Mathematical and Stochastic Modeling for Salt Transport in Soil: Leaching of Heavy Metals

A Thesis

Submitted for the Award of Ph.D. degree of

UNIVERSITY OF KOTA

in the

Faculty of Science

By

AJAY SHARMA

Under the Supervision of

Dr. ARUN KUMAR
Lecturer (Associate Professor)

RESEARCH CENTER
(Department of Mathematics, Government College, Kota)
UNIVERSITY OF KOTA,
KOTA (RAJ)

2017

Dedicated

To

My Parents

C E R T I F I C A T E

I feel great pleasure in certifying that the thesis entitled "Mathematical and Stochastic Modeling for Salt Transport in Soil: Leaching of Heavy Metals" by Ajay Sharma under my guidance. He has completed the following requirements as per Ph.D regulations of the university.

(a) Course work as per the university rules.
(b) Residential requirements of the university (200 days)
(c) Regularly submitted annual progress report
(d) Presented his work in the departmental committee
(e) Published/accepted two research papers in a referred research journal,

I recommend the submission of thesis.

Date:

Dr. Arun Kumar
(Supervisor)
Lecturer (Associate Professor)
Department of Mathematics,
Government College Kota, Kota

Candidate's Declaration

I hereby certify that the work, which is being presented in the thesis, entitled "Mathematical and Stochastic Modeling for Salt Transport in Soil: Leaching of Heavy Metals" in partial fulfilment of the requirement for the award of the Degree of Doctor of Philosophy, carried under the supervision of Dr. Arun Kumar and submitted to the (Department of Mathematics, Govt. College Kota, Kota), University of Kota, Kota represents my ideas in my own words and where others ideas or words have been included. I have adequately cited and referenced the original sources. The work presented in this thesis has not been submitted elsewhere for the award of any other degree of diploma from any institutions. I also declare that I have adhered to all principles of academic honesty and integrity and have not misrepresented or fabricated or falsified any idea/data/fact/source in my submission. I understand that any violation of the above will be cause for disciplinary action by the University and can also evoke penal action from the sources which have thus not been properly cited or from whom proper permission has not been taken when needed.

(Signature)

(Name of the student)

Date:……

This is to certify that the above statement made by Ajay Sharma (Enrolment No……) is correct to the best of my knowledge.

Date:……

(Research Supervisor)
Department of Mathematics
Government College Kota, Kota

Acknowledgement

The success of this work would have been uncertain without the help and guidance of dedicated band of people. Thus as a token of appreciation of their effort in making of Ph.D. work a success, I would like to express my true and sincere acknowledgements to their contributions.

I express my sincere thanks to the Guide/Supervisor Dr. ARUN KUMAR, Associate Professor, Department of Mathematics Govt. College, Kota (Rajasthan) for his valuable guidance during entire phase of Ph.D. thesis work.

I am thankful to staff members of the Department of Mathematics Govt. College, Kota who have helped me directly or indirectly during this course of time.

I am grateful to Prof. ASHU RANI, University of Kota, Kota (Rajasthan) also for her constant encouragement and valuable suggestions throughout the preparation of the thesis.

My special thanks are due to my friends, Mr. Mohan, Mr. Manish, Mr. Triveni and Mr. Suresh for their inspiration, cooperation and support.

I am extremely thankful to my dear sister Dr. Arti Sharma for her cooperation and whole-hearted support in preparation of the thesis. I shall never forget her valuable support during this thesis work.

Last but not the least I would like to convey my heartfelt gratitude to my beloved parents, my wife Shikha and my family members for their incessant support, encouragement and inspiration throughout my career without which this Ph. D. thesis would only have been a dream. My loving cheers to the kids Adamya and Rishon.

Kota (AJAY SHARMA)

The present thesis entitled **"Mathematical and Stochastic Modeling for Salt Transport in Soil: Leaching of Heavy Metals"** consists of the following research papers:-

1. **Arun Kumar**, Ajay Sharma and Ashu Rani (2015) "Transport of solutes under transient flow conditions" International Soil and Water Conservation Research, Volume 3, Issue 3, 209-223.
2. Ajay Sharma, **Arun Kumar** (2016) **"**Assessment of Heavy Metal Contamination in Soil Sediments of Jaipur and Kota Industrial Areas, Rajasthan, India" International Journal of Engineering, Management & Sciences (IJEMS), Volume-3, Issue-10, 1-7.

CONTENTS

1. INTRODUCTION 1-24

1.1 Soil 2

1.2 Soil Constituents 3

1.3 Soil Processes 5

1.4 Soils of Jaipur and Kota District 9

1.5 Adsorption and Migration of Heavy Metals 10

1.6 Mathematical Techniques 18

1.7 Aim and Objective 20

1.8 Importance of Proposed Research Work 21

2. REVIEW OF LITERATURE 25-51

2.1 Heavy Metal Polluted Soils 26

2.2 Brief Overview of Heavy Metals 28

2.3 Heavy Metal Contamination Sources 29

2.4 Leaching 30

2.5 Factors Affecting Heavy Metals Leaching 31

2.6 International and National Status of Work Done 33

2.7 Mathematical Modeling of Heavy Metal Leaching 36

3. MODEL FOR HEAVY METAL TRANSPORT IN SOIL 52-82

3.1 Introduction 53

3.2 Mathematical Statement of Transport Problem 53

3.3 Stochastic Approach to Study Transport of Solute under Gravity 56

3.4 Concentration Distribution 58

3.5 Concentration Distribution for Dispersive Transport 65

3.6 Stochastic Transport in Non-steady Vertical Flow 72

4. TRANSPORT OF SOLUTES UNDER TRANSIENT FLOW CONDITIONS 83-98

4.1 Introduction 84

4.2 Estimation of Soil Hydraulic Properties 85

4.3 Soil Moisture Retention Curves 86

4.4 Soil Water Infiltration and Movement (Swim) Model 87

4.5 Analytical Solution 92
4.6 Results 95
5. KINETIC MULTIREACTION APPROACH FOR LEACHING OF HEAVY METALS 99-115
5.1 Introduction 100
5.2 Kinetic Multireaction Approach 102
5.3 Formulation of Models 102
5.4 Initial and Boundary Conditions 106
5.5 Results 110
6. ASSESSMENT OF HEAVY METAL CONTAMINATION IN SOIL SEDIMENTS OF JAIPUR AND KOTA INDUSTRIAL AREAS 116-142
6.1 Method and Material 117
6.2 Distribution of Studied Heavy Metals in Different Locations of Jaipur District 120
6.3 Distribution of Studied Heavy Metals in Different Locations of Kota District 124
6.4 pH Analysis 137
6.5 Correlation between Heavy Metals 138

Mathematical and Stochastic Modeling for Salt Transport in Soil: Leaching of Heavy Metals

Chapter 1

Introduction

1.1 SOIL

Soil is the natural, unconsolidated, mineral and organic matter occurring on the surface of the Earth [1], i.e., soil consists of mineral solid particles mixed with organic matter and water. The standard soil classification is carried out based on the size distribution of mineral solid particles which can be divided into three different categories; sand, silt and clay. The characteristic size distribution of sand, silt and clay particles is shown in following table.

Soil particle size [2]

Particle	Diameter (mm)	Number per 1 gram of soil	Surface area (cm^2) per 1 gram of soil
Sand	0.05−2	$89\times10^5-112$	15−308
Silt	0.002−0.05	2×10^7	888
Clay	<0.002	4×10^{11}	4×10^5 (non-swelling)
			8×10^6 (swelling)

A valid concept of the nature of soil must avoid the common error that soil is simply a mixture of unconsolidated material resulting from the weathering processes of underlying rocks. Soil is a natural body, having mineral and organic component as well as physical, chemical and biological properties, and therefore, cannot be simple reflection of the combined properties of all soil components. Any classification of soil suffers from the disadvantage that it is impossible to relate it to the great complexities of soil genesis and properties. The terms used in defining the soil in different systems seldom is exactly equivalent.

The composition of soil is extremely diverse and, although governed by many different factors, climatic conditions and parent material predominant most commonly. Soil is composed of three phases: solid (mineral and organic), liquid and gaseous and exhibits properties resulting from the physical and chemical equilibrium of three phases. The important factors influencing soil properties are the chemical compositions of the solid component, its mineral structure and the state of dispersion.

Two stages are involved in the formation of soil from parent material. The first is the alternation of the primary mineral constituents of the parent rock by the physical and chemical processes of weathering. The second stage (pedogenesis) results in the formation of a soil profile from the weathered rocked material, leading to the development of a mature soil as the end product of the interacting processes. Weathering and pedogenic processes cannot be easily distinguished and separated because they may take place simultaneously at the same sites and most largely control the kind of soil that finally develops.

1.2 SOIL CONSTITUENTS

Generally speaking soil is a three-dimensional system, made of a solid, a liquid and a gaseous phase, each in an amount depending on the quantity of its constituents and their kinetic roles in the complex series of reactions, leading to soil formation. Following figure illustrates the composition by volume of an average soil.

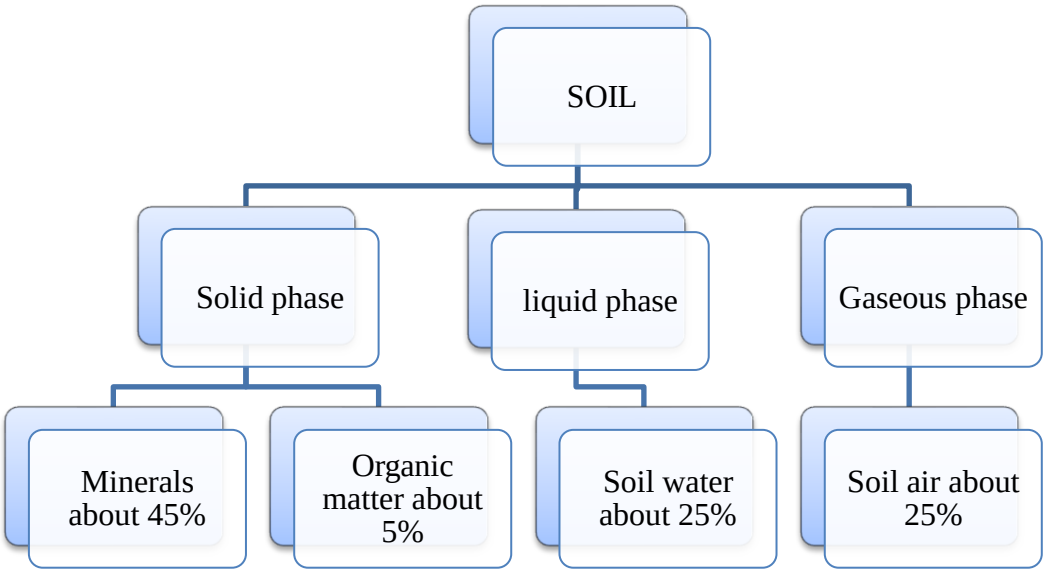

Figure 1: Composition by volume of an average soil

MINERALS-

The mineral constituents of soil inherited from the parents rocks have been exposed for various periods of time to weathering and pedogenic processes. The

soil mineral system, which is not necessarily in equilibrium with the soil solution, is complicated by the processes of degradation and neo formation of minerals, as well as by mineral reaction with organic compounds. The common primary minerals in soil inherited from the parent material can be arranged in to parallel series, according to their susceptibility to weathering processes:

- Series of felsic minerals; plagioclase > K-feldspar muscovite > quartz,
- Series of mafic minerals; olivcne > pyroxenes > amphiboles > biotic.

They are, however, considered to be the source of certain micronutrients elements. The approximate composition of mineral constituents of surface soil shows that quartz is the most common mineral in the soil, constituting 50 – 90% of the solid phase. Even in geochemical condition favourable for the leaching of silicates, quartz remains as basic soil mineral. Feldspar is of low relative resistance to weathering in the soil environment and their alternation usually provides materials for clay mineral formation. Carbonates and metal oxides are usually accessory mineral in soil of humid climatic zones, while in soil of arid climatic zones they may be significant soil constituents.

THE LIQUID PHASE – SOIL WATER

Soil water is principally derived from two sources: precipitation and groundwater. Each contributes to the amount of moisture in the soil, depending mainly on the climate and the water balance between the atmosphere and the plant-soil system. The amount of water lost to the atmosphere comprises the sum of the water transferred by evaporation and of that transferred by plant transpiration, forming together the evapotranspiration. This depends directly on the climatic conditions as well as the properties of the plant-soil system. The evapotranspiration that would take place under optimum precipitation conditions and soil moisture capacity is known as the potential evapotranspiration.

THE GASEOUS PHASE – SOIL AIR

Soil air, or soil atmosphere, is the characteristic name given to the mixtures of gases moving in the aerated zone above the water and filling the soil pores, where these are not already occupied by interstitial water. Mass flow of

these gases in the aerated zone will be wholly controlled by atmospheric factors such as temperature, pressure, and moisture conditions. As far as major constituents are concerned, soil air has a composition slightly different from that of atmospheric air. Although soil air contains 1–6% less oxygen by volume than atmospheric air, we find that it contains about 10 to 150 times more CO_2.

These differences in the concentration of CO_2 and O_2, between soil air and the atmosphere, result in partial pressure gradients between the two systems along which CO_2 moves from the soil to the atmosphere, while the oxygen flow takes place in the opposite direction. Gas exchange between soil air and the atmosphere occurs also along temperature gradients and in sites where rainwater introduces atmospheric gases into the soil. Beside the major constituents, minor or trace amounts of other gases may occur in the soil air, originating from deep-seated sources or as products of organic or mineral reactions in the soil environment.

1.3 SOIL PROCESSES

Transport

The transport of dissolved heavy metals may take place through the soil solution (diffusion) and also with the moving soil solution (mass flow, leaching). Generally, in soils formed under a cool and humid climate, the leaching of heavy metals downward to the profiles is greater than their accumulation, unless there is a high input of these elements into the soils. In warm, dry climate, and also to some extent in humid climate, upward translocation of heavy metals in the soils profiles is the most common movement. However, specific soils properties, mainly its cation exchange capacity, control the rates of heavy metal migration in the profiles.

Heavy metals budgets have been calculated for various ecosystems. Input/ output differences show that for the majority of elements the accumulation rate in the surface soil is positive.

Adsorption

The term “adsorption” is commonly used for the process of sorption of chemical elements from solution by soil particle. Adsorption is thus the kinetic reaction based on thermodynamic equilibrium rules. The forces involved in the

adsorption of ionic species at charge surfaces are electrostatic and can be explained by Coulomb's law of attraction between unlike charges and repulsion between like.

Surface charges in soil materials caused primarily by ironic substitutions are exhibited mainly by colloids. At a low pH a positively charge surface prevails, while at a high pH a negatively charge surface develops. The colloids of the majority of soils, therefore, carry negative charges and can be electro-neutralized by cations present in the surrounding solutions. In the presence of an excess of cations, the process of exchanging the cations for other others maintain the eletro-neutrality of the system. Thus, the cation adsorbed by the solid phase can be replaced by other cations, most often by H ions. An increase stability of adsorbed metals may result from dehydration and recrystallisation processes that occur on the surface of the colloids, especially in alkaline soils.

From the above information it can be summarised that geochemically, an element introduce in to the soil may end up in one or more of the following form:

- Occluded or fixed into soil minerals,
- Incorporated into biological material,
- Dissolved in soil solution,
- Precipitated with other compounds in soils, and
- Held into exchanged sites of organic solids or in ordinate constituents.

Weathering processes

Weathering, the basic soil forming processes, has been extensively studied and reviewed as the complex interactions of the lithosphere, the atmosphere, and the hydrosphere that occur in the biosphere empowered by solar energy. Weathering can be chemically described as the process of dissolution, hydrolysis, hydration, oxidation, reduction, and carbonation. All of these processes are based on rules of enthalpy and entropy, and they lead to the formation of minerals and chemical components that are relatively stable and equilibrated in the particular soil environments. Chemical weathering leads to the destruction of parent minerals

and removal of the elements from the minerals into solution and suspensions. Greatly simplified, basic weathering processes can be characterized as follows:

- Oxidation-incorporation of the oxygen into chemical components or increase of the element potential
- Hydration-minerals increase their water content
- Reduction-reaction that are reverse of oxidations
- Dissolution-minerals are soluble in the aquatic phase
- Hydrolysis-reaction of minerals with water producing new ions and/or insoluble components
- Carbonation alternations of compounds into carbonates due to the incorporation of CO_2. All these reactions are controlled led by chemical equilibria of the particular earth surface environment.

Dissolution

Chemical reactions leading to solution of each species of ions can be characterized by thermodynamic equations. At each equilibrium states the reaction rates of both directions compensate and keep the composition of the soil phases- (solid, liquid and gaseous) constant. The diversity of ionic species of heavy metals and their various affinities to complex with inorganic and organic legends make possible the dissolution of each element over a relatively wide range of pH and Eh. Each element can also be quite readily precipitated and/ or add sorbed even under a small change of the equilibrated conditions.

However, usually the most mobile fractions of ion occurred at a lower range of pH and at a lower redox potential. It can then be anticipated that with increasing pH of the soil substrate the solubility of most trace cations will decrease. The concentration of heavy metal is lower in soil solution of alkaline and neutral soil then in those of light acid soils.

Pedogenic processes

Several specific reactions, in addition to those involved in weathering, lead to the formation of a particular soil profile. Although there is a great diversity in pedogenic processes, they include the following similar stages-

- Translocation of these materials within the soil, both vertically and horizontally
- Losses of this materials from the soil
- Addition of organic and mineral material to the soil
- Transformation of organic and mineral metal in the soil.

These processes can be constructive or destructive in soil formation. Six factors that largely control the kind of soil that finally develops are-

- Topography (open or close systems)
- Vegetation and other soil biota
- Anthropogenic activity (degradation, contamination, re-cultivation)
- Climate (temperature, rainfall)
- Time
- Parent material (the nature of minerals)

Thus, dynamic equilibrium between soil components is governed by various interactions between the soil, solid and gaseous phases, biota and the soil solutions.

Sorption

Soils are considered as sinks for heavy metals; therefore, they pay an important role in environmental cycling of these elements. They have a great ability to fix many species of trace ions. The term "sorption" refers to all phenomenonat the solid solution boundary, including the following intermolecular interaction:

- Magnetic bonding
- Charge transfer

- Ion dipole forces
- Chemisorptions
- Ion and legend exchanges
- Hydrophobic and hydrogen bonding
- Van-der-waals forces

Soils component involved in sorption of heavy metals are oxides (hydrous, amorphic mainly of Fe and Mn and, to a much lesser extent, Al and Si); organic matter and biota; carbonates, phosphate, sulphides, and basic salts; and clays.

1.4 SOILS OF JAIPUR AND KOTA DISTRICT

JAIPUR

Jaipur district, covering geographical area of 11,061.44 sq. km and extending between north latitudes $26^0 25'$ and $27^0 51'$ and east longitudes $74^0 55'$ and $76^0 15'$ forms east-central part of the Rajasthan State.

Soils in the district may be classified as:

a) Loamy sand to sandy loam
b) Sandy clay loam
c) Sandy clay
d) Windblown sand
e) River sand

KOTA

Kota district lies in south eastern part of the state, between $24^0 25'$ and$25^0 51'$ North latitude and $75^0 17'$ and $76^0 00'$ East Longitude. It covers a geographical area of 5198 sq. km. The soil of the Kota district is characterized by deep, mediumand black shallow alluvium soils. The soils ranges in depth from shallow to verydeep with lime concretion or lime encrusted gravels at varying depths. The soils in general are clay loam to clay in texture and moderately to less permeable anddeveloping cracks in dry season. The soils can be classified as Chromusterts great group of Vertisols order.

1.5 ADSORPTION AND MIGRATION OF HEAVY METALS

Soil is a major reservoir for contaminants as it possesses an ability to bind various chemicals. These chemicals can exist in various forms in soil and different forces keep them bound to soil particles. It is essential to study these interactions because the toxicity of chemicals may strongly depend on the form in which they exist in the environment. Another thing is that soil variability and some environmental properties (e.g. climate factors) may change equilibrium found in soil and cause leaching of trace toxic elements like heavy metals tightly bound to soil particles.

Leaching is one of the most important physical process responsible for migration of soil nutrients and pollutants occurs either by active transport or passive permeation accompanied by diffusion of energy and matter through soil matrix. Over fertilized agricultural areas possess a threat to the ground water quality mainly because of leaching of salts through macropores along with percolating water [3]. As the water moves through the soil profile, it dissolves additional salts from the soil and transports them to subsurface and ground water [4]. The leaching rates of salts are basically the relative mobility or fluidity of water along with salt movement as diffusion of salt is not possible without diffusion of water in saturated soils. One of the worst consequence of leaching from polluted sites as well as from over fertilized agricultural fields during irrigation, rain events and water percolation is contamination of subsurface and ground water [5]. Leaching may depend on macro porosity of soil [6] as well as laminar flow of water in cracks and channels found in soils [7]. It also depends on soil quality, applied water quality, ion exchange [8], salt solubility, initial water content of soil [9], pH [10], temperature etc. of various types of soils.

Chemicals having heavy metals once introduced to the environment by one particular method may spread to various environmental components, which may be caused by the nature of interactions occurring in this natural system. Heavy metals may chemically or physically interact with the natural compounds, which change their forms of existence in the environment. In general they may react with particular species, change oxidation states and precipitate [11]. Heavy metals may be bound or sorbed by particular natural substances, which may

increase or decrease mobility. Studying the dissipation of heavy metals is called speciation [12]. Literature study shows that the speciation may be understood in different ways and in various aspects [13]. In general, two forms of speciation are distinguished by environmental scientists: chemical and physical.

Properties Influencing Sorption of Heavy Metals in Soil

Soil has the ability to immobilise introduced chemicals like heavy metal ions. The immobilisation of xenobiotics is mainly due to sorption properties which are determined by physicochemical properties of the soil such as: amount of clay and organic fraction, pH, water content, temperature of the soil and properties of the particular metal ion [14].

The solid state of soils composes an average of 45% of soil bulk. It consists of mineral particles, organic matter and organic-mineral particles. They all play a very important role in giving the soil the ability to absorb, exchange, oxidise, reduce, catalyse and precipitate chemicals and metal ions in particular [14].

The inorganic colloidal fraction of soil is the most responsible for sorption by its mineral particles. It is comprised of clay minerals, oxides, sesquioxides and hydrous oxides of minerals. The total amount of clay minerals in soil bulk is very important, as they are the major inorganic component of soil sorption complex.

The distribution of xenobiotics like, for instance, heavy metals between different size classes of organic-mineral particles is important because the physical movement of these particles leads to their re-distribution in the landscape. The content of heavy metals usually decreases from clay to coarse silt [15]. It is caused by the high surface area of clay minerals and weak pH dependence of C.E.C (Cation Exchange Capacity). Hence, soils with high amounts of clay fraction and organic matter can be more contributed with heavy metals than others.

Contaminant Transport Processes

Solute transport processes control the extent of contaminant migration in the subsurface. It involves mainly three processes: advection, diffusion and dispersion. These processes are available only to deal with the transport of nonreactive contaminants in the subsurface. Nonreactive contaminants are

dissolved contaminants that are not influenced by chemical reactions or microbiological processes. In case of reactive contaminants, these transport processes are considered along with various mass transfer and microbial degradation processes.

Diffusion

Diffusion is a micro-scale process which causes movement of a solute in water from the area of its higher concentration to the area of its lower concentration. The difference in concentration is called concentration gradient. Diffusion ceases when there is no concentration gradient. It can occur even when the fluid is not flowing or is flowing in the direction opposite to the contaminant movement. Diffusion is characterized using Fick's first law of Diffusion.

Advection

Advection is the movement of the dissolved contaminant in groundwater, and it refers to the average linear flow velocity of the bulk of contaminant. Due to advection the contaminant moves with the flow at a velocity equal to the seepage velocity of the groundwater in the porous medium. The seepage velocity can be represented as-

$$v_s = \frac{K_c h}{\alpha} \quad (1)$$

Where K_c is the hydraulic conductivity, h is the hydraulic gradient and α is the porosity of the porous material.

Dispersion

At the macroscale level, the contaminant transport is defined by the average groundwater velocity. However, at the microscale level, the actual velocity of water may vary from point to point and can be either lower or higher than the average velocity. The difference in microscale water velocities arises due to pore size, path length and friction in pores. Due to these differences in velocities, mixing occur along the flow path.

This mixing is called mechanical dispersion or hydrodynamic dispersion or simply dispersion. The mixing that occurs along the direction of the flow path is called longitudinal dispersion and along direction normal to the direction of the flow path is called transverse dispersion. Figure 2(c) represents the one-dimensional dispersion of the contaminant results in a dilution of the

contaminants at the advancing edge of flow by considering only longitudinal hydrodynamic dispersion [16-17].

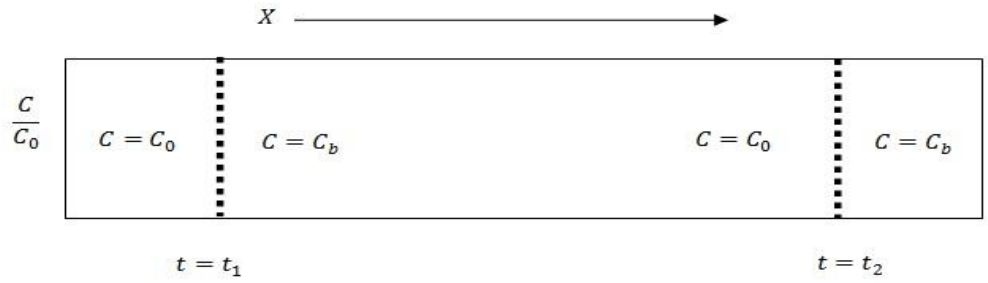

(a) Advection only (Where C_0 =Initial Concentration, C_b =Background Concentration)

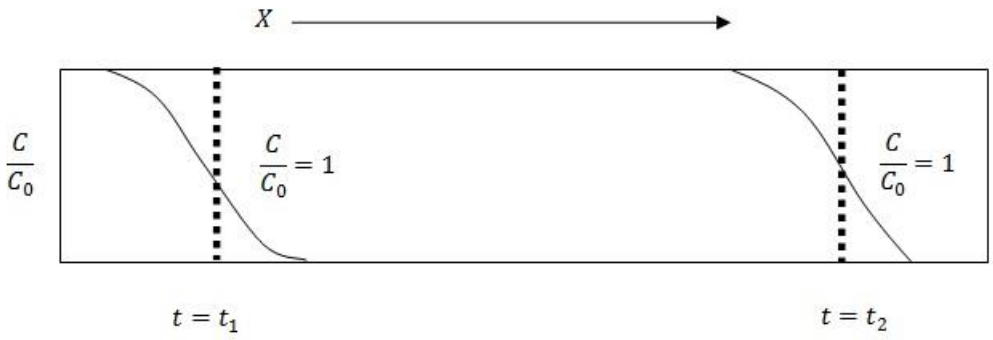

(b) Diffusion only

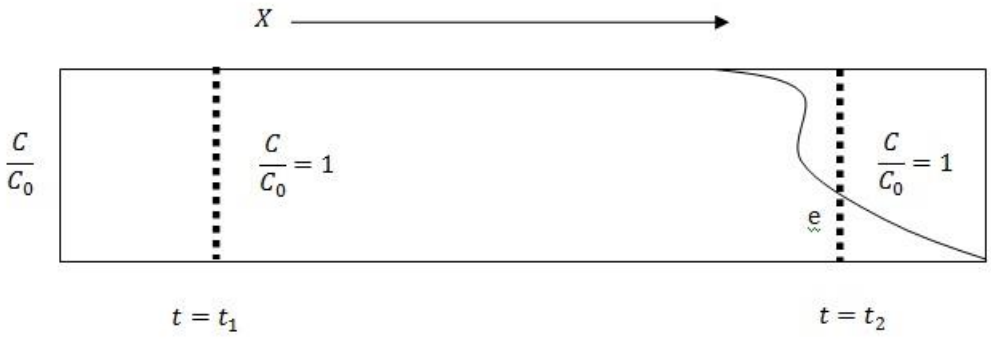

(c) Advection and Dispersion

Figure 2: Contaminant transport processes

Hydrodynamic Dispersion Equation

The general equation governing the hydrodynamic dispersion of a homogeneous fluid is the fundamental advection-dispersion equation. It is based on conservation of mass and Fick's first law of diffusion.

Fick's first law

Fick's first law relates the diffusive flux to the concentration gradient. It states that the rate of transfer of diffusive substance through the unit area of a section is proportional to the concentration gradient normal to that section.

$$J_D = -D' \frac{\partial c}{\partial x} \tag{2}$$

Where J_D is the diffusive mass flux, D' is the diffusion coefficient. Negative sign indicates that contaminant moves from zone of higher concentration to the zone of lower concentration.

Advection-dispersion Equation

Let $c(x, y, z)$ be the concentration of the fluid at any point (x, y, z) and u_x, u_y, u_z are the velocity components parallel to the co-ordinates axes. Consider a small element of volume $dxdydz$ in the form of a rectangular parallelepiped shown in Figure 3, whose sides are parallel to the axes of co-ordinates.

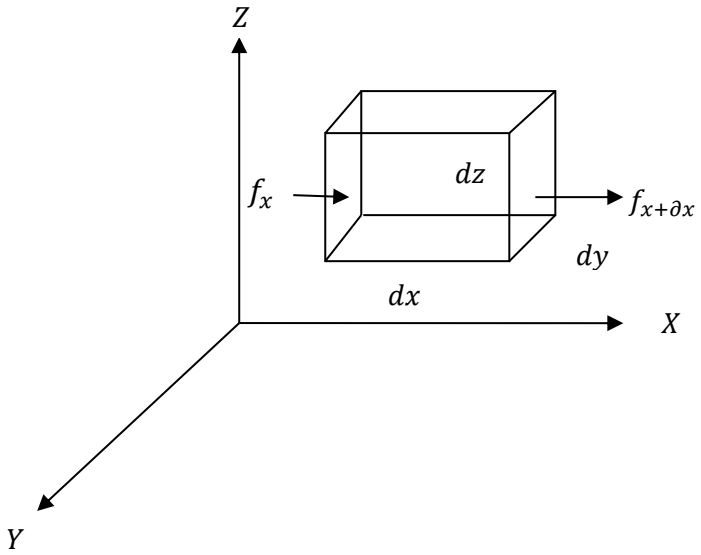

Figure 3: Small rectangular parallelepiped

The dispersive mass flux $\bar{J}_{diff}(J_x, J_y, J_z)$ from Fick's first law of diffusion

$$J_x = -D_x \frac{\partial c}{\partial x}, J_y = -D_y \frac{\partial c}{\partial y}, J_z = -D_z \frac{\partial c}{\partial z} \quad (3)$$

and, the convective mass flux $\bar{J}_{conv}$ through the element can be written as,

$$\bar{J}_{conv} = \bar{u}c, \quad (4)$$

Where D_x, D_y and D_z are the dispersion coefficients and $\bar{u}$ (u_x, u_y, u_z) is the flow velocity.

Therefore, the total flux including advection and diffusion transport is

$$\bar{J}(J_1, J_2, J_3) = \bar{J}_{conv} + \bar{J}_{diff} \quad (5)$$

The total flux entering the element along x-direction

$$J_1 = \left(u_x c - D_x \frac{\partial c}{\partial x}\right) \partial y \partial z = f_1(x, y, z) \quad (6)$$

And the total flux leaving the element from x-direction

$$f_1(x + \partial x, y, z) = f_1(x, y, z) + \partial x \frac{\partial f_1(x,y,z)}{\partial x} + \cdots \quad (7)$$

The excess of solute flow along x-axis can be written as-

Difference of mass per unit time = Mass entering the element – Mass leaving the element

$$= -\partial x \frac{\partial}{\partial x} f_1(x, y, z)$$

$$= -\partial x \frac{\partial}{\partial x}\left(u_x c - D_x \frac{\partial c}{\partial x}\right) \partial y \partial z \quad \text{(Using Eq. 6)} \quad (8)$$

Similarly, the excess of solute flow along y-axis

$$= -\frac{\partial}{\partial y}\left(u_y c - D_y \frac{\partial c}{\partial y}\right) \partial x \partial y \partial z \quad (9)$$

And the excess of solute flow along z-axis

$$= -\frac{\partial}{\partial z}\left(u_z c - D_z \frac{\partial c}{\partial z}\right) \partial x \partial y \partial z \quad (10)$$

Total excess of solute flow in over the solute flow out from all the co-ordinates axes of the element, i.e. difference of mass of solute per unit time

$$= -\left[\frac{\partial}{\partial x}\left(u_x c - D_x \frac{\partial c}{\partial x}\right) + \frac{\partial}{\partial y}\left(u_y c - D_y \frac{\partial c}{\partial y}\right) + \frac{\partial}{\partial z}\left(u_z c - D_z \frac{\partial c}{\partial z}\right)\right] \partial x \partial y \partial z \quad (11)$$

Since, the dissolved substance is assumed to be non-reactive, the difference between the flux into the element and the flux out of the element equals the amount of dissolved substance accumulated in the element. Therefore, the rate of mass change per unit time is given by-

$$\frac{\partial c}{\partial t}\,\partial x\partial y\partial z \tag{12}$$

By the principal of conservation of mass, we have,

Rate of change of solute concentration = Rate of solute flow in - Rate of solute flow out

$$\frac{\partial c}{\partial t}\,\partial x\partial y\partial z = -\left[\frac{\partial}{\partial x}\left(u_x c - D_x\frac{\partial c}{\partial x}\right) + \frac{\partial}{\partial y}\left(u_y c - D_y\frac{\partial c}{\partial y}\right) + \frac{\partial}{\partial z}\left(u_z c - D_z\frac{\partial c}{\partial z}\right)\right]\partial x\partial y\partial z \tag{13}$$

$$\Rightarrow \frac{\partial c}{\partial t} = \left[\frac{\partial}{\partial x}\left(D_x\frac{\partial c}{\partial x} - u_x c\right) + \frac{\partial}{\partial y}\left(D_y\frac{\partial c}{\partial y} - u_y c\right) + \frac{\partial}{\partial z}\left(D_z\frac{\partial c}{\partial z} - u_z c\right)\right] \tag{14}$$

This is known as hydrodynamics dispersion equation or advection-dispersion equation in three-dimensional case.

Here, D_x, D_y and $D_z$are the dispersion coefficients may be considered as function of time or position or constant.

For one-dimensional case, the advection-dispersion equation with constant coefficient can be written as

$$\frac{\partial c}{\partial t} = D_x\frac{\partial^2 c}{\partial x^2} - u_x\frac{\partial c}{\partial x} \tag{15}$$

Initial and Boundary Conditions

The advection-dispersion equation represents the expressions of mass balance and dimensions. It does not contain any information related to any specific case of flow, not even the shape of the domain within which this flow occurs. Therefore, each equation has an infinite number of possible solutions, each of which corresponds to a particular case of flow through a porous medium. To obtain one particular solution corresponding to a certain specific problem of interest, it is necessary to provide supplementary information that is not contained in the equation. This supplementary information defines the initial and boundary condition of the problem.

Initial Condition

The initial conditions describe the distribution of the values of the considered state variables at some initial time, usually taken as $t = 0$, at all points within the considered domain. The initial condition representing concentration of

contaminant transport in general form for a three-dimensional system can be written as

$$c(x, y, z, t) = f_2(x, y, z); t = 0 \quad (16)$$

Where $c(x, y, z, t)$ is the required state variables, and $f_2(x, y, z)$ is a known function or constant or zero, depending on the physical model of the problem.

Boundary Conditions

Boundary conditions represent the way the considered domain interacts with its adjacent environment. It can be described by three types of mathematical conditions enlisted as follows:

A. **Neumann boundary condition:**

In case of specified flow boundaries, the derivative of head (flux) across the boundary is given. It is used to describe fluxes to surface water bodies, spring flow, underflow and seepage to or from bedrock underlying the modelled system. It prescribes normal gradient of concentration over a certain portion of the boundary. Mathematically it can be written as

$$\left(D_{ij} \frac{\partial c}{\partial x_j}\right) n_i = f_3(x, y, z, t) \quad (17)$$

Where f_3 is a known function and n_i is directional cosine. For impervious boundaries, f_3 becomes zero.

B. **Robin boundary condition:**

It is also known as Cauchy or mixed boundary condition. The head dependent flow boundaries relate with boundary heads and boundary flows. The flux across this type of boundary is dependent on the difference between a user-supplied specified head on one side of the boundary and the model calculated head on the other side. Robin type boundary condition prescribes linear combination of concentration and its gradient along the boundary. Mathematically, it can be represented as-

$$\left(D_{ij} \frac{\partial c}{\partial x_j} - v_i c\right) n_i = f_3(x, y, z, t) \quad (18)$$

Where f_3 is a known function. The first term on the left-hand side represent flux by dispersion and the second term represent the effect of advection. These descriptions of boundary conditions have been explored [18].

C. **Dirichlet boundary condition**:

A specific head boundary is simulated by setting the head at the relevant boundary nodes equal to known head values. It prescribes concentration along a portion of the boundary. Mathematically, it can be expressed as-

$$c = f_4(x, y, z, t) \tag{19}$$

Where $f_4(x, y, z, t)$ may be constant or a given function of space or time or both for that particular portion of the boundary.

1.6 MATHEMATICAL TECHNIQUES

Mathematical modeling is the major tool to predict the mobility and the persistence of pollutants within soil systems. Therefore, the objective of this research is to show Mathematical and Stochastic representation for Salt Transport in Soil and process governing Leaching of Heavy Metals.

The advection-dispersion equation with different initial and boundary conditions in combined form is known as advection-dispersion model or solute transport model. Analysis of contaminant transport problem requires the use of mathematical model commensurate with the application. In literature, there are several mathematical techniques available to solve the advection-dispersion model. These techniques generally involve two main approaches such as numerical method and analytical method.

Numerical Method

The numerical methods such as finite differences, finite elements, integrated finite differences, the boundary integral equation, and analytical element can be used in groundwater modeling. The boundary integral equation method [19-20] and analytic elements [21-22] are relatively new techniques which are not yet widely used. Integrated finite difference (IFD) technique is closely related to the finite element method. Finite difference and finite element methods are more commonly used to solve groundwater modeling problems [23].

Finite Difference Method

Advection-dispersion equation subject to different initial and boundary conditions can be solved by approximating the first and second order derivatives contains in the equation by forward, backward and central difference

approximations. The numerical solution can be obtained by finite-difference techniques such as Explicit finite difference method and Crank-Nicolson implicit method.

i. **Explicit Finite-difference Method:**

It is a second order accurate method. Let us consider a one-dimensional domain on which problem is defined. This is rectangular with *x* ranging from x_{min} to x_{max} and time domain *t* ranging from *0* to *T*. Divide the interval $[x_{min}, x_{max}]$ into *M* equal subinterval with length Δx, indexed by $i = 0,1,2, \dots, M$ and interval [*0,t*] into equal subintervals with length Δt, indexed by $j = 0,1,2, \dots$ .Let C_{ij} denote the approximation of grid point at $x_i = x_0 + i\Delta x$ and $t_i = t_0 + j\Delta t$. The partial order derivative can be approximated as follows:

$$\frac{\partial C}{\partial t} \approx \frac{C_{i,j+1} - C_{i,j}}{\Delta t} \quad \text{(Forward difference formula)} \quad (20)$$

$$\frac{\partial C}{\partial x} \approx \frac{C_{i+1,j} - C_{i-1,j}}{2\Delta x} \quad \text{(Central difference formula)} \quad (21)$$

$$\frac{\partial^2 C}{\partial x^2} \approx \frac{C_{i+1,j} - 2C_{i,j} + C_{i-1,j}}{\Delta x^2} \quad \text{(Central difference formula)} \quad (22)$$

Using these approximations in one-dimensional solute transport model, all the values of $C_{i,j+1}$ can be calculated for the entire grid at each time level. This method is known as Explicit finite-difference method. It is second order accurate in x-direction and first order accurate in t-direction, and easy to implement. The Explicit finite-difference solution is unstable unless the ratio $\frac{\Delta t}{\Delta x^2}$ is sufficiently small. This means that small errors may come either due to arithmetic inaccuracies or due to the approximate nature of the derivative expressions which tends to accumulate and grow as one proceeds rather than dampen out.

ii. **Crank-Nicolson Implicit Method:**

In Crank-Nicolson implicit method, the time derivative of advection-dispersion equation can be approximated by forward difference approximation, first order space derivative can be approximated by average of central difference approximation of n^{th} level and $(n+1)^{th}$ level and second order space derivation can be approximated as average of central difference approximation n^{th} level and $(n+1)^{th}$ level. After

computing the set of approximations, it gives a system of equation which can be solved by tri-diagonal method or Gauss elimination method. This method is assumed to be unconditionally stable. However, to calculate the system of equations at each time step, especially in two-dimensional model, makes the problem more complex.

Analytical Method

Analytical methods are useful for providing initial and approximate studies of alternative pollution scenario, conducting sensitivity analyses to investigate the effects of various parameters or processes on contaminant transport, extrapolating result over large time and spatial scales where numerical solutions become impractical. The literatures contain many analytical solutions for advection-dispersion type transport problem in one-, two- and three-dimension.

There are several analytical methods available to find the analytical solution of advection-dispersion model named as- Laplace transform technique, Fourier transform technique, generalized integral transform technique, Green's function method, Power series method, Hankel transform technique, Method of superposition principle. The methods are used according to the physical model, dimensions, types of initial and boundary conditions, temporally and spatial dependency of the coefficient in the equation of the problem.

1.7 AIM AND OBJECTIVE

Large areas of cultivated land worldwide are affected by soil salinity. Salinity refers to large 20 concentrations of easily soluble salts present in water and soil on a unit volume or weight basis (typically expressed as electrical conductivity (EC) of the soil moisture in ds/m, i.e. deci siemens per meter at 25^0C; for NaCl 1mg/l). High salinity causes both ion specific and osmotic stress effects, with important consequences for plant production and quality. Prevention or remediation of soil salinity is usually done by leaching of heavy metals, and has resulted in the concept of leaching requirement [24-26].

An understanding of the factors that affect the fate and transport of contaminants in the unsaturated soil and in groundwater is important for many applications. This understanding is necessary for determining the assimilative

capacity of a soil and whether chemicals are likely to accumulate within the soil profile or leach to contaminate groundwater. An understanding of these factors will help in identification of suitable remediation methods and proper land disposal sites. The factors also determine what happens to chemicals under closure conditions and how to avoid groundwater contamination.

Mathematical modeling is the major tool to predict the mobility and the persistence of pollutants to and within groundwater systems. Several comprehensive institutional models have been developed in recent years for this purpose. However, evaluation procedures are not well established for models of soil-water flow and chemical transport. The models may be used to determine the potential concentrations at receptor points and the necessity & immediacy of remedial action. The factors and processes that are important include those that affect losses, retardation, solubility and transport. For protection of public health and the environment, particularly groundwater, it is desirable to enhance losses and retardation.

Objective

- Formulate Mathematical model for salt transport in soil.
- Formulate Kinetic multireaction approach for leaching of heavy metals in soil.
- The present research work endeavours to find out the total concentration of some specific heavy metals in the soil.
- The total concentration of heavy metal provides pollution information at different locations of Jaipur and Kota cities.
- In this work, metals like copper, zinc, lead, chromium, nickel, and cadmium have been estimated at different locations and established correlation between the total metal content.

1.8 IMPORTANCE OF PROPOSED RESEARCH WORK

A quantitative description of heavy metals transport in the saturated and unsaturated zone of the soil is required to predict the impact of human influence on the environment.

In this study, we will deal with heavy metals transport and pollutant transport in soil by using mathematical and stochastic modeling. We first introduce the underlying physical concept, and then translate the concept into a mathematical model.

Moreover, additional research is required to develop accurate and rapid measurement techniques for the necessary input parameters. To be useful in real environmental problems, modeling concepts should be coupled in one overall mathematical framework. This work will be primarily devoted to various issues related to the modeling of heavy metals transport in soil.

With respect to the stochastic approach, special emphasis is given to the characterization of spatial variability and the prediction of effective parameters. As heterogeneity increases, modeling approaches evolve from a purely deterministic description to a stochastic analysis.

References:

1. Allaby, M. 1998. A Dictionary of Plant Sciences. Oxford University Press.
2. Barber, S.A. 1984. Soil Nutrient Bioavailability. A Mechanistic Approach. A Wiley-Interscience Publication, New York.
3. Ritter, W.F., Scarborough, R.W., and Chimside, A.E.M. 1991. Nitrate leaching under irrigation on coastal plain soils. Journal of Irrigation and Drain Energy. 6: 116.
4. Kross, B.C., Hallberg G.R., Bruner, D.R., Cherry holmes, K., and Johnson, J.K. 1993. The nitrate contamination of private well water in Iowa. American Journal of Public Health. 83: 270-272.
5. Carefoot, J.P., and Whalen, J.K. 2003. Phosphorus concentrations in subsurface water as influenced by crop-ping systems and fertilizer sources. Canadian Journal of Soil Science. 83: 203-212.
6. Jonge, de W.L. P., Rubaek, G., Hschede, K., and Djurhuus, J. 2004. Particle Leaching and Particle–Facilitated Transport of Phosphorous at Field Scale. Soil Science Society of America Journal. 3: 462-470.
7. Willfried, W., Manfred, T., and Uwe, P. 2006. Prediction of the P leaching potential of arable soils in areas with high livestock densities. Journal of Zhejiang University Science. B 7: 515-520.
8. Oster, J.D., Willardson, L.S., and Hoffman, G.J. 1972. Transactions of American Society of Agriculture Engineers. 15: 115
9. Verma, S.K., and Gupta, R.K. 1989. Leaching behaviour of saline clay soil under two modes of water application. Journal of the Indian Society of Soil Science. 37: 803-808.
10. Ernani, P.R., Fingueiredo, O.R.A., Becegato, and V. Aloneido, J.A. 1996. Decrease of phosphorus retention in soil with increasing pH. Journal of Soil Science. 20: 159-162.
11. Dube, A., Kowalkowski, T., Zbytniewski, R., Ko-Sobucki P., Cukrowska, E, and Buszewski, B. 2000. Proceedings of the XVth International Symposium on Physico-chemical Methods of the

Mixtures Separation - ArsSeparatoria' 2000, June 14 - 17, 2000, Borowno n. By dgoszcz. pp.21.

12. Hulanicki, A. 2000. Chromatografia i innetechnikiseparacyjne u progu XXI wieku, B. Buszewski (red. nauk.), SAR Pomorze, Bydgoszcz. pp. 19.
13. Kot, A., Namiesnik, J. 2000. Trends in Analytical Chemistry. 19: 69.
14. Weber, J.B. 1991. Applied Plant Science. 5: 1.
15. Shulten, H.R. 2000. Biol. Fertil. Soils. 20: 399.
16. Batu, V. 2006. Applied Flow and Solute Transport Modeling in Aquifers. CRC Press, Taylor & Francis Group.
17. Sharma, H.D., and Reddy, K.R. 2004. Geo-environmental Engineering. John Willy & sons INC.
18. Aral, M.M. 1990. Groundwater Modeling in Multilayer Aquifers: Steady flow. LEWIS Publishers.
19. Ligette, J.A. 1987. "Advances in the boundary integral equation method in subsurface flow." Water Resources Bull. 23(4): 637-651.
20. Ligette, J.A., and Liu, P.L.F. 1983. The Boundary Integral Equation Method for porous Media Flow. Allen and Unwin. 255p.
21. Strack, O.D.L. 1987. "The analytic element method for regional groundwater modeling in: Solving ground water problems with models." National Water Well Assoc., Columbus, Ohio. 929-941.
22. Strack, O.D.L. 1988. Groundwater Mechanics. Prentice-Hall, Enlgewood Cliffs, N. J. 732 p.
23. Anderson, M.P., and Woessner, W.W. 2002. Applied Groundwater Modeling: Simulation of Flow and Advective Transport. Academic Press, Elsevier.
24. Richards, L. 1954. Diagnosis and Improvement of Saline and Alkali Soils. USDA Hand- book No.60, Washington.
25. Hillel, D. 1998. Environmental Soil Physics. Academic Press, London
26. Schleiff, U. 2008. Analysis of water supply of plants under saline soil conditions and conclusions for research on crop salt tolerance. J. Agron. Crop Science. 194(1): 1–8.

Chapter 2

Review of Literature

Environmental pollution is creating an increased load on resources of our environment, especially on soil and air. Heavy metals polluted soil is present around industrial areas, metropolises and also near transportation roads. Soils have capacity to assimilate heavy metals for many years without the observable signs of their severe toxic results. However, the purifying/filtering capability of soils is limited and soils are no more competent to take these elements after a certain level; and the soil itself become sources of pollution. These toxic substances are incorporated into water and absorbed by plants and crops; and finally they enter into the food-web to cause long-term harmful effect.

According to L. Fodor and L. Szabó [1], the interaction of soil and heavy metals varies in diverse conditions. For example- conversion and immobilisation rate of toxicants in soils changes according to elements. A clear differentiation of pollutants elements can be easily established between mobile pollutants in soils (Pb, Cd, Cu, Zn) and the elements which rapidly transform into bonded insoluble forms (As, Hg, Cr). Secondly, other pollutants and heavy metals that are present over soils assimilate in the cultivated soil horizons where root mass is dense. Cu, Cd, Pb, Zn and Hg are present as bonded form in the cultured horizons, whereas deeper horizon (30-60 cm) is moderately polluted. Ultimately, leaching of heavy metal is also responsible for acidic soil. Subterranean water sources are also jeopardized by these elements as a consequence of rapid leaching.

2.1 HEAVY METAL POLLUTED SOILS

Heavy metals display metallic properties such as malleability, ductility, conductivity, ligand specificity and cationic stability. These elements are categorized by their high density and relatively high atomic weight [2]. Few heavy metals (Fe, Co, Cu, Mn, Ni, V, Zn and Mo) are required in very small amount by organisms and high concentration of these elements are harmful to organisms. Heavy metals for example Hg, Pb, As and Cd do not contain any beneficial effect and considered as the “main threats” because they are very injurious to both animals and plants. Metals can occur either as combined form or as separate entity. These forms can consist of exchangeable ions which are absorbed on the exterior of non-exchangeable ions, inorganic solids and insoluble

inorganic metal compounds (phosphate and carbonate), free metal ions in the soil solution or soluble metal compound, metals attached to silicate minerals and metal complex of organic materials [3].

Metals attached to silicate minerals signifies the conditions of metal accumulation in soil and they are not responsible for pollution/contamination issues as compared to metals that occur as distinct entity or those which exist in elevated concentration in soil [4]. Soil property mainly influences metal concentration in different ways. The soil pH is the main factor which affects metal availability in soil [5]. Wang *et al.* [6] reported decrement of Zn and Cd concentration in the roots of *Thlaspi caerulescens* with augmentation of soil pH. Organic matter and hydrated Fe_2O_3 also resulted in low heavy metal accessibility through immobilization of these metals [7]. Important positive relationship has also been established between heavy metals and physical properties of soil such as water retaining capacity and moisture content [8].

Other aspects that influence the metal accessibility in soil comprises- density and nature of charge in soil particle, relative soil surface area and extent of complex formation with ligands [3]. The great interface and particular surface areas presented by soil colloids assist in controlling the amount of heavy metal deposition in soils. In addition, soluble metals in polluted soils may be lowered by soil particles which have more specific surface area, although it may be metal specific [3]. It was reported that accumulation of alteration consisting of hydroxides (OH^-) with more reactive surface region lowered the solubility of Cd, As, Pb, Cu and Mo, while the solubility of Zn and Ni did not change [9]. Microbial activity, mineral composition and soil aeration also influenced heavy metal concentration in soils [10].

Conversely, heavy metals can also modify soil characteristics related to soil biological properties [11], indicating alteration in soil biochemical and microbiological properties after pollution can be used to assess the intensity of soil contamination. Moreover, these methods are more accurate and results can be analyzed at a faster rate as compared to examining soil's physical and chemical characteristics [12]. Heavy metals are also known to influence the diversity, number and behaviour of soil micro-organisms. The toxic behaviour of these

heavy metals on microbes depends on a number of variables for example- soil pH, temperature, organic matter, clay minerals, inorganic ions and type of the metal [11].

There are discrepancies in studies comparing the effect of heavy metals on soil biological properties. While some researchers have recorded negative effect of heavy metals on soil biological properties [11-13], others have reported no relationship between high heavy metal concentrations and some soil (micro) biological properties [14]. Some of the inconsistencies may arise because some of these studies were conducted under laboratory conditions using artificially contaminated soils while others were carried out using soils from areas that are actually polluted in the field.

2.2 BRIEF OVERVIEW OF HEAVY METALS

Heavy metal term is used for those metals and metalloids which are related to contamination. Their atomic density is more than 6 g/cm^3 [15-17] for example- Lead, Copper, Zinc, mercury, zinc, nickel, chromium, arsenic, silver, tin and cadmium. Trace heavy metals are those metals which are found relatively low natural concentrations in sediments, soils, water and organisms. Usually, heavy metals exist in cationic forms, though some may exist as oxy-anions for example, arsenate (AsO_4^{3-}) [17]. However, some heavy metals such as Zn and Cd are weakly adsorbed to sediments and soils, and other heavy metal such as Cu and Pb adsorb strongly and are discharged into solution slowly under favourable condition only. Moreover, they are not biodegradable and most of them possess toxic, carcinogenic and mutagenic properties. As a result, heavy metal tend to assimilate in sediments and pose a high risk to the atmosphere mainly when they meet conditions that enhance their solubility and concentration in soils, water, sediments and organisms above their permissible limits [18-22].

The accumulation of heavy metals to the atmosphere has escalated enormously after industrialization. The release of deleterious heavy metal has occurred through various pathways such as water, air and soil. Emanation through air is of huge concern because high concentration is involved, the pervasive spreading and its potential for immense human exposure [23].

Heavy metals could be present in amorphous materials; sorbed on clay; precipitated as oxides or sulphides; or complexed with organic matter (OM) [24].

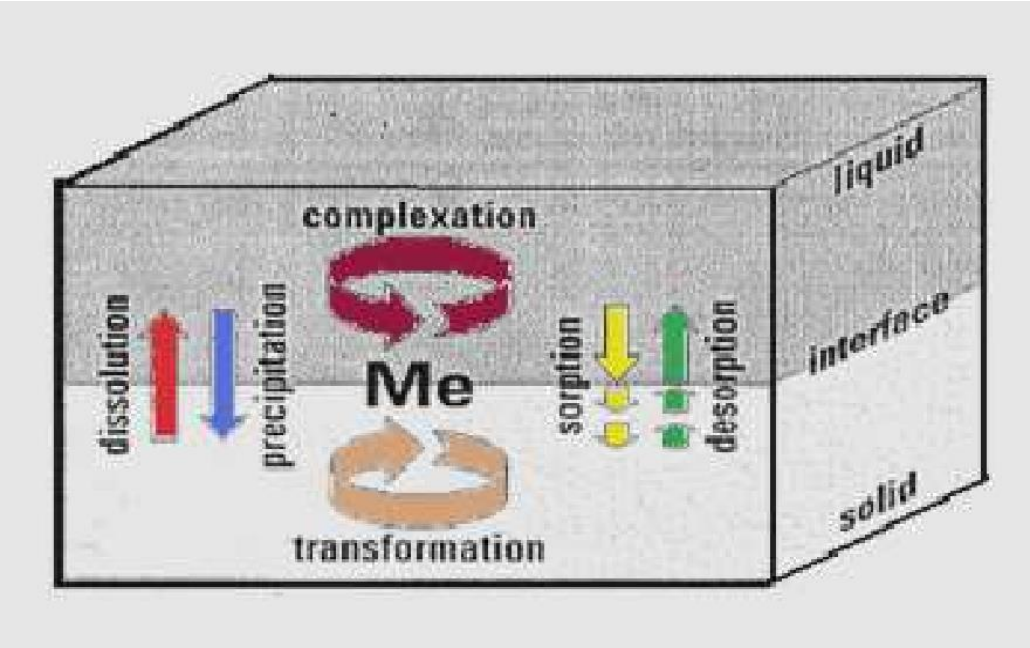

Figure 1: Schematic representation of the various processes of heavy metals undergo in sediments (Adapted and modified from Ziegler) [25]

2.3 HEAVY METAL CONTAIMINATION SOURCES

Heavy metals contamination of soil can occur in various ways. On the basis of source, they are divided into two main categories- natural and anthropogenic sources. Anthropogenic activities contribute excess heavy metals to the environment as compared to the natural inputs.

Natural sources-

Naturally, heavy metals pollution occurs during weathering of rocks. Weathering of rocks results due to hydration and hydrolysis reactions; loss of mineral components via leaching and volatilization; dissolution and dissociation of minerals; oxidation and reduction reaction; immobilization by precipitation; and chemical exchange processes such as cation exchange. Heavy metals are present naturally in rocks as constituents. During natural geological weathering, heavy metals can discharge into the surroundings and it is often called as background concentrations. Background concentrations are not essentially a warning to the atmosphere but it is considered as a threat only when their concentration increases above the acceptable value in the environment. They can

provide as point source contamination or they may be carried out to different places by surface erosion or runoff and results in diffused pollution [17].

Anthropogenic resource-

Now a day, there is no dispute in many scientific arguments that anthropogenic action is the major source for the observed elevation of heavy metal concentration worldwide. Major anthropogenic resources of heavy metals are- sewage sludge, leaching from building materials, addition of fertilizers both of organic and inorganic origins, industrial disposal and discharges, and atmospheric consequences. Heavy metals discharge by anthropogenic action is generally unsteady and highly soluble, and easily accessible as compared to their natural forms [15, 17, 26, 27]. Anthropogenic discharge of heavy metals in the atmosphere escalated significantly in the 19^{th}century. This resulted in increased universal concern for the implementation of method that would decrease their concentrations in the environment. With the execution of environmental rules and advancement in technology, there has been considerable reduction in the discharge of heavy metals to the surroundings [17].

2.4 LEACHING

Leaching is defined as the removal of materials from solids via dissolving away by "the action of a percolating liquid." [28]. Perry's Chemical Engineers' Handbook [29] defines leaching as "the removal of a soluble fraction, in the form of a solution, from an insoluble, permeable solid phase with which it is associated." In this work we employ the definition given in the Chemical Engineers Handbook.

While technologies have been developed to counter flow regime impact on mobilizing solidified contaminants [30-32], restraining leaching in acidic environments, usually created by acid forming bacteria, continues to be a challenge [33].

2.5 FACTORS AFFECTING HEAVY METALS LEACHING

The principal geochemical parameters that govern the mechanisms of heavy metals leaching/immobilization in sediments include redox potential, pH and the presence of complexing agents. These parameters affect the chemical forms of the metals. Although several studies have shown the effects of pH to be enormous in immobilization of heavy metals [34], the effects of the other factors cannot be overemphasised.

Influence of pH on charge development-

Surface chemistry of minerals greatly affects the solubility and hence the mobility of contaminants in the environment in that, reactions between solutions and solids often involve the interface between these phases. Hydroxyl groups as a result of the interaction of sediments with and the subsequent dissociation of water molecules usually occupy the surfaces of sediments and soils in water. At high or low pH, negative or positive charges, respectively, can be developed on the mineral surfaces. This dictates the type of ionic compounds that can be sorbed onto mineral surfaces. Generally, the surfaces of C-S-H in basic solutions are deprotonated. This potentially attracts positively charged metals in solution, thereby affecting their mobility. Thus, adsorption of cationic metals is greatly enhanced in basic media.

$$S - OH + OH^- \rightleftharpoons S - O^- + H_2O$$

On the other hand, lowering the pH would lead to the development of positive charges on the surfaces of the minerals. This favours the adoption of negatively charged metals or compounds. This explains why most cationic heavy metals are found in acidic solutions.

$$S - OH \; + \; H^+ \rightleftharpoons S - OH_2^+$$

The pH value where surface charge becomes zero, is called as point of zero charge (ZPC). Different materials have different ZPCs. Anion adsorption increases with decreasing pH whereas cation adsorption increases with increasing pH. As the pH increases, the percentage of cationic heavy metals bound to the surface increases and for anionic metals, their percentage adsorption increases with decreasing pH.

Effect of pH on leaching of heavy metals-

As stated above, pH plays an enormous role in mineral surface charge development which in turn, controls the adsorption of charged species. The dissolution and portability of heavy metals in sediments and soil can further more influenced by pH. Metals in solution usually exist in hydrated forms due to their interaction by water molecules.

$$M(H_2O)^{+n} \; + \; H_2O \rightleftharpoons M(H_2O)OH^{+(n-1)} \; + \; H_3O^+$$

$$M(H_2O)^{+n} \; + \; H_2O \rightleftharpoons M(OH)_n(S) \; + \; nH_3O^+$$

It follows from the equilibrium reactions above that adding more acid, H_3O^+ shifts the reaction to the left producing more dissolved species. On the other hand, if the pH is increased by increasing the OH^-concentrations, the reaction shifts to the right precipitating more insoluble metal hydroxides. Increasing the pH further will result in the metal hydroxide forming complexes with OH with negative charges. This negatively charged poly hydroxide metal can, however, be engaged in a strong interaction with water molecules which eventually can result in their dissolution.

$$Cu(OH)_2(S) + \; OH^- \rightleftharpoons Cu(OH)_3^-$$

In cement stabilized sediments, the pH of fluid that fills the pore structures is usually alkaline in nature. This aids in the precipitation of insoluble species, particularly metal hydroxides. It is therefore imperative for the pore fluid to be maintained at high pH to ensure long term retention of contaminants. This, however, is independent of the amount of hydrated phases in the cement which have the potential of raising the pH but rather, by keeping the quasi-equilibrium between solid and aqueous phases constant [35]. However, studies have shown that over time, the equilibrium between the solid and the liquid phases can be disrupted due to changes in the conditions of the waste form. In some cases, however, high pH favours the mobility of certain cations.

The two metals under investigation Pb and Cu are referred to as amphoteric metals i.e. their hydroxide forms can dissolve when the solution pH is very low or high [36-38]. The pH at which metals begin to dissolve defers for

each metal. For instance, Cu begins to solubilise again from pH 9 and above whereas that of Pb begins from 9.4 and above. The influence of pH on discharge of heavy metals for the different sediments was investigated by NGI.

2.6 INTERNATIONAL AND NATIONAL STATUS OF WORK DONE

Mathematical models are used to resolve hydrological efforts and some models are categorized into 4 main groups. It is advised that models with limitation calculated by computing the smallest of a least squares objective function signifies an application of famous non-linear regression theory to conditions in which the supposition normally made in this theory are rarely applicable. The correction necessarily is not the use of objective functions other than those based on sums of squares, but the application of additional realistic statement relating the stochastic structure of the model residuals. Numerous denotations are specified to the term "model" in the hydrological. Acclimatizing a additional general description given by Dooge [39], a hydrological system is described as a set of chemical, physical and/or biological processes depending upon an input variable or variables to change it (them) into an output variable or variables (A variable is unstated to be a attribute of a system which may be calculated and which presume a dissimilar numerical values when calculated at altered times, the terms variable and variate being synonymous; a parameter is a quantity describing a hydrological system, which remains constant in time). A model is a simplified depiction of a complex system, hydrological models (that is, models of hydrological systems) being either: (a) analog, such as the resistance-capacitance analog of a coastal aquifer used by Hunter Blair [40] and of a complete catchment used by Ishihara and Ishihara [41], (b) physical, such as a scaled-down facsimile of the full-scale prototype [42-43].

Various factors can results in non-ideal solute transport, together with non-homogeneous soil physical property (e.g., soil-water content, hydraulic conductivity, bulk density), non-homogeneous soil chemical properties (e.g., sorption equilibrium constant), physical non-equilibrium, sorption non-equilibrium, sorption isotherm non-linearity and sorption-desorption non-singularity. Factors associated to the physical nature of the porous medium, such

as structure (i.e., non-homogeneous soil physical non-equilibrium and physical properties), will apparently manage non-ideality for transfer of non-sorbing solutes. It is advised that the main factors which cause non-ideal transfer of organic solutes are non-homogenous soil characteristics (both chemical and physical) and non-equilibrium (both sorption and transport) [44-45].

The literature is complete with information on effect of soil structure on solute migration. These reports are more than 100 years old [46-47], as reported by White [48]. The description for obtained non-ideal behaviour (e.g., "macropore flow", "preferential flow", "changeling", "bypassing", "short-circuiting", "subsurface storm flow", "partial displacement") is the result of non-unimodal pore-size distributions (i.e., a non-uniform velocity field) is usually approved. For such systems, a continuum approach [44] is frequently used. In this approach, the porous medium is considered to be made up of two domains: an "immobile" domain, in which least advective flow is present and a "mobile" domain, where solute migrate by dispersion and advection. The mobile-immobile conceptualization for soils dates back at least 30 years, when it was used by Gardner and Brooks [49]. Early mathematical models utilizing this conceptualization were assessed by Skopp and Warrick [50] and by Van Genuchten *et al*. [51]. Fast transport in the mobile domain is escorted by diffusive mass transfer of solutes between the mobile and immobile domains, which cause latter behaving as sink/source components. Solute transport, as depicted by breakthrough curves (BTC's), in such systems is categorized by early initial breakthrough and by "tailing" or delayed approach to relative concentration values of either 0 or 1. Because access to some portion of the porous medium is controlled by diffusive mass transfer, solute in the system may be present in a state of non-equilibrium. This incident has been named as physical or transport non-equilibrium (TNE). It was suggest that "dead water" can result in non-ideal BTC's [52]. Behavior attributable to TNE has been seen in aggregated, heterogeneous (with relation to hydraulic conductivity) and fractured porous media as well as in macroporous media. Some of the initial work on solute transport in aggregated soils, where the non-ideality detected in experimentally-derived BTC's was attributed to TNE, was performed for non-sorbing solutes

($C1^-$) and for sorbing inorganic solutes (Mg^{2+}) [53], and for organic compounds (pesticides) [54-57].

All the experiments were performed with packed soil columns and demonstrated the effect of soil aggregation on solute migration; they are not main representative of field conditions. In an effort to further strongly initiate field conditions, miscible displacement studies have been carried out by using uninterrupted soil core. Early experiments of this nature demonstrating non-ideal solute transport of Clorine, which was attributed to macro pore flow, were reported by Elrick and French [54]. Numerous studies of a similar nature have since been reported for C1- and for other non-sorbing solutes [48, 58]. Numerous field investigation of solute transport in controlled situation, where detected non-ideality was contributed to TNE, has been carried out for inorganics [59]. An early investigation of TNE in field-scale transport of an organic solute (herbicide picloram) was carried out by Rao *et al*. [60].

The bicontinuum model can relate to heterogeneous porous media, such as aquifers made up of laminae containing different hydraulic conductivities (K). In this event, the low-K layer corresponds to the "immobile zone" and the high-K layer to the "mobile zone". Solute dispersal is influenced by mass transport among the low and high K layers. This solute advection is more in the high-K than in the low-K layers. Differential solute-front progression happens in the diverse layers, which produce inter-layer concentration incline. Consequently, inter-layer diffusive solute transport arises and results in TNE. A diffusion-based model was given by [61-62] to acquire data from a natural-gradient field experimentation. Movement in fractured media can also be modelled with a bicontinuum approach. These fractures provide as zones of better transport, with the inter-fracture matrix acting as a diffusional source.

Various mechanisms are implicated in the solute-transfer phenomenon for a system of the immobile-mobile concept: (1) diffusive transport across the adsorbed water (i.e., film diffusion); (2) advective-dispersive transfer from bulk solution to boundary layer (i.e., adsorbed water surrounding the sorbent); and (3) pore and surface diffusion within the immobile region (i.e., intra-aggregate diffusion). Some or all of these three components may be a rate-limiting step. It is

frequently thought that one of the three steps is slow compared to the other two and that it may be designated as the primary rate-limiting step. The advective-flow domain is usually alleged to be well-mixed, therefore reducing the significance of mass-transfer resistances within these regions.

The amount of deadly trace metals in the soil sample obtained from Jaipur, India, has been measured by Omprakash *et al.* [63]. Concentrations of lead, nickel, cadmium and zinc were determined by using DC polar grams in soil sample. The heavy elements concentrations in digested soil samples were as follows: Pb about 7.70 ppm, Ni 2.41 ppm, Cd 7.35 ppm and Zn 2.68 ppm.

A study was carried out at a wastewater irrigated site, Mansarovar in Jaipur city of Rajasthan, India to estimate the accumulation of heavy metals (Cd, Pb, Zn and Ni) in soil during the pre monsoon and post monsoon period [64]. Their study revealed accumulation of Cd above the safe limits whereas Zn, Ni and Pb were found under permissible limits. Concentration of metals was found to be elevated throughout pre monsoon period in comparison to post monsoon period. The concentrations of all the metals found in the study are high enough to accumulate in the crops grown on this soil.

Manju *et al.* [65] examined seasonal variations in average concentrations of metals in free fall dust samples collected from 5 diverse zones of Kota industrial area, Rajasthan, India. The amount of heavy metals (Zn, Cu, Pb and Cd) was elevated in winter and less in summer and reverse behaviour was detected for crustal metals (Fe, Mg and Ca). In general, the sequence of mean amount of heavy metals were Zn > Pb > Cu > Cd in both seasons. Seasonal dissimilarity in metal concentrations was due to variation in wind strength, wind direction, relative humidity temperature and anthropogenic activities at sampling sites.

2.7 MATHEMATICAL MODELING OF HEAVY METAL LEACHING

A number of mathematical models explaining mechanical and/or physiochemical leaching of heavy metals from non-stabilized and/or stabilized forms are available in literature. Bishop [66] studied the long term effect of heavy metals leaching from solidified/stabilized matrices. Using diffusion based model shown below, we simulated a series of up-flow column leaching tests.

$$\left(\frac{\sum a_n}{A_0}\right)\left(\frac{V}{S}\right) = 2\left(\frac{D_e}{\pi}\right)^{1/2} t_n^{1/2} \quad (1)$$

Where:

a_n =Contaminant loss during nth leaching period (mg)

A_0 =Initial amount of contaminant present in the specimen (mg)

V =Volume of specimen (cm^3)

S =Surface area of specimen (cm^2)

t_n =Time to end of nth leaching period (sec)

D_e= effective diffusion coefficient (cm^2/sec)

For a linear leaching rate over the leaching period, Bishop [66] suggested the following equations to decide the effective diffusion coefficientD_e:

$$D_e = \pi\left(\frac{a_n}{A_0}\right)^2\left(\frac{V}{S}\right)^2\left(\frac{1}{\Delta t}\right)^2\left(t_n - \frac{\Delta t_n}{2}\right) \quad (2)$$

Where

Δt_n =duration of nth leaching period (sec)

$\left(t_n - \frac{\Delta t_n}{2}\right)$ = elapsed time at the middle of leachant nth renewal period (sec) and the leachability index, LX:

$$LX = \frac{1}{7}\sum_{n=1}^{7} log\left(\frac{1}{D_e}\right) \quad (3)$$

The leachability index was applied to evaluate the relative mobility of different contaminants on a 'uniform scale that differes from 5 (D_e = 10^{-5}cm^2/s, very mobile) to 15 (D_e = 10^{-15}, immobile)'. Simulation results indicated that the diffusion coefficients did not stay constant and changed with time as the speciation of the metals changed to more soluble forms. Other important factors affecting the leaching rate included: particle size (surface-to-volume-ratio in particular) leachant velocity and acidity.

Cheng and Bishop [67] have argued that leaching mechanism in the pozzolanic-based solid matrices is regulated by the free H^+ accessible in the leachate.

Measuring alkalinity of leachate, they suggest that H^+ ions penetrate inside the solid matrix and reduce the effect the alkalinity generated by the binder in the leach facade. As the pH drops due to H^+ penetration, the metals precipitated at high pH environment dissolve and diffuse away into the leachate. Considering untimely phases of leaching, an 'unsteady diffusion with fast chemical reaction', authors developed a kinetic leaching model to be used for prediction of the acid diffusion in the pozzolanic-based paste. Diffusion from a solid with constant surface concentration in a semi-infinite medium having initial zero concentration, was shown to be proportional to the square root of time [68] and involves a single dimensionless parameter: $z/\sqrt{4D_e t}$, where z is penetration distance and D_e the effective diffusion coefficient. The concentration of diffusing substance $C(z,t)$ and the flux of diffusion $J(z,t)$are given by:

$$C(z,t) = C_0(1 - \text{erf}(z/\sqrt{4D_e t})) \tag{4}$$

$$J(z,t) = C_0(\sqrt{D_e/\pi t})exp(-z^2/4D_e t) \tag{5}$$

The mass balance of H^+ in a small shell within the solid can be written as: Hydrogen ion H^+ diffusion in amount H^+ produced accretion out by chemical reactions

$$\begin{pmatrix} Hydrogenion \\ accumulation \end{pmatrix} = \begin{pmatrix} H^+ \ diffusion \ in \\ -out \end{pmatrix} + \begin{pmatrix} amount \ H^+ \ produced \\ by \ chemical \ reactions \end{pmatrix} \tag{6}$$

In differential form:

$$\frac{\partial C_H}{\partial t} = \frac{\partial}{\partial z}\left(D_e \frac{\partial C_H}{\partial z}\right) - \frac{\partial \theta f(C_H)}{\partial t} \tag{7}$$

Where θ is the density of the sample with mass/volume unit and $f(C_H)$is acid neutralization capacity (ANC). Assuming constantD_e and θ, with $f(C_H) = KC_H$, and using the boundary conditions:

$$C_H(z,0) \approx 0 \quad \forall\, z$$

$$C_H(0,t) \approx C_0 \text{for } t > 0$$

$$C_H(z,t) \approx 0 \quad for\ z = \infty \tag{8}$$

The solution was given as:

$$C_H(z,t) = C_0(1 - \text{erf}(z\sqrt{(1+\theta K)}/\sqrt{4D_e t})) \tag{9}$$

$$J(z,t) = C_0(\sqrt{D_e(1+\theta K)/\pi t})exp(-z^2(1+\theta K)/4D_e t) \tag{10}$$

Equation (9) was used to find the H^+ concentration at any given distance and given time.

Batchelor [69] developed a 'numerical leaching' model which considered interactions between calcium (as a measure of the alkalinity of the treated waste), hydrogen ion, lead (as the contaminant that can precipitate as hydroxide) and acetate (as a measure of acidity of the leaching solution). The model was applied to a rectangular solid of finite thickness containing contaminant, held in an acidic bath of finite volume.

The diffusion path for the molecules through the solid was assumed on the order of half of the pore radius and that for the molecules in the liquid was taken on the order of half of the pore length. The model assumed presence of two solids ($Ca(OH)_2$, $Pb(OH)_2$), six soluble species (Ca^{2+}, H^+, Ac^-, Pb^{2+}, OH^-, HAc) and reactions between them (providing the equilibrium constant for each reaction) Equation (11-14):

$$H_2O \leftrightarrow H^+ + OH^- \qquad Log\ K_w = -14.0 \tag{11}$$

$$H^+ + Ac^- \leftrightarrow HAc \qquad Log\ K_{HAc} = 4.76 \tag{12}$$

$$Ca^{2+} + 2H_2O \leftrightarrow Ca(OH)_2 + 2H^+ \qquad Log\ K_{Ca(OH)_2} = -22.675 \tag{13}$$

$$Pb^{2+} + 2H_2O \leftrightarrow Pb(OH)_2 + 2H^+ \qquad Log\ K_{Pb(OH)_2} = -8.15 \tag{14}$$

Writing a material balances relating the total concentration of each species per unit volume (T_{ss}) to the concentration of contaminant in mobile phase and assuming the Fickian diffusion with local chemical equilibrium, resulted in Equation (15).

$$\frac{\partial T_{ss}}{\partial t} = D_e \frac{\partial^2 C_m}{\partial X^2} \quad (15)$$

To simplify solving this equation, Batchelor [69] defined the concentration in mobile phase in terms of total concentration of each species using a factor G, representing mobile fraction of the species.

$$\frac{\partial T_{ss}}{\partial t} = D_e \frac{\partial^2 (G T_{ss})}{\partial X^2} \quad (16)$$

A modified Crank-Nicholson algorithm was employed to solve the dimensionless form of Equation (16) numerically. The model predictions agreed with those obtained analytically for infinite bath conditions.

Hinsenvel and Bishop [70] used Fick's bulk diffusion model to determine contaminant leaching out of solid form:

$$\frac{\partial C}{\partial t} = D_e \frac{(\partial^2 C)}{(\partial x^2)} \quad (17)$$

Where:

D_e =Effective diffusion coefficient, corrected for porosity and tortuosity (cm^2s^{-1})

C =Concentration of the contaminant (g cm^{-3})

t =Time (sec)

x =Distance (cm).

Equation (17) was solved for contaminant concentration profile in a specimen as a function of dimensionless time, which can be used to determine leaching rate:

$$C(x,t) = 3C_0 erf\left[\frac{x}{4D_e t}\right] \quad (18)$$

where:

C_0 =initial contaminant concentration in the solid

erf =standard error function

x =distance into the solid

t =leaching time.

Baker and Bishop [71], based on research that showed leaching of contaminants is a result of the dissolution of the outer shell of the waste form which then results in a solubilisation and release of contaminants from the leached shell, modelled contaminants release using shrinking unreacted core (SUC). They used acid exposure, rather than time, as the key variable in evaluating leaching behavior. Acid exposure is defined as 'the amount of acid a specimen is exposed to under acidic conditions' which is equivalent to the acid concentration X time/volume. To compensate for the change in acid concentration over time, the authors define the exposure integral, $I(t)$, as:

$$I(t) = \int_0^t \overline{C_r}\, dt \tag{19}$$

Where

$\overline{C_r}$ is the average acid concentration.

For flat specimens, this is simply the acid penetration depth (APD) and for cylindrical or spherical shape specimens, conversion is a dimensionless number relating the original specimen radius to the core radius. Under the leached shell diffusion limitation, the conversion, as measured by acid penetration depth (cm), has been shown to follow the relationship:

$$\zeta = \sqrt{\frac{2D_{e,S}(C_{H,i}-C_{H,c})}{\beta_c}\, t} \tag{20}$$

where:

$D_{e,s}$ = Effective diffusion coefficient (for acid species)(cm^2s^{-1})

$C_{H,i}$ = Hydrogen ion concentration at the liquid interface (kmole m^{-3})

$C_{H,c}$ =Hydrogen ion concentration at the liquid core boundary (kmole m^{-3})

β_c =Acid neutralization capacity (ANC), the quantitative capacity of cement to react with a strong acid to a pre-determined pH, (k mole eq m^{-3})

Assuming the H^+ concentration at the leaching front is much less than that in the bulk liquid, the exposure integral , Equation (19), can be substituted into Equation (20) to give:

$$\zeta = \sqrt{\frac{2D_{e,s}I(t)}{\beta_c}} \quad (21)$$

The authors corroborate validity of their formulation studying 'the behavior of real-world' solidified wastes.

Halim *et al*. [72] simulated the leaching of Pb, Cd, As, and Cr from cementitious wastes. Four different matrices were examined namely calcite, portlandite, calcium-silicate-hydrate (C-S-H) matrix, and the free metal compounds. The model used the following equation to describe the dissolution rates of these

$$\frac{dM}{dt} = 50x10^4 k_{system} A(c_1 a_{H^+} + c_2 a_{H_2CO_3} + c_3 a_{OH^-} - c_4 a_{Ca^{2+}} a_{CO_3^{2-}} + C_5) \quad (22)$$

Where:

$\frac{dM}{dt}$ =Dissolution rate of each matrix

k_{system} = Constant

A = Surface area of the matrix (in $m^2 g^{-1}$of waste)

$a_{H^+}, a_{H_2CO_3}, a_{OH^-}, a_{Ca^{2+}}, a_{CO_3^{2-}}$ = activities of $H^+, H_2CO_3, OH^-, Ca^{2+}$, and$CO_3^{2-}$

By using both kinetic terms and equilibrium thermodynamics of key compounds, the model provided information on leachate and precipitate speciation. The model predicted leaching of Pb, Cd, As, and Cr from cement and indicated that Pb and As were predominantly incorporated within the calcium-silicate-hydrate matrix while a greater portion of Cd was seen to exist as discrete particles in the cement pores and Cr (VI) existed mostly as free CrO_4^{2-}ions. Schiopu *et al*. [73] used PHREEQC united with the Lawrence Livermore National Laboratory (LLNL) thermodynamic data base, to model and simulate leaching from concrete under

outdoor exposure conditions. The model was tested using experimental data. Assuming that in a porous monolith like the concrete slabs, diffusion is the main transport mechanism in the solid, for each chemical element α of concentrationC_α^{Pores} in the pores water, the mass balance equation is:

$$\frac{\partial C_\alpha^{Pores}}{\partial t} = D_e \frac{\partial^2 C_\alpha^{Pores}}{\partial z^2} - \sum_{n=1}^{N} \frac{\partial S_{\alpha,n}^{Pores}}{\partial t} \tag{23}$$

$$\begin{cases} if\ S_{\alpha,n}^{Pores} \geq 0\ and\ C_\alpha^{Pores} > C_\alpha^{sat-Pores}\ then\ \frac{\partial S_{\alpha,n}^{Pores}}{\partial t} = R_{\alpha,n} \\ else: \frac{\partial S_{\alpha,n}^{Pores}}{\partial t} = 0 \end{cases} \tag{24}$$

where

$S_{\alpha,n}^{Pores}$ is the concentration in the pore water of the element α in a solid phase n,

$C_\alpha^{sat-Pores}$ is the saturation concentration in pore water, and D_e is the effective diffusioncoefficient. Equation (23) is solved subject to boundary conditions:

$$\left.\frac{\partial C_\alpha^{Pores}}{\partial t}\right|_{z=0} = 0 \tag{25}$$

at the bottom face, $z = 0$and:

$$D_e \left.\frac{\partial C_\alpha^{interface}}{\partial t}\right|_{z=h} = k_{SL}\left(C_\alpha^{leachate} - C_\alpha^{interface}\right) \tag{26}$$

at monolith/leachate interface, $z = h$.

For demonstrating the role of soil in ecosystems, various models of diverse heavy metals transportation and sorption in this matrix have given. The most famous sorption models are categorized into two main groups:

a) Models, which do not comprise this interaction
b) Models, which takes description of bonding and electrostatic forces.

In classical models remained to second group sorption process was depicted by Langmuirs isotherm:

$$S_i = \frac{b.K.C}{1+K.C} \tag{27}$$

Where :

S_i =Concentration of sorbent in solid state;

C =Concentration of solution in equilibrium;

K =Equiibrium constatnt;

b =Capacity of monolyers;

Or

Freundlich isotherm:

$$S_i = K.C^{1/n} \quad (28)$$

Where n is constant.

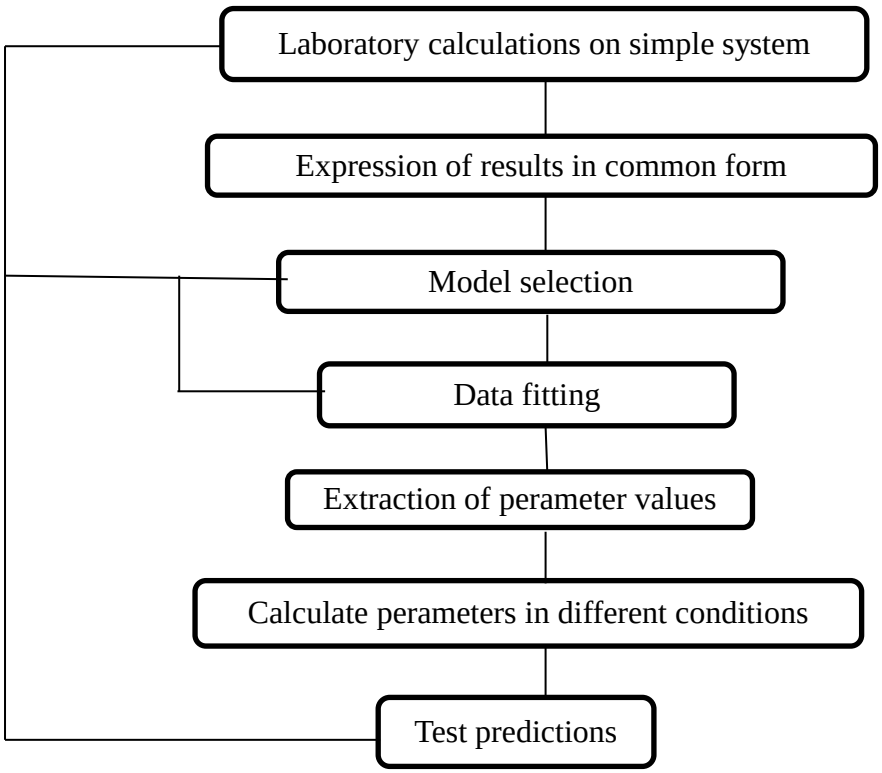

The modeling cycle according to Hestenberg *et al.* [74].

References:

1. Fodor, L., and Szabó, L. 2004. Study of heavy metal leaching in the soil. 13th International Soil Conservation Organisation Conference – Brisbane. Conserving Soil and Water for Society: Sharing Solutions. Paper No. 216.
2. Raskin, P.B., Kumar, A.N., Dushenkov, S., and Salt, D.E. 1994. Bioconcentration of heavy metals by plants. Current Opinion in Biotechnology. 5(3): 285–290, 1994.
3. Marques, P.G.C., Rangel, A.O.S.S., and Castro, P.M.L. 2009. Remediation of heavy metal contaminated soils: phytoremediation as a potentially promising clean-up technology. Critical Reviews in Environmental Science and Technology. 39(8): 622–654.
4. Ramos, L., Hernandez, L.M., and Gonzalez, M.J. 1994. Sequential fractionation of copper, lead, cadmium and zinc in soils from or near Donana National Park. Journal of Environmental Quality. 23(1): 50–57.
5. Harter, R.D. 1983. Effect of soil pH on adsorption of lead, copper, zinc, and nickel. Soil Science Society of America Journal. 47(1): 47–51.
6. Wang, S., Angle, J.S., Chaney, R.L., Delorme, T.A., and Reeves, R.D. 2006. Soil pH effects on uptake of Cd and Zn by Thlaspicaerulescens. Plant and Soil. 281(1-2): 325–337.
7. Yi, L., Hong, Y., Wang, D., and Zhu, Y. 2007. Determination of free heavy metal ion concentrations in soils around a cadmium rich zinc deposit. Geochemical Journal. 41(4): 235–240.
8. Rakesh Sharma, M.S., and Raju, N.S. 2013. Correlation of heavy metal contamination with soil properties of industrial areas of Mysore, Karnataka, India by cluster analysis. International Research Journal of Environment Sciences. 2(10): 22–27.
9. Mcbride, M.B., and Mart´ınez, C.E. 2000. Copper phytotoxicity in a contaminated soil: remediation tests with adsorptive materials. Environmental Science and Technology. 34(20): 4386– 4391.
10. Magnuson, M.L., Kelty, C.A., Kelty, K.C. 2001. Trace metal loading on water-borne soil and dust particles characterized through the use of Split-flow thin-cell fractionation. Analytical Chemistry. 73(14): 3492–3496.

11. Friedlov´a, M. 2010. The influence of heavy metals on soil biological and chemical properties. Soil and Water Research. 5(1): 21–27.
12. Nannipieri, P., Badalucco, L., Landi, L., and Pietramellara, G. 1997. Measurement in assessing the risk of chemicals to the soil ecosystem in Ecotoxicology: Responses, Biomarkers and Risk Assessment. Zelikoff, J.T. Ed., pp. 507–534, OECDWorkshop, SOS Publ., Fair Haven, NY, USA.
13. ˇSmejkalova, M., Mikanova, O., and Borˇuvka, L. 2003. Effects of heavy metal concentrations on biological activity of soils micro-organisms. Plant, Soil and Environment. 49: 321–326, 2003.
14. Castaldi, S., Rutigliano, F.A., and Virzo de Santo, A. 2004. Suitability of soil microbial parameters as indicators of heavy metal pollution. Water, Air, & Soil Pollution. 158(1): 21–35.
15. Alloway, B.J. 1995. Soil Processes and the behaviour of Metals. In: Heavy Metals in Soil. Edited by: B.J. Alloway, Blackie Academic & Professional, London.
16. Wild, A. 1993. Soils and the Environment. Cambridge University Press. 189-210.
17. Van der Perk, M. 2006. Soil and water contamination from molecular to catchment scale. Taylor and Francis/ Balkema Pp 389.
18. MacCarthy, P, Klusman, R.W., Cowling, S.W. *et al*. 1991. Water analysis. Anal Chem. 63: 301–342.
19. Volesky, B. 1994. Advances in biosorption of metals: selection of biomass types. FEMS Microbiology Reviews. 14(4): 291-302.
20. Clement, R.E., Eiceman, G.A., Koester, C.J. 1995. Environmental analysis. Anal Chem. 67: 221R–225R D.W.
21. Volesky, B., & Holan, Z.R. 1995. Biosorption of heavy metals. Biotechnology progress. 11(3): 235-250.
22. Bozkurt, S., Moreno, L. and Neretnieks, I. 2000. Long term processes in waste deposits. The science of total environment. 250: 101-121.
23. Jarup, L. 2003. Hazards of Heavy Metal Contamination. Brit Med Bull. 68: 167- 182.

24. Tessier, A., Campbell, P.G., & Bisson, M. 1979. Sequential extraction procedure for the speciation of particulate trace metals. Analytical chemistry. 51(7): 844-851.
25. Ziegler, F. 2000. Heavy Metal Binding in Cement-Based Waste Materials: An Investigation of the Mechanism of Zn Sorption to Calcium Silicate Hydrate. Diss. ETH No. 13 569, ETH Ziirich, Switzerland.
26. Dudley, L.M., McLean, J.E., Furst, T.H. and Jurinak, J.J. 1991. Sorption of Cadmium and Copper from an Acid Mine Waste Extract by two Calcareous Soils: Column Study. Soil Sci. 151: 121-135.
27. Anderson, S., Rasmussen, G., Snilsberg, P., Amundsen, C.E., and Westby, T. 1996. Assessing Toxicity and Mobilization of Impregnation Salts at a Contaminated Site. Fresenius J. Anal. Chem. 354: 676-680.
28. Merriam Webster Dictionary. 2011. Retrieved April 2011 from http://www.merriam-webster.com/dictionary/leaching.
29. Perry, R.H. & Green, D.W. 1997. Perry's Chemical Engineers' Handbook. McGraw Hill, 7th Edition. pp. 18-55.
30. Fleming, E.C. & Cullinane Jr., M.J. 1992. Evaluation of solidification/stabilization for treating contaminated soils from the frontier hard chrome site. USAE Waterways Experiment Station, Environmental Laboratory Technical Report, 3909 Halls Ferry Road, Vicksburg, MS 39180-6199 EL-92-22.
31. Bobrowski, A. & Gawlicki, M. 1997. Analytical evaluation of immobilization of heavy metals in cement matrices. Environmental Science & Technology. 31: 745-749.
32. Pagilla, K.R., and Canter, L.W. 1999. Laboratory studies on remediation of chromium-contaminated soils. J. Environ. Eng. 125: 243-248.
33. Löser, C., Zehnsdorf, A., Görsch, K., & Seidel, H. 2005. Bioleaching of heavy metal polluted sediment: Kinetics of leaching and microbial sulfur oxidation. Engineering in Life Sciences. 5(6): 535-549.
34. Brown, S., Chaney, R., and. Angle, J.S. 1997. Surface Liming and Metal Movement in Soil Amended with Lime-Stabilized Bio solids. J. Environ. Qual. 26: 724-732.

35. Bone, B.D., Barnard, L.H., Boardman, D.I., Carey, P.J., Hills, C.D., Jones, H.M., MacLeod, C.L. and Tyrer, M. 2004. Review of Scientific Literature on the Use of Stabilisation/Solidification for the Treatment of Contaminated Soil, Solid Waste and Sludges. Environment Agency - United Kingdom 343 pp.
36. Conner, J.R. 1990. Chemical Fixation and Solidification of Hazardous Wastes, Van Nostrand Reinhold, NY, USA.
37. Li, X.D. 2001. Heavy metal speciation and leaching behaviours in cement based solidified/stabilized waste materials. Journal of Hazardous Materials. A82: 215–230
38. Huang, P.M. 1993. An Overview of Dynamics and Bio toxicity of Metals in the Freshwater Environment. Water Poll. Res. J. Canada. 28: 1-5.
39. Dooge, J.C.I. 1968. The hydrologic cycle as a closed system. Bull. Int. Ass. Scient. Hydrol. 13 (1): 58-68.
40. Hunter Blair, A. 1966. A ground water analogue investigation of a multi-well pumping scheme at Otterbourne. Water research association technical paper. 56.
41. Isihara, T. and Isihara, Y. 1961. Runoff analysis by analogue computer. 9th general assembly of the international association for hydraulic research, Dubrovnik. 749-759.
42. Chery, D.L. 1963. Runoff studies with a physical model of watershed. Trans. Am. Geophys. Union. 44: 869-870.
43. Chow, V.T. 1967. Laboratory studies of watershed hydrology. Proc. Int. Hydrol. Symp. 1: 194-202.
44. Brusseau, M.L., and Rao, P.S.C. The influence of sorbateorganic matter interactions on sorption nonequilibrium, Chemosphere, 18(9/10), 1691-1706, 1989a.
45. Brusseau, M. L., and Rao, P.S.C. Sorption nonideality during organic contaminant transport in porous media, CRC Crit. Rev. Environ. Control, 19(1), 33-99, 1989b.
46. Schumacher, W. 1864. Die physik des Bodens, Berlin, Germany.

47. Lawes, J.B., Gilbert, J.H., and Warington. 1882. On the amount and composition of the rain and drainage waters collected at Rothamsted. William Cloves and Sons, London.
48. White, R.E. 1985. The influence of macropores on the transport of dissolved and suspended matter through soil. Adv. Soil Science. 3: 95.
49. Gardner, W.R. and Brooks, R.H. 1956. A descriptive theory of leaching. Soil Sci. 83: 295.
50. Skopp, J., and Warrick, A.W. 1974. Two-phase model for the miscible displacement of reactive solute in soils. Soil Sci. Soc. Am. Proc. 38: 545.
51. Van Genuchten, M.Th., Davidson, J.M., and Wierenga, P.J. 1974. An avaluation of kinetic and equilibrium equations for the prediction of pesticide movement through porous media. Soil Sci. Soc. Am. Proc. 38: 29.
52. Danckwerts, P.V. 1953. Continuous flow systems. Chem. Eng. Sci. 2: 1.
53. Biggar, J.W., and Nielsen, D.R. 1963. Miscible displacement: V. Exchange processes. Soil Sci. Soc. Am. Proc. 27: 623.
54. Elrick, D.E. and French, L.K. 1966. Miscible displacement patterns on disturbed and undisturbed soil cores. Soil Sci. Am. Proc. 30: 153.
55. Elrick, D.E., Erh, K.T. and Krupp, H.K. 1966. Applications of miscible displacement techniques to soils. Water Resour. Res. 2: 717.
56. Davidson, J.M., and Chang, R.K. 1972. Transport of picloram in relation to soil physical conditions and pore water velocity. Soil Sci. Soc. Am. Proc. 36: 257.
57. Green, R.E., Rao, P.S.C., and Corey, J.C. 1972. Solute transport in aggregated soils: Tracer zone shape in relation to pore-velocity distribution and adsorption. In: Proc. Second Syrup. Transp. Porous Media, IAHR and ISSS, Guelph, Canada. 2: 733.
58. Beven, K., and Germann, P. 1982. Macropore and water flow in soil. Water Resour. Res. 18: 1311.
59. Balasubramanian, V., Kanehiro, Y., Rao, P.S.C., and Green, R.E. 1973. Field study of solute movement in a highly aggregated Oxisol with intermittent flooding: I. Nitrate, J. Environ. Qual. 2: 359.

60. Rao, P.S.C., Green, R.E., Balasubramanian, V., and Kanehiro, Y. 1974. Field study of solute movement in a highly aggregated Oxisol with intermittent flooding. II. Picloram. J. Environ. Qual. 3: 197.
61. Gilham, R.W., Sudicky, E.A., Cherry, J.A., and Frind, E.O. 1984. An advection-diffusion concept for solute transport in heterogenous unconsolidated geological deposits. Water Resour. Res. 20: 369.
62. Goltz, M.N., and Roberts, P.V. 1986. Interpreting organic solute transport data from a field experiment using physical non-equilibrium models. J. Contam. Hydrol. 1: 77.
63. OmPrakash Meena, Ashish Garg, Mahipat singh, and Rajayashree Pandey. 2011. Determination of Toxic Trace Metals Pb, Cd, Ni, and Zn in Soil by Polarographic Method. International Journal of ChemTech Research. 3(2): 599-604.
64. Charu Jhamaria, Mridula Bhatnagar. 2015. Accumulation of Heavy Metals in Soil Due to Wastewater Application International Journal of Scientific Research. 4(6).
65. Meena Manju, *et.al.* 2014. Seasonal Variations and Sources of Heavy Metals in Free Fall Dust in an Industrial City of Western India. Iranica Journal of Energy & Environment. 5(2): 160- 166.
66. Bishop, P.L. 1986. Prediction of heavy metal leaching rates from stabilized/solidified hazardous wastes. Toxic and Hazardous Waste: Proceedings of the Mid-Atlantic Industrial Waste Conference. 18: 236-252.
67. Cheng, K.Y., & Bishop, P.L. 1990. Developing a kinetic leaching model for solidified/ stabilized hazardous wastes. Journal of Hazardous Materials. 24: 213-224
68. Crank, J. 1975. The mathematics of diffusion. Oxford, Clarendon Press, Cary, NC.
69. Batchelor, B. 1992. A numerical leaching model for solidified/stabilized wastes. Water Science Technology. 26(1-2): 107-115.
70. Hinsenveld, M., & Bishop, P.L. 1994. Use of the shrinking core/exposure model to describe the leachability from cement stabilized wastes,

stabilization and solidification of hazardous, radioactive, and mixed wastes. ASTMSTP 1240, T. Gilliam and C.C. Wiles (Eds.), American Society for Testing and Materials, Philadelphia, PA.

71. Baker, P.G., & Bishop, P.L. 1997. Prediction of metal leaching rates from solidified/stabilized wastes using the shrinking unreacted core leaching procedure. Journal of Hazardous Materials. 52: 311-333.

72. Halim, C.E., Short, S.A., Scott, J.A., Amal, R., & Low, G. 2005. Modeling the leaching of Pb, Cd, As, and Cr from cementitious waste using PHREEQC. Journal of Hazardous Materials. 125(1-3): 45-61.

73. Schiopu, N., Tiruta-Barna, L., Jayr, E., Mehu, J., & Moszkowicz, P. 2009. Modeling and simulation of concrete leaching under outdoor exposure conditions. Science of the Total Environment. 407: 1513-1630.

74. Hestenberg I., Bril J., Del Castilho P.J. 1994. Environ. Qual. 22: 681.

Chapter 3

Model for Heavy Metal Transport in Soil

3.1 INTRODUCTION

Transport phenomena refers to the study of the motion and balance of momentum, heat and mass. To make a calculation for heavy metal concentration in terms of time and space through partial differential equation is required. In the process of continuation it is concerned with boundary conditions. To regard the field as the unit of same properties pertaining to traditional numerical modeling approach is suitable for dispersion-convection equation in relation to saturated-unsaturated soil.

In terms of space coverage fields in connection with laboratory soil columns expose hydraulic characteristics as in (K_s). The traditional approach is not beneficial but despite of it actual heterogeneous field is considered almost suitable pertaining to vertical homogeneous columns having distinctions in hydraulic characteristics. As a consequence of it, heavy metal transport will be different from profile to profile relying on local merits. So far as practical term is considered one is neither enthusiastic nor able to calculate the solute concentration at each point of the field is interested. Considering the hydraulic characteristics for example (K_s) as random, water content (θ), flow velocity ($V = q/\theta$), that is why solute concentration are related to characteristics by their PDF. So logical result is that transport model differs from traditional one described in [1].

3.2 MATHEMATICAL STATEMENT OF TRANSPORT PROBLEM

Soil characteristics are considered to be uniform along the vertical (but are different in the horizontal) plane, and flow is vertical. The soil lies at the bottom of plane x, y and z, a vertical coordinate, directed downward. Let q be the vertical flux, θ the soil moisture, Ψ the suction head, and K the hydraulic conductivity. The one dimensional Richard's equation for θ is:

$$\frac{\partial \theta}{\partial t} + \frac{\partial}{\partial z}\left(K \frac{d\Psi}{d\theta}\frac{\partial \theta}{\partial z}\right) + \frac{\partial K}{\partial z} = 0 \qquad (1)$$

Many analytical representations that fit measurements with several degree of success have been suggested. The type of relationship of [1] is accepted here, as

$$\frac{K(\Psi)}{K_s} = \left(\frac{\Psi_w}{\Psi}\right)^{\eta} \tag{2}$$

$$S = \frac{\theta-\theta_r}{\theta_s-\theta_r} = \left(\frac{\Psi_w}{\Psi}\right)^{\beta} \tag{3}$$

Here K_s is the hydraulic conductivity at saturation, Ψ_w is the air entry value. S is the reduced water content (saturation), θ_s and θ_r are moisture content for saturation and for K→ 0, respectively, and η and β are constant, empirical coefficients ($\eta \sim 2.0-3.5, \beta \sim 0.25-0.5, \frac{\eta}{\beta} \sim 7.2$). Thus, the soil hydraulic merits are characterized by the six constant $\theta_s, \theta_r, \Psi_w, K_s, \eta$ and β.

In line with many studies of the PDF of K_s, it is considered that it is related to scaling parameter δ, which is, in turn, lognormal, that is,

$$Y = In\ \delta \tag{4}$$

and its PDF f_Y is given by

$$f_Y(Y) = \frac{1}{(2\pi)^{1/2}\sigma_Y} exp\left[\frac{(Y-m_Y)^2}{2\sigma_Y^2}\right] \tag{5}$$

The relationship between K_s and δ is obtained as from same determinations about the microscopic flow equation,

$$k_s = \lambda d^2 \qquad \text{or} \qquad K_s^{1/2} = \lambda^{1/2} d \quad \text{and} \quad E\left[K_s^{1/2}\right] = \lambda^{1/2} E[d]$$

Where d is the characteristic length of the pores and λ is the proportionality constant. If we define δ by $\delta = d/E[d]$ then

$$\frac{K_s^{1/2}}{E\left[K_s^{1/2}\right]} = \frac{\lambda^{1/2} d}{\lambda^{1/2} E[d]} = \left[\frac{K_s}{K_s^*}\right]^{1/2} = \delta$$

or

$$\frac{K_s}{K_s^*} = \delta^2 \tag{6}$$

Where

$$K_s^* = \left[E(K_s^{1/2})\right]^2 = \left[\int_0^\infty K_s^{1/2} f(K_s) dK_s\right]^2 \tag{7}$$

For some problems we do not need the velocity profile or information about the details of the transport to get the information we need. For these problems we do macroscopic balances. There are three types of macroscopic balances: mass, momentum, and energy. Here we take macroscopic mass balance

equation governing heavy metal dispersion in one-dimensional transport through a homogeneous column may be expressed as

$$\frac{\partial C}{\partial t} + V\frac{\partial C}{\partial z} = D_p\frac{\partial^2 C}{\partial z^2} + \frac{1}{\theta}\frac{\partial}{\partial z}(\theta D_h\frac{\partial C}{\partial z}) \quad (8)$$

Where C is the heavy metal concentration, θ is the volumetric water content, z is the vertical coordinate positive downward, t is the time, D_h is the mechanical dispersion coefficient, and D_p is the effective molecular diffusivity for a static fluid in the soil system. A rough approximation for D_p is (2/3)D_0, where D_0 is the diffusivity in the solution phase. It is considered that $\theta = \theta(z,t)$ and the pore velocity, $V(z,t) = q/\theta$ (where q is the specific discharge), are given solutions of the flow equation independent of C. The concentration C is made dimensionless with respect to the difference between the initial concentration in the soil. Hence, C varies between zero to unity. For flow through saturated media ($\theta = \theta_s = \text{constant}$), it has been exhibited that under quite general conditions [2-3]

$$D_h = \lambda V \quad (9)$$

in which λ is the dispersivity for longitudinal dispersion. Equations (8) and (9) are adopted, although with some reservations as authentic for unsaturated flows [4-5], with values of λ that differ in the range of 0.1-3 cm for most soils [6-7].

Equation (8) refers to soil lying in the horizontal x, y plane and beneath $z = 0$ with z positive downward. Salt transport takes place due to application of recharge q_0 on the surface, at the soil moisture content θ, and at the pore water velocity *V*. It is considered that instead of heterogeneity and eventual nonuniform application, transport is vertical. This hypothesis is bound to be quite precise for the upper layer of thickness on the order of 1 to a few meters. Furthermore by [8], that the length scale characterising the variation of hydraulic properties in the x,y plane is much larger than the depth and, henceforth, lateral transports are just small compared with the vertical transport. So problem is solved significantly, and derivatives with respect to t and z are preserved in the solute motion equation (Equation 8).

3.3 STOCHASTIC APPROACH TO STUDY TRANSPORT OF SOLUTE UNDER GRAVITY

The simplest solution of Equation (8) is calculated for uniform transport (i.e.,V = constant and θ = constant) and for initial and boundary conditions: C = 1 at $z = 0$, C = 0 at t = 0, $z > 0$, in a column extending along $z > 0$. Subsequently, the next simplifying assumption is that the transport of salt is steady, that is, the vertical specific discharge q does not depend on z or t (q is constant in each profile, but differs in the x, y plane). This can be acceptable after the short time required for the wetting front to move away from the soil surface has passed, and if the recharge q_0 does not alter with time in the period.

Under these conditions, the dispersion-convection equation (Equation 8) becomes

$$\frac{\partial C}{\partial t} + V\frac{\partial C}{\partial z} = D\frac{\partial^2 C}{\partial z^2} \tag{10}$$

with V and D independent of z.

Under these assumptions and for boundary and initial conditions,

$$C = 1 \qquad z = 0, \qquad t > 0$$
$$C = 0 \qquad z > 0, \qquad t = 0 \tag{11}$$

The concentration profile of a noninteracting solute is explained by the solution of Equation (10) confined Equation (11) as follows:

$$C = (0.5)(1 - \mathrm{erf}\frac{z - Vt}{2\sqrt{Dt}}) \tag{12}$$

Where C is the dimensionless concentration and $D = D_p + D_h$. The estimate given by Equation (12) is valid for $t \gg D/V^2$ Furthermore, D_p is normally negligible compared with D_h.

Although for a homogeneous column *V* and *D* are constant, in a heterogeneous field they vary with x and y, so this variation is observed as random and the real field is considered as a realization of an ensemble of fields with the same probability distribution functions (PDF) of the variables of interest. Additionally, it is considered that these PDF are statistically stationary, and under exact ergodic assumptions the whole averaging and space averaging in the given realization over x, y plane are equivalent. Returning now to Equation (12), C is a random

function of the random variables *V* and *D* (because of the random nature of *V* and θ), and it depends certainly upon *z* and *t.* Hence, the value of C cannot be judged deterministically, as it relies on the random variables *V* and θ. The main purpose is to calculate $f(z,t;C)$, the PDF of concentration for fixed *z* and *t* or the related cumulative probability:

$$P(z,t;C) = \int_0^A f(z,t;C)dC \tag{13}$$

Where *P* is the probability that $C \leq A$ at depth *z* and time *t.*

Under the ensemble and space equivalence, *P* represents the ratio between the area of the field whose solute concentration is less than *A,* and the total area, at given *z* and t. The first moment, the average, is given by

$$E[C] = \int_0^1 Cf(C)dC = \int_0^1 C\,dP = [CP]_0^1 - \int_0^1 P\,dC = 1 - \int_0^1 P\,dC$$

Hence, the expectation

$$E[C(z,t)] = \int_0^1 Cf(z,t;C)dC = 1 - \int_0^1 P(z,t;C)dC \tag{14}$$

is the average concentration of the field at depth z at time *t.* If the field is viewed as a imaginary equivalent homogeneous column, then it is logical to consider $E[C(z,t)]$ as the concentration in the equivalent field. The variation of C over the horizontal plane is characterized by the variance, the second central moment which is extracted as follows:

$$\sigma_c^2 = \int_0^1 (C-\bar{C})^2 f(C)dC = \int_0^1 (C-\bar{C})^2 dP$$

$$= [(\bar{C}-C)^2 P]_0^1 - 2\int_0^1 (C-\bar{C})PdC$$

$$= (1-\bar{C})^2 - 2\int_0^1 CP\,dC + 2\bar{C}\int_0^1 P\,dC$$

Putting the value of $E[C]$ from Equation (14) for $\bar{C}$, yields

$$\sigma_c^2 = (1-\bar{C})^2 + 2\bar{C}(1-\bar{C}) - 2\int_0^1 CP\,dC$$

$$= 1 - \bar{C}^2 - 2\int_0^1 CP\,dC$$

Thus, the second moment, the variance of C(z,t), is evaluated with the aid of $P(z,t;C)$ from

$$\sigma_c^2(z,t) = \int_0^1 (C-\bar{C})^2 f(z,t;C)dC$$

$$= 1 - \bar{C}^2 - 2\int_0^1 CP(z,t;C)dC \tag{15}$$

A measure of the symmetry of the distribution of C about its average is given by the skewness,

$$\gamma_c(z,t) = \int_0^1 (C-\bar{C})^3 f(z,t;C)dC$$

$$= (1-\bar{C})^2 - 2\int_0^1 (C-\bar{C})^2 P(z,t;C)dC \tag{16}$$

The randomness of C satisfying Equation (12) stems from that of *V* and of *D (D* being in turn a function of *V* and θ). Hence, the moments of C are calculated with the aid of the PDF of these two variables (because C is a function of *V* and θ).

The randomness of C is related with the boundary and initial conditions in addition to its dependence on the variability of the soil variables. In the case of steady gravitational flow, which is the practical case of leaching applied on the soil surface, the rate q_0 (Equation 10) is also a random variable denoted by R and characterized by a PDF $f(R)$. A simple authentic approximation to the PDF of the random variation of the recharge density R with x, y is the uniform PDF:

$$f(R) = 0 \quad \text{for} \quad R < \bar{R} - d_R \quad \text{and} \quad R > \bar{R} + d_R$$

$$f(R) = \frac{1}{2d_R} \quad \text{for} \quad \bar{R} - d_R < R < \bar{R} + d_R \tag{17}$$

defined by the two parameters $\bar{R}$ and d_R so that the PDF of *R* is constant in the interval of width $2d_R$ around the average $\bar{R}$. In the case of rainfall over the field, d_R is very small, but for many cultivating methods or rainfall over large areas, $d_R/\bar{R}$ may be quite large.

3.4 CONCENTRATION DISTRIBUTION

If dispersion is taken as unimportant in problems of solute displacement, an approximation [9] for solute transport can be explained by ignoring the diffusion

and dispersion terms in Equation (8). Then the convection equation without diffusion-dispersion can be explained for any $q = V\theta$. Hence, C is constant for

$$\frac{dz}{dt} = \frac{q(z,t)}{\theta(z,t)} \tag{18}$$

and for steady uniform transport, C is augmented along fronts of the equation

$$z = \left(\frac{q}{\theta}\right) t + \text{constant} = Vt + \text{constant} \tag{19}$$

For the boundary and initial conditions indicating to Equation (12), the value of C from Equation (19) is given by the simple expression

$$C(z,t) = H(Vt - z) \tag{20}$$

where H is the Heaviside step function (i.e., $H(x) = 0$ for $x < 0, H(x) = 1$ for $x > 0$). Equation (20) is also the limit case of Equation (12), for $D \to 0$ signifying a sharp front, separating the area with $C = 1$ from $C = 0$, which moves downward at constant velocity *V*. Now Equation (8) can be solved for specified θ and *V* in terms of z and *t* at any given point of coordinates x and *y* in the field. Equivalently, in the statistical methodology, *V* and θ are functions of the random parameters characterizing the field $(\text{e.g.}, \psi_w, \eta, \beta, \theta_s, \theta_r, K_s)$ and random parameters characterizing the transport $(e.g., q_0 = R, t_i, \theta_n)$.(To simplify, K_s has been singled out as the only stochastic parameter representing the field spatial variability, and R is the only one representing the transport at the boundary.) Hence, the concentration outline on the coordinates x and y, which is random and can be expressed in terms of the frequency function (PDF) $f(K_s, R \ldots,)$. To derive explicitly a solution for the concentration probability distribution in a spatially variable field for steady gravitational transport, a steady recharge *R* with PDF (Equation 17) is assumed. If *R* is applied for a enough long time, a steady transport is acquired in each profile such that the transport is gravitational with constants θ and *V*. At any point in the field, one of two situations are arise:

(1) if $R \geq K_s$, then in that area of the field, the transport is saturated, and with neglect of additional head on the surface (i.e., for unit gradient), Darcy's law yields

$$V = K_s/\theta_s \tag{21}$$

(2) for $R < K_s$, the soil is unsaturated and the velocity is given by

$$V = \frac{K(\theta)}{\theta} \quad \text{and} \quad K(\theta) = R \tag{22}$$

Substituting Equation (6) into Equation (21), and Equation (2) & (3) into Equation (22) and inserting Equation (4) in Equation (6), outcome for Equations (21) and (22)

$$V = K_s^* \exp(2Y) / \theta_s \text{ for } [R > K_s^* \exp(2Y)] \quad (23)$$

$$V = \frac{R\, exp(2\omega Y)}{\theta_s (R/K_s^*)^{\omega}} \text{ for } [R < K_s^* \exp(2Y)] \quad (24)$$

Where $\omega = \beta/\eta$. It can be exposed that since $\theta_r \ll \theta_s$ dropping θ_r from Equation (3) would have a negligible effect upon the resulting *V* in Equation (23). The two expressions, Equations (23) and (24), incorporate the entire kinematical information needed in order to solve Equation (8) for this simple transport configuration. In Equations (23) and (24), *V* depends on the deterministic parameters K_s^* and θ_s and on the random variables *R* and *Y*, the PDF of which may be approximated by Equations (17) and Equation (5). The cumulative probability distribution of *V* can be computed in a general method from

$$P(V) = \int dY \int f(R,Y) dR \quad (25)$$

Where $f(R,Y)$ is the joint probability density function of *R*, *Y* and the integration region in the double integral depends on *V* and *Y* through Equation (24) and (23). Because the recharge *R* and K_s are independent variables, then

$$f(R,Y) = f(R)f(Y) \quad (26)$$

With $f(Y)$ and $f(R)$ given by Equation (5) and Equation (17), respectively. The cumulative probability *P(V)* are calculated in an analytically solution of Equation (25) when $f(R,Y)$ is substituted from Equation (26).

In the simplified transport model, the concentration (C) depends on the velocity *(V)* through Equation (20), from which C can be zero or unity. Thus, for given z and *t*, if $V > z/t$ then $C = 1$, but if $V < z/t$ then $C = 0$. The PDF of *C* is therefore represented by two Dirac distributions at $C = 0$ and $C = 1$ [10], so that the region at $C = 0$ is

$$P(\varepsilon) = P(V \leq z/t) \quad (27)$$

Conversely, the area at $C = 1$ is

$$1 - P(V \leq z/t) \quad (28)$$

Where $\varepsilon \to 0$. Substituting $V = z/t$ in Equations (22), (23), and (24), the cumulative probability Equation (27) or (28) is calculated. Since $P(z/t)$ gives the

ratio for a given t and at a depth z between the region of a field for which $C = 0$ and the total region, the average concentration (C) over the field is given by

$$\bar{C}(z,t) = 1 - P(z/t) = 1 - P(V) \quad (29)$$

Physically, $\bar{C}$ is the ratio between the area of the field for which $C = 1$ and the total area of the field. This is because in this simplified transport model, the concentration front separating the zone of $C = 1$ from the zone of $C = 0$ is a surface propagating downward at velocity $V = z/t$, which changes from profile to profile due to the variability of K_s (or Y). At the soil surface $(z = 0)$, the cumulative probability $P(V = z/t = 0) = 0$ and therefore $\bar{C} = 1$, but on the other side, at large z and small $t, P(z/t) = 1$ and therefore $\bar{C} = 0$. At intermediate z values of $C(0 \leq C \leq 1)$ can be calculated.

To measure Average Field Concentration $\bar{C}(z,t)$ from Equation (29), the cumulative probability $P(V = z/t)$ are computed by Equation (25) (with Equation (26) substituted for $f(R,Y)$) with the complete field of integration $-\infty < Y < \infty, \bar{R} - d_R < R < \bar{R} + d_R$.The complication raises in calculating $\bar{C}$ in analytical form, and therefore we get the lengthy equation of $\bar{C}$. Consequently, we divide the calculations into two different expressions at

$$Y = 0.5In(R/K_s)$$

The end points are at

$$Y = 0.5In\frac{\bar{R}-d_R}{K_s^*} \quad \text{and} \quad Y = 0.5In\frac{\bar{R}+d_R}{K_s^*}$$

For the range of recharge rate $\bar{R} - d_R \leq R \leq \bar{R} + d_R$, there are generally three cases:

(1) $V < (\bar{R} - d_R)/\theta_s$ so that Equation (23)

$$Y \leq Y_2 = 0.5In(V\theta_s K_s^*) \quad (30)$$

(2) $V > (\bar{R} + d_R)/\theta_s$ so that Equation (24)

$$Y \leq Y_3 = (1/2\omega)In\frac{V\theta_s(R/K_s^*)^{\omega}}{R} \quad (31)$$

With

$$Y_b = (1/2\omega) In[V\theta_s(\bar{R} - d_R)^{-1}(K_s^*)^{-\omega}] \quad (32)$$

And if $Y_a > Y_b$ then

$$Y_a = (1/2\omega) In[V\theta_s(\bar{R} + d_R)^{\omega-1}(K_s^*)^{-\omega}] \quad (33)$$

(3) Transport velocity is within the entire range of R, that is, $(\bar{R} - d_R)/\theta_s < V < (\bar{R} + d_R)/\theta_s$.

To develop expressions for P(V) in each of these three cases, normal PDF f(Y) from Equation (5) and uniform PDF f(R) (Equation 17) are substituted to Equation (26) and then to Equation (25) and are integrated over the relevant domain. For this integration, we use the following auxiliary formulas:

$$\int_{-\infty}^{A} e^{\alpha Y} f(Y) dY = 0.5 exp(\alpha m_Y + \frac{\alpha^2 \sigma_Y^2}{2})(1 + erf \frac{A - \alpha\sigma_Y^2 - m_Y}{\sqrt{2}\sigma_Y}) \quad (34)$$

$$\int_{B}^{A} e^{\alpha Y} f(Y) dY = 0.5 exp(\alpha m_Y + \frac{\alpha^2 \sigma_Y^2}{2})(1 + erf \frac{A - \alpha\sigma_Y^2 - m_Y}{\sqrt{2}\sigma_Y} - erf \frac{B - \alpha\sigma_Y^2 - m_Y}{\sqrt{2}\sigma_Y}) \quad (35)$$

This outcomes for the above-mentioned three cases the following expressions:

(1) For $V < (\bar{R} - d_R)/\theta_s$,

$$P(V) = \int_{\bar{R}-d_R}^{\bar{R}+d_R} dR \int_{-\infty}^{Y_2} dY \, f(R) f(Y)$$

Which gives, after integration, using Equation (34) with $\alpha = 0$

$$P(V) = (0.5)\left[1 + \text{erf} \frac{(0.5) In \frac{V\theta_s}{K_s^*} - m_Y}{\sqrt{2}\sigma_Y}\right] \quad (36)$$

(2) For $V > (\bar{R} + d_R)/\theta_s$,

$$P(V) = \int_{\bar{R}-d_R}^{\bar{R}+d_R} dR \int_{-\infty}^{Y_2} dY \, f(R) f(Y)$$

$$= \int_{R-d_R}^{R+d_R} dR \int_{-\infty}^{Y_a} dY \, f(R) f(Y) + \int_{Y_a}^{Y_b} dY \int_{R-d_R}^{R(Y_3)} dR \, f(Y) f(R)$$

Which gives, after integration, using Equation (34) for the first term on the right-hand side and Equation (35) for the second term,

$$P(V) = 0.5\left[1 + \text{erf} \frac{Y_a - m_Y}{\sqrt{2}\sigma_Y}\right] - \left[\frac{\bar{R} - d_R}{4d_R}\right]\left[\text{erf} \frac{Y_b - m_Y}{\sqrt{2}\sigma_Y} - \text{erf} \frac{Y_a - m_Y}{\sqrt{2}\sigma_Y}\right]$$

$$+ 0.25 d_R \left(\frac{V\theta_s}{K_s^{*\omega}}\right)^{1/(1-\omega)} \left[exp\left[-\frac{2\omega m_Y}{1-\omega}\right] + \left[\frac{2\omega^2 \sigma_Y^2}{(1-\omega)^2}\right]\right]$$

$$\times \left[\text{erf}\frac{Y_b - m_Y + (2\omega\sigma_Y^2)/(1-\omega)}{\sqrt{2}\sigma_Y} - \text{erf}\frac{Y_a - m_Y + (2\omega\sigma_Y^2)/(1-\omega)}{\sqrt{2}\sigma_Y}\right] \quad (37)$$

Where Y_b *and* Y_a are given explicitly by Equations (32) and (33), respectively.

(3) For $(\bar{R} - d_R)/\theta_s < V < (\bar{R} + d_R)/\theta_s$,

$$P(V) =$$

$$= \int_{\bar{R}-d_R}^{\bar{R}+d_R} dR \int_{-\infty}^{Y_2} dY\, f(R)f(Y) + \int_{Y_2}^{Y_b} dY \int_{R-d_R}^{R(Y)} dR\, f(Y)f(R)$$

Which gives, after integration, using Equation (34) and Equation (35),

$$P(V) = \quad 0.5\left[1 + \text{erf}\frac{Y_2 - m_Y}{\sqrt{2}\sigma_Y}\right] - \left[\frac{\bar{R} - d_R}{4d_R}\right]\left[\text{erf}\frac{Y_b - m_Y}{\sqrt{2}\sigma_Y} - \text{erf}\frac{Y_2 - m_Y}{\sqrt{2}\sigma_Y}\right]$$

$$+ \left(\frac{0.25}{d_R}\right)\left(\frac{V\theta_s}{K_s^{*\omega}}\right)^{1/(1-\omega)}\left[exp\left[-\frac{2\omega m_Y}{1-\omega}\right] + \left[\frac{2\omega^2\sigma_Y^2}{(1-\omega)^2}\right]\right]$$

$$\times \left[\text{erf}\frac{Y_b - m_Y + (2\omega\sigma_Y^2)/(1-\omega)}{\sqrt{2}\sigma_Y} - \text{erf}\frac{Y_2 - m_Y + (2\omega\sigma_Y^2)/(1-\omega)}{\sqrt{2}\sigma_Y}\right] \quad (38)$$

Where Y_2 is given by Equation (30).

In the particular simple case of uniform transport, that is,

$d_R = 0$ ($or\ S_R = d_R/\bar{R} = 0$),

$$\bar{C} = 0.5\left[1 - \text{erf}\frac{0.5\ In\ \xi - m_Y}{\sqrt{2}\sigma_Y}\right]\ for\ (\xi < r) \quad (39)$$

$$\bar{C} = 0.5\left[1 + \text{erf}\frac{(0.5\omega)\ In(\xi r^{\omega-1}) - m_Y}{\sqrt{2}\sigma_Y}\right]\ for\ (\xi > r) \quad (40)$$

Where

$$\xi = \frac{z\theta_s}{tK_s^*}, \qquad r = \bar{R}/K_s^*, \qquad and \qquad S_R = d_R/\bar{R} \quad (41)$$

are easier dimensionless forms. Equation (41) enable to calculate the value of $\bar{C}$, from Equations (29),(36), (37), and (38) in terms of the dimensionless variables $\xi, r\ and\ S_R$ and in addition to $m_Y, \sigma_Y, and\ \omega$.

3.4.1 Results

Average concentration profiles $\bar{C}(z,t)$, for the transport of heavy metals, derived by Equations (1-41). The values of the parameters, K_s^*, m_Y, σ_Y, and ω for the soil are given by [11]. So, evaluation of $\bar{C}(z,t)$, is straight forward for any

combination of $r = \bar{R}/K_s^*$and $S_R = d_R/\bar{R}$, characterizing the average and variance of the rate of application and of the soil parameters describing the transport.

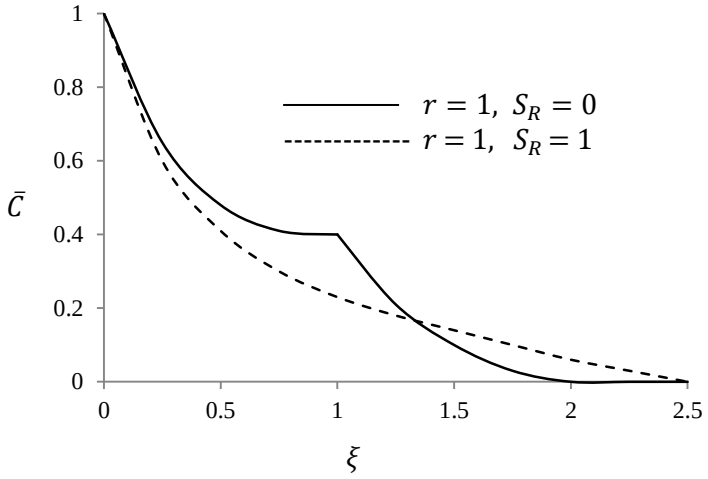

(A)

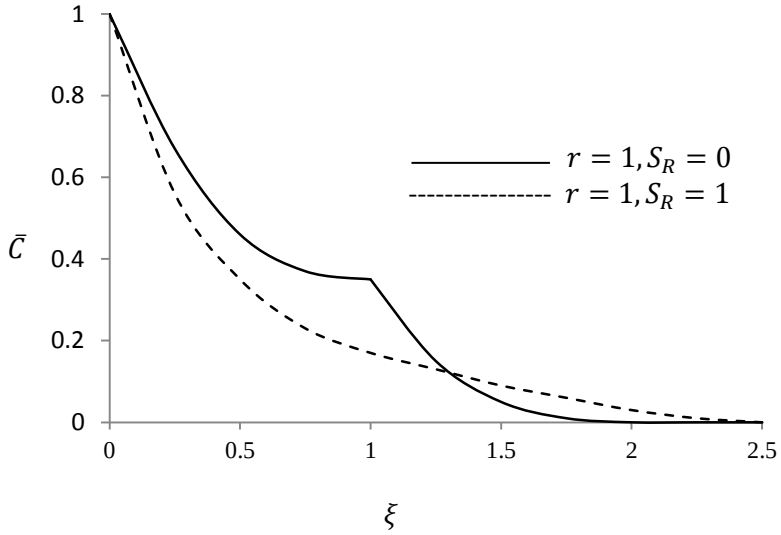

(B)

Figure 1: Average concentration profile $\bar{C}$ as a function of $\xi = \frac{z\theta_s}{tK_s^*}$ for one value of the dimensionless application rate ($r = \bar{R}/K_s^*$) for deterministic ($S_R = 0$) and stochastic ($S_R = 1$) rates. (A): for the soil of Jaipur area, (B): for the soil of Kota area.

Assume first the simplest case of $S_R = 0$ (i.e., deterministic uniform recharge on the soil surface). In this case, the concentration profile for the zone extending from the soil surface to $\xi = r$ (i.e.,$\xi \leq r$) is described by Equation (39). This is demonstrated by the curves lying above the breaking points. In this area, which lies between $\xi = 0$ and $\xi = r$, heavy metal transport is controlled by the saturated flow. For the area in which $\xi > r$, the $\bar{C}(\xi)$ profile is given by Equation (40), which relates here to the unsaturated flow. Therefore, $S_R = 0$ curve differs mainly in the location of the breaking point of change of shape of the profile at $\xi = r$ and $\bar{C}(\xi)$ profiles for other values of r can be obtained easily by translation. For cases where $S_R > 0$, the $\bar{C}(\xi)$ profiles are calculated by Equations (36) through (38). The curves are smooth as $\bar{C}$, at a given depth, is influenced by front translation either in the saturated or in the unsaturated area because of the altogether but independent, variation of K_s and R.

Thus for a given S_R the transport of heavy metals spreading over the complete field is greater for large values of r than for small values. This is because a larger portion of the field has greater value of r and hence the saturated transport plays a dominant role. So in this region, the front velocity varies in a wide range because of relatively high K_s variation. In contrast, in the unsaturated part of the field, the variation of V depends on θ (Equation 22), which varies less widely than K_s.

3.5 CONCENTRATION DISTRIBUTION FOR DISPERSIVE TRANSPORT

To relate the variables V and D in Equation (12) to the spatially variable soil characteristics and the rate of application boundary conditions, the stochastic steady transport velocity (V) is determined from previous Equations, also the dispersion coefficient (D) in Equations (8) through (12). Taking Equation (9) as the representative expression for $D(V)$, the soil parameter, λ, i.e., the dispersivity, fits lognormal distribution [11]. Hence, if we define μ as

$$\mu = \ln \lambda \tag{42}$$

Then $f(\mu)$ is given by Equation (5) after substituting Y by μ with the statistical parameters σ_μ and m_μ.

Now *C* is a function of *V* and λ (Equations 9 and 12), which, in turn, are functions of *Y*, *R*, and μ (Equations 17, 21, 22, and 42). The PDF of *C* can then be written in a general manner

$$f(C) = f(Y, R, \mu) dY dR\, d\mu \tag{43}$$

Furthermore, Y, *R*, and μ are taken as independent random variables. This is obvious for *R* and the two others, but it is less probable for *Y* and μ, which are both soil characteristics. Thus, Equation (43) becomes

$$f(C)dC = f(Y)f(R)f(\mu) dY dR\, d\mu \tag{44}$$

with $f(Y)$, $f(R)$ (Equation (17)), and $f(\mu)$ similar to $f(Y)$.

To sum up the procedure in principle, the input parameters of the problem are $\sigma_Y, \beta, \theta_s, \theta_r, d_R, m_Y, D_P, K_S^*, \bar{R}, \sigma_\mu$ and m_μ. They define fully the random variable *V* by Equations (17), (21), and (22) and, therefore, $f(C)$ (Equation 44) is defined by them as well.

3.5.1 Computational Procedure

To simplify the computations, only two of the three variables *Y*, *R*, and μ are taken as random and the third one as deterministic. The fundamental function to be evaluated is the cumulative probability of C (Equation 13). In the first case in which *Y* and μ are random though *R* is deterministic and equal to *R*, *P(C)* is given by the combination of $f_Y(Y)$ and Equations (13), and (44),

$$P(z,t;C) = \frac{1}{\sqrt{2\pi}\sigma_\mu} \int_{-\infty}^{\infty} \exp\left[-\frac{(\mu - m_\mu)^2}{2\sigma_\mu^2}\right] d\mu \int_{-\infty}^{Y} \frac{1}{\sqrt{2\pi}\sigma_Y} \exp\left[-\frac{(\alpha - m_Y)^2}{2\sigma_Y^2}\right] d\alpha \tag{45}$$

Where $Y = Y(z, t; C, \mu, \bar{R})$.

By integration once over α, Equation (45) becomes

$$P(z,t;C) = \frac{1}{2\sqrt{2\pi}\sigma_\mu} \int_{-\infty}^{\infty} \exp\left[-\frac{(\mu - m_\mu)^2}{2\sigma_\mu^2}\right] \left[1 + erf\, \frac{Y(z,t;C,\mu,\bar{R}) - m_Y}{\sqrt{2}\sigma_Y}\right] d\mu \tag{46}$$

so that *P* is evaluated by a quadrature that has to be carried out numerically. Similarly, for *Y*, *R* (random), and $\lambda = \bar{\lambda}$ (deterministic), by Equations (13), (17), and (44)

$$\begin{aligned} P(z,t;C) &= \int_{R-d_R}^{R+d_R} f(R) dR \int_{-\infty}^{Y} f(Y)\, dY \\ &= \frac{1}{4d_R} \int_{\bar{R}-d_R}^{\bar{R}+d_R} \left[1 + erf\, \frac{Y(z,t;C,\mu,\bar{R}) - m_Y}{\sqrt{2}\sigma_Y}\right] dR \end{aligned} \tag{47}$$

Again *P* is calculated by a numerical quadrature with small truncation error.

The function $Y(z,t;C,\mu,\bar{R})$, which appears in Equations (46) and (47), is given by inverting Equation (12) after replacing Equation (9) for *D*, as follows:

$$\frac{z-V(R,Y)t}{2\sqrt{\lambda V(R,Y)t+D_p t}} = \phi(C) \tag{48}$$

Where

$$\phi(C) = erf^{-1}(1-2C) \tag{49}$$

From Equation (48), which is a quadratic equation in *V*,

$$V = \left[z + 2\phi^2\lambda - 2\phi\left\{\sqrt{\lambda z + \phi^2\lambda^2 + D_p t}\right\}\right]/t \tag{50}$$

This can be written also with the help of the dimensionless variable $\xi = z\theta_s/tK_s^*$. substituting *t* (Equation 41) as follows:

$$V = \frac{K_s^*\xi}{\theta_s} + \frac{K_s^*\xi}{z\theta_s}\left[2\phi^2\lambda - 2\phi\sqrt{\lambda z + \phi^2\lambda^2 + \frac{D_p z\theta_s}{K_s^*\xi}}\right]$$

With these preliminary steps, the computation of $P(z,t;C)$ is carried out as follows:

a. Given values of z, t, C (i.e., ϕ of Equation 49), $D_p, \lambda = \exp(\mu)$, and *R* are substituted in Equation (50) to get *V*.

b. To evaluate which one of the two relationships Equation (21) or (22) holds, *V* is compared with R/θ_s, which is the value demarcating unsaturated transport (Equation 22) from Equation (21). If $V < R/\theta_s$, transport takes place and Equation (21) is effective. Then,

$$V = \frac{K_s}{\theta_s} = \frac{K_s^*\exp(2Y)}{\theta_s} \tag{51}$$

Or

$$Y = (1/2)\ln(V\theta_s/K_s^*) \tag{52}$$

If $V > R/\theta_s$, the transport is unsaturated, Equation (22) is valid, and

$$V = \frac{R}{\theta} = R/[\theta_r + (R/K_s^*)^{\omega}(\theta_s - \theta_r)exp(-2\omega Y)] \tag{53}$$

or

$$Y = \frac{1}{2\omega} ln \frac{(R/V)-\theta_r}{(R/K_s^*)^{\omega}(\theta_s-\theta_r)} \tag{54}$$

Hence, for given $K_s^*, \theta_s, \theta_r$ and ω, $Y(z,t;C,R,\mu)$ is determined from Equation (52) or (54).

c. This value of Y is replaced in Equation (46) with $R = \bar{R}$ or in Equation (47) with $\lambda = \bar{\lambda}$, and P are evaluated by numerical integration by augmenting the values of μ or R by small increments.
d. Once $P(z, t; C)$ is calculated numerically for a set of C values, several moments of C are found from Equations (14) and (15) by an additional integration over C, in Equation (46) or (47).

3.5.2 Results

To demonstrate the capability of the model $P(z, t; C)$, computations from Equations (46) and (47), the curves of cumulative probability $P(z, t; C)$ have physical clarification. They characterize the area of the field relative to the total area, which is at a concentration smaller than C at depth z and time *t.* For these computations, values of m_Y, σ_Y are adopted from [12]; and the values of m_μ, σ_μ and $\bar{\lambda}$ are calculated from [7, 14] as

$$m_\mu = 0.41, \sigma_\mu = 1.17, \text{and } \bar{\lambda} = 3\ cm, \theta_s = 0.43, K_s^* = 0.22\ cm/hr\ , S_R = 0.$$

The curves $P(z, t; C)$ in Figure 2 have physical interpretation. It represents the area of the field relative to the total area, which is at a concentration smaller than C at depth z. After evaluating $P(z, t; C)$ the average concentration distribution $\bar{C}(z, t)$, the variance $\sigma_C^2(z, t)$, and skewness $\gamma_C(z, t)$ are computed from Equations (14), (15) and (16), respectively, by numerical evaluation of the integrals. Several combinations of the parameters $r = \bar{R}/d_R, K_s^*$ and $S_R = d_R/\bar{R}$ can be used

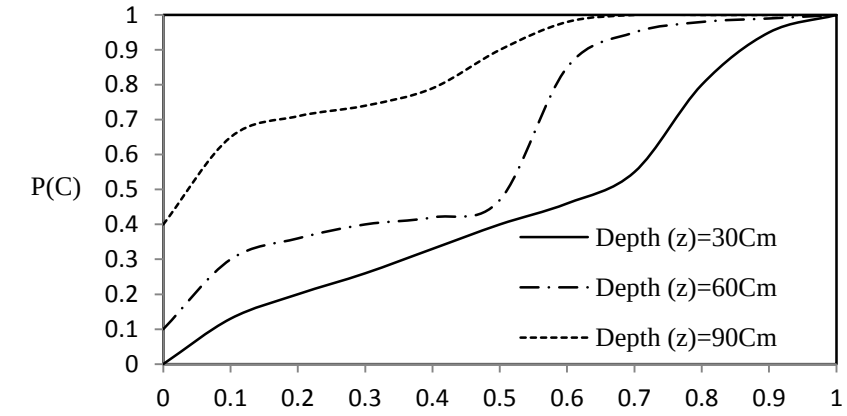

A

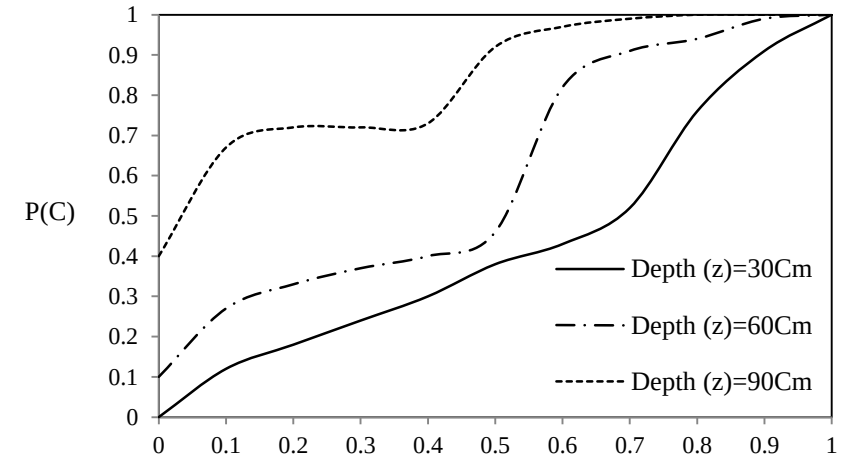

B

Figure 2: Cumulative probability $P(z,t;C)$ as a function of concentration C, for various z in cm. A: for the soil of Jaipur area, B: for the soil of Kota area.

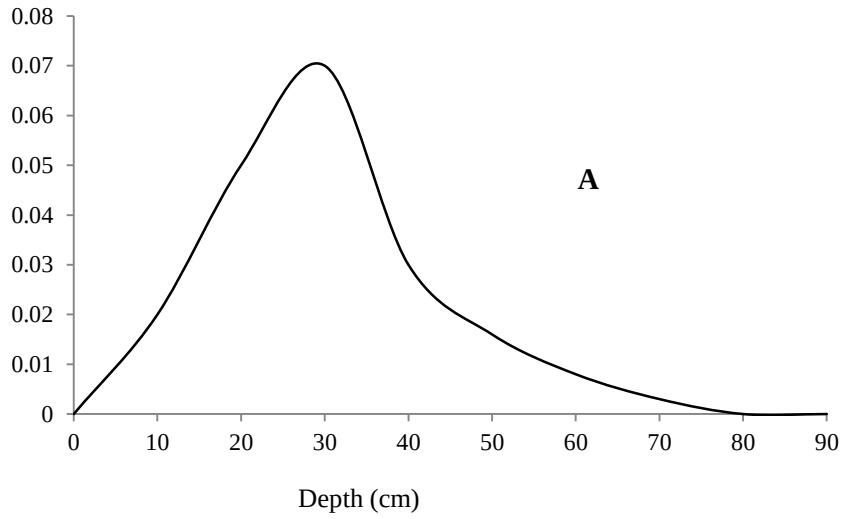

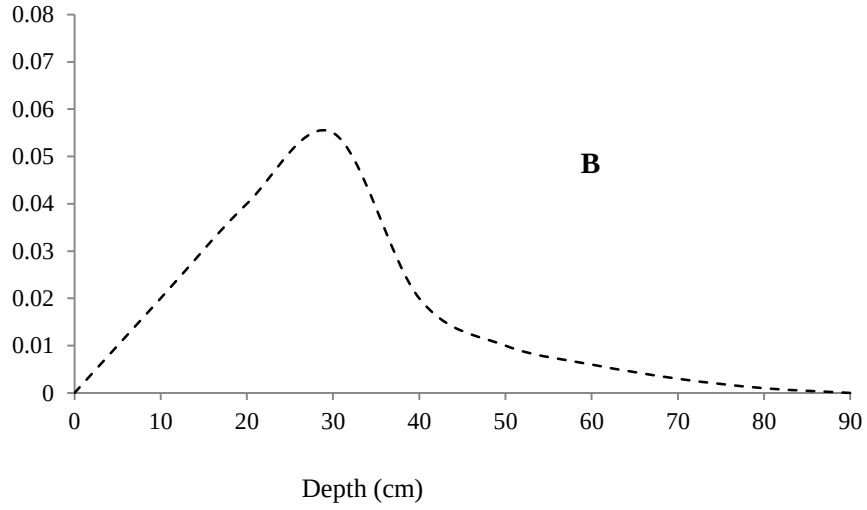

Variance of C as a function of depth, A: for the soil of Jaipur area, B: for the soil of Kota area

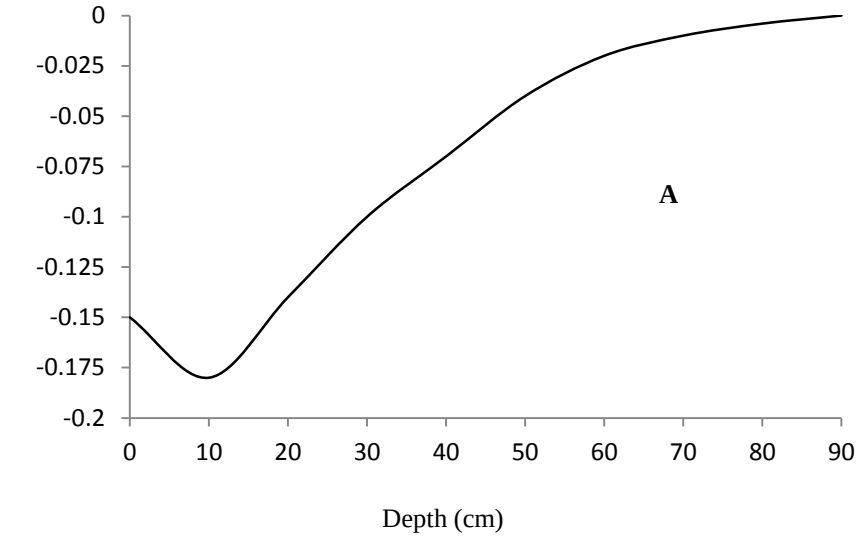

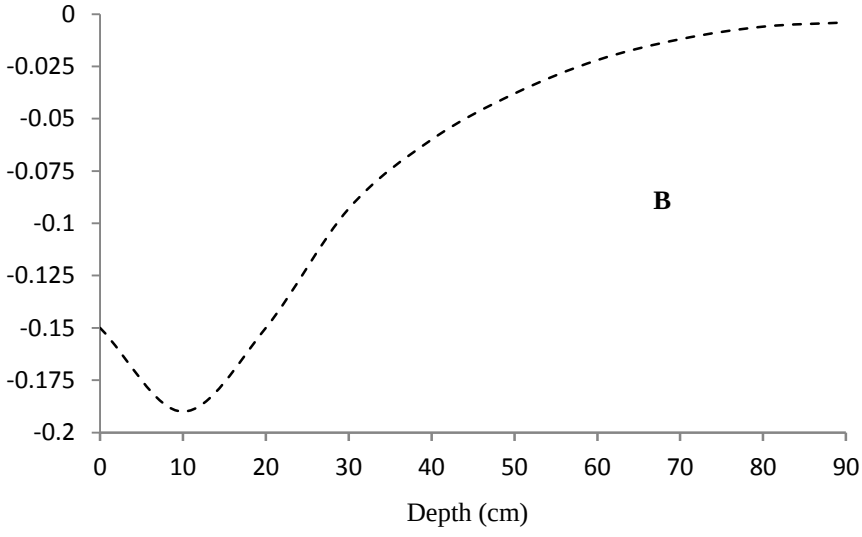

Skewness of C as a function of depth, A: for the soil of Jaipur area, B: for the soil of Kota area

Figure 3: Variance and Skewness of C as a function of soil depth (z).

The moments describing the function $f(z,t;C)$ by Equations (15), and (16) are given in Figure 3 for two soils: soil of Jaipur area and soil of Kota area.

The second central moment: the variance of the concentration $\sigma_C^2(z,t)$, being analysed in Equation (15). It describes the degree of variation of the concentration of salt over the horizontal plane at a depth z. The third central moment, the skewness, being evaluated by Equation (16). Being a measure of the symmetry of the distribution about its average value, the deviation of the skewness shows that the distribution of $C(z,t)$ in the x,y plane about $\bar{C}(z,t)$ is not symmetric. In addition, since the values of $\gamma_C(z)$ are always negative, the distribution of $C(z,t)$ is skewed to the left. Also, maximum skewness is connected with maximum deviation and γ_C is zero at $z=0$ and disappears for large depths. The whole statistical information about the concentration distribution is given by curves in Figure 2 and 3.

3.6 STOCHASTIC TRANSPORT IN NON-STEADY VERTICAL FLOW

Here a stochastic approximate model of transport of heavy metals in a spatially variable field is established. The model is undertaken by the following principles: the transport of metals is vertical, spatial variability takes place in the horizontal plane, variability is connected with the saturated conductivity, deterministic uniform recharge is applied on the soil surface during $t \le t_i$ and the soil is with uniform $\theta = \theta_n$. Solute concentration prior to leaching (C_n) is uniform, whereas water with uniform concentration $C_0 > C_n$ is applied at the surface during $0 < t < t_i$.The purpose is to calculate the expectation $E(C)$ and the variance σ_C^2 as a function of z and *t* under these conditions. For this purpose, a simplified model of salt transport are formulated to calculate mean concentration and its variance in a spatially variable field.

3.6.1 Derivation of Approximate Solution of Salt Transport

For vertical one-dimensional transport of deterministic pore velocity $V(z,t)$,the equations of transport (Equations 8 and 11) for an inert solute can be given as follows:

$$\frac{\partial C}{\partial t} + V\frac{\partial C}{\partial z} = \frac{\partial}{\partial z}\left(D\frac{\partial C}{\partial z}\right) \tag{55}$$

$$C = 0 \qquad t = 0 \qquad z > 0 \tag{56}$$

$$C = 1 \qquad 0 < t < t_i \qquad z = 0 \tag{57}$$

$$\frac{\partial C}{\partial z} = 0 \qquad t_i < t \qquad z = 0 \tag{58}$$

Assuming that the actual moisture content profile is substituted by one of uniform $\theta = \bar{\theta}$ or $\bar{S} = (\bar{\theta} - \theta_r)/(\theta_s - \theta_r)$ extending from the soil surface $z = 0$ to the equivalent front $z = L$, while ahead of the front $(z > L)$ the moisture content has the initial θ_n. In the stage of transport with constant recharge q_0 applied on $z = 0$ and for redistribution as well, $\bar{V} = \bar{q}/\bar{\theta} = \bar{q}[\bar{S}(\theta_s - \theta_r) + \theta_r]$ is also constant in the profile and depends on *t*. Thus, the equations satisfied by the concentration C, replacing Equation (55), become

$$\frac{\partial C}{\partial t} + \bar{V}(t)\frac{\partial C}{\partial z} = \frac{\partial}{\partial z}\left(D\frac{\partial C}{\partial z}\right) \qquad 0 < z < L \tag{59}$$

To simplify the problem further, $\bar{V}$ is related to *L* by the equation

$$\bar{V}(t) = dL/dt \tag{60}$$

which is exact in the gravitational, late stage of leaching. Equation (60) is quite accurate even at the beginning of the leaching process. Another simplification is attained by ignoring the molecular diffusivity term so that Equation (59) becomes

$$\frac{\partial C}{\partial t} + \frac{dL}{dt}\frac{\partial C}{\partial z} = \lambda\frac{dL}{dt}\frac{\partial^2 C}{\partial z^2}; \qquad 0 < z < L \tag{61}$$

Carrying out the of variables

$$\zeta = z - L(t); \qquad \tau = \int_0^t \frac{\lambda}{\lambda_{max}}\frac{dL}{dt'}dt' \tag{62}$$

gives $C(z,t) = C(\zeta,\tau)$. replacing Equation (62) into Equation (61) yields

$$\frac{\partial C}{\partial \tau} = \lambda_{max}\frac{\partial^2 C}{\partial \zeta^2} \qquad -L < \zeta < 0 \tag{63}$$

while the initial and boundary conditions for Equations (56), (57), and (58) become, respectively,

$$C = 0 \qquad \tau = 0 \qquad \zeta > 0 \tag{64}$$

$$C = 1 \qquad \zeta = -L(\tau) \tag{65}$$

$$\frac{\partial C}{\partial \zeta} = 0 \qquad t > t_i \qquad \zeta = -L \tag{66}$$

In the moving frame ζ (Equation 62), the problem is therefore of heat conduction with conditions in Equation (65) or (66) along the moving boundary $\zeta = -L$. An additional boundary condition required in order to solve Equation

(63) is the existing at the front $z = L, \zeta = 0$. In a numerical exact solution of the transport problem, the suitable condition is $\frac{\partial C}{\partial z} = 0$ for $z = L_F(t)$. However, by the definition of L, the equivalent front is above the real one, (i.e., $L < L_F$).Hence, it is considered that the condition $\frac{\partial C}{\partial z} = 0$ applies sufficiently far from $z = L$ to justify accepting for C the solution pertaining to a vertical column of indefinite length. Furthermore, except for exceedingly short times, L is sufficiently large to allow eliminating boundary conditions in Equations (65) and (66) from $\zeta = -L$ to $\zeta = -\infty$. Under these simplifying conditions, the solution of Equation (63) is obtained by [13]:

$$C(\zeta, \tau) = erf\left[-\frac{\zeta}{2\sqrt{\lambda_{max}\tau}}\right] \qquad 0 > \zeta > -L \tag{67}$$

By the definition of τ and with the expected variation of λ from $\lambda = 0$ to $\lambda = \lambda_{max}$ [14], from Equation (62),

$$\tau = \frac{L^2}{26\lambda_{max}} \qquad \text{for } \frac{L}{\lambda_{max}} < 13 \tag{68}$$

$$\tau = L - \frac{13}{2}\lambda_{max} \qquad \text{for } \frac{L}{\lambda_{max}} > 13 \tag{69}$$

Hence, $C(\zeta, \tau)$ of Equation (67) is given by the following approximate expressions, after substitution of Equations (62), (68), and (69)

$$C(z, t; Y) = erf\left[\frac{L(t;Y) - z}{\left(\frac{2}{26}\right)^{\frac{1}{2}} L(t;Y)}\right] \qquad L < 13\lambda_{max} \tag{70}$$

$$C(z, t; Y) = erf\left[\frac{L(t;Y) - z}{2\lambda_{max}^{\frac{1}{2}}\sqrt{(L - 6.5)}}\right] \qquad L > 13\lambda_{max} \tag{71}$$

for $L > 13\lambda_{max}$ the dispersivity becomes constant and equal to λ_{max}.

The derivation of the expectation $E(C)$ and the variance σ_C^2 is straight-forward by replacing Equations (70) and (71) (with values of $L(t; Y)$)

$$E[C(z, t)] = \int_{-\infty}^{\infty} C(z, t; Y) f_Y(Y) dY \tag{72}$$

and

$$\sigma_C^2(z, t) = \int_{-\infty}^{\infty} (C - E(C))^2 f_Y(Y) dY \tag{73}$$

for f_Y normal as expected to be a normal PDF defined by Equation (5). PDF of C, $f_C(z, t; C)$ can be calculated by using the relationships

$$f_C dC = f_Y dY \qquad P_c = \int_0^C f_C dC = \int_{-\infty}^{Y(z,t;C)} f_Y dY \tag{74}$$

in terms of spatial distribution. It is used to analyse the fractional area of the whole field for which C is smaller than a given number.

The integration over $f_Y dY$ is also achieved when computing the various statistical moments of S at different z, and it is very simple to incorporate C in the same integration procedure.

3.6.2 Statistical computation of Concentration

With values of m_Y, σ_Y, and six deterministic parameters ($\eta, \beta, \theta_s, \theta_r, K_s^*$ and ψ_w, characterizing the field), the required moments of $C(z,t)$ are computed for several combinations of the initial and boundary parameters ($R = q_0, t_i,$ and θ_n, characterizing the transport).

The mean $E(C)$ and the variance σ_C^2 are calculated by two methods: (1) by using the numerical exact solution of the salt transport problem and, consequently, the numerical solution by finite differences as explained by [4]; and (2) by employing the approximate model of salt transport to calculate $L(t;Y)$, which is substituted in Equation (70) or (71) to find $C(z,t;Y)$.

The computation process for the approximate model includes the following steps:

a. First we set $i = 1$ then we define t, and calculate $L_i(t)$ from $L = \frac{V}{\theta - \theta_n} = \frac{(q_0 - K_n)t}{[(\theta_s - \theta_r)(\bar{S} - S_n)]}$, then we have

$$L_i(t) = V_i(t)/((\theta_s - \theta_r)(\bar{S} - S_n))$$

b. Then we define various values of z.

c. Now, compare $L_i(t)$ with the input values of z. If $L_i(t) \geq z$, then we have to compute for each input value of z, $C_i(z,t) = C(z,t;Y_i)$ from Equations (70) and (71). Otherwise, $C_i(z,t) = 0$.

d. Again, we set $i = 2,3,\ldots,N$ and repeat the above steps.

e. Once $C_i(z,t)$ are calculated for the whole set of N values, the three moments of C (averages, variances, and skewness) are calculated from

$$E[C(z,t)] = \frac{1}{N}\sum_{i=1}^{N} C_i(z,t) \tag{75a}$$

$$\sigma_C^2(z,t) = \frac{1}{N}\sum_{i=1}^{N}\{C_i(z,t) - E(C(z,t))\}^2 \quad (75b)$$

$$\gamma_C(z,t) = \frac{1}{N}\sum\{C_i(z,t) - E(C(z,t))\}^3 \quad (75c)$$

f. Now again change t and repeat the steps.

For the numerical model, finite difference equations to approximate the partial differential equation (Equation 55), the initial conditions Equation (56), and the boundary conditions (Equation 58) are first framed and then solved numerically [4]. The boundary condition (Equation 57) given at the soil surface $(z = 0)$and at $0 < t \leq t_i$ is substituted by the flux condition

$$-D(\zeta,t)\frac{\partial C}{\partial z} + V(0,t)C(0,t) - q_0/\theta(0,t) = 0 \quad (76)$$

Where $\zeta \to 0$ from the positive direction of z and the dimensionless concentration is equal to unity. Hence, the value of $D(\xi,t) = D_m[\theta(0,t)] + \lambda[L(t)]V(0,t)$ is evaluated as follows: for $L(t) < 13\lambda_{max}$

$$\lambda = \lambda_{pore} + L(t)(\lambda_{max} - \lambda_{pore})/(13\lambda_{max}) \quad (77)$$

While for $L(t) \geq 13_{max}$,

$$\lambda = \lambda_{max}$$

in which $\lambda_{max} = 3$ cm from [7] and $\lambda_{pore} = 0.1$ cm from [6]. Furthermore, $D_m[\theta(0,t)]$ is extracted from [4] $D_m(0,t) = D_0 a \exp(b\theta(0,t))$, with $D_0 = 0.04$ cm^2/hr,$a = 0.002,$ and $b = 10.$

The soil moisture retention curves that are suitable for the numerical computations are those of Equation (3), with the same values of $\beta, \psi, \theta_s \; and \; \theta_r$. Hysteresis in the $\theta(\psi)$ relationship is not assumed in the computations. The hydraulic conductivity function is also evaluated as in the approximate model with the same deterministic $\eta, K_s^*, m_Y \; and \; \sigma_Y$ and the same values of $K_s^i, i = 1,2,\ldots,N$. The calculated results of $C_i(z,t;Y_i), i = 1,2,\ldots,N$ are replaced into Equations (75a), (75b), and (75c) to compute the three central statistical moments of C. The numerical computations [4] were carried out with 90 cm depth.

3.6.3 Results

The results are demonstrate in following figures with m_Y, σ_Y and all other soil parameters. The capacity of the approximate model to simulate deterministic field conditions during transport of heavy metals are displayed by Figure 4.

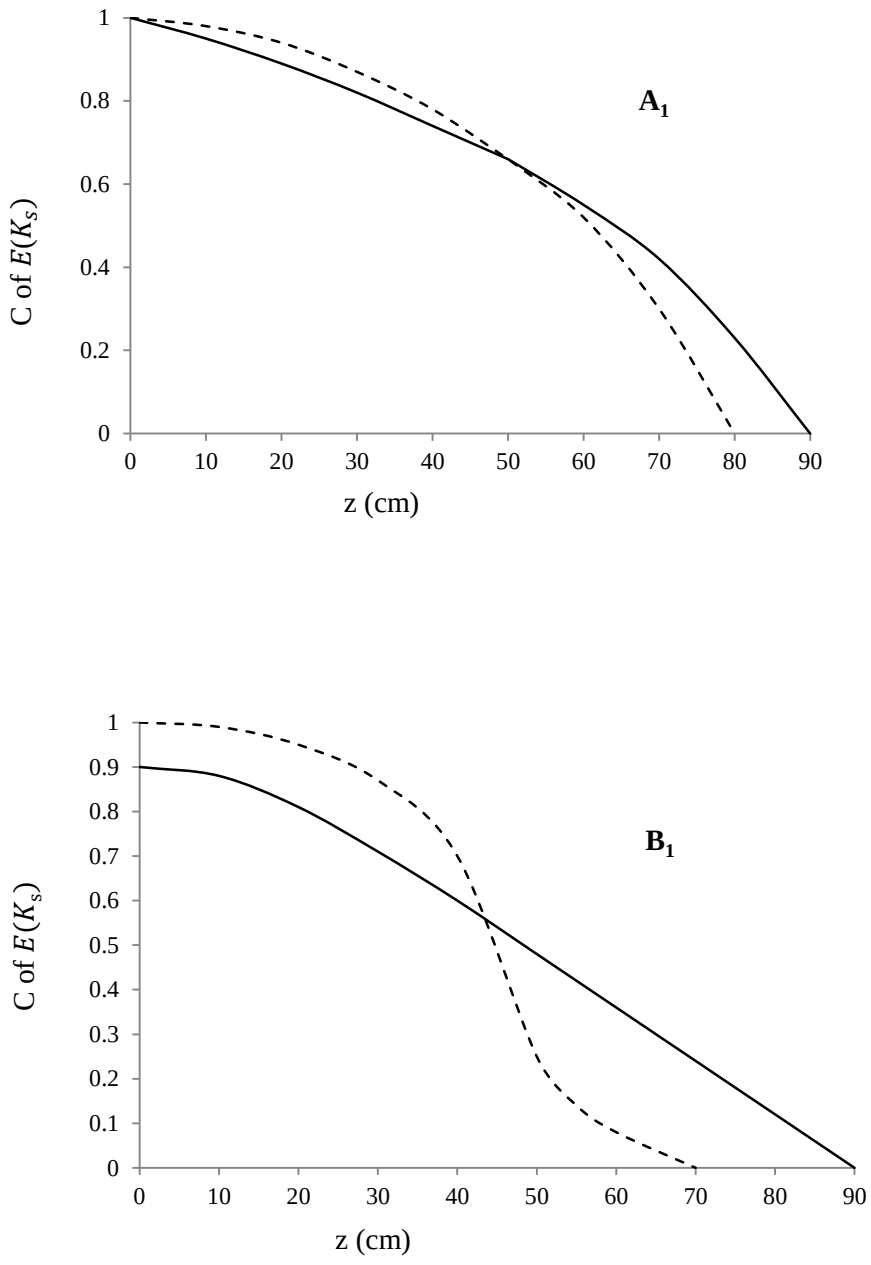

Figure 4: Computed profile of C as a function of depth (z).

A_1 : for the soil of Jaipur area. B_1 : for the soil of Kota area.

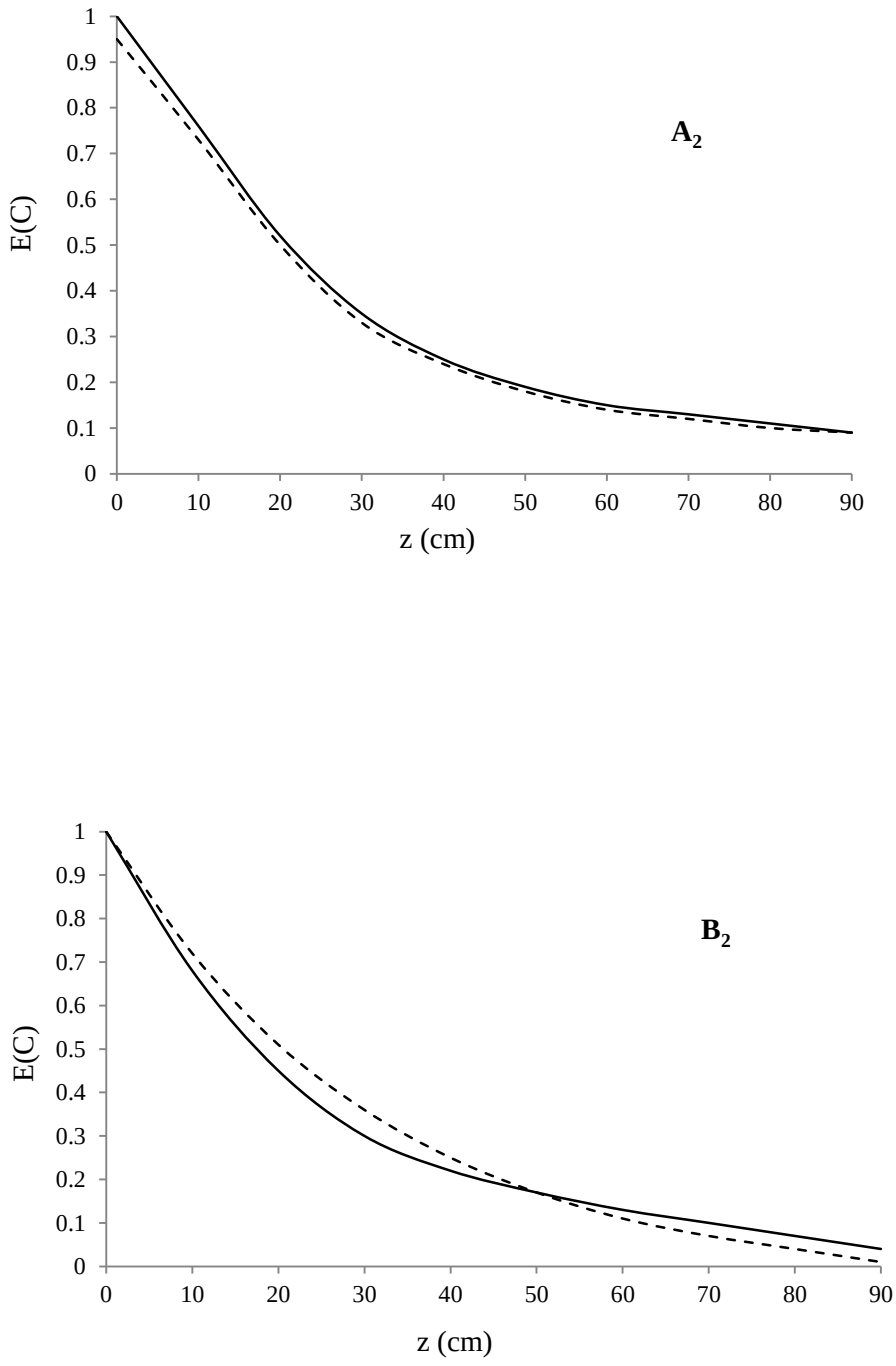

Figure 5: Expected value of C as a function of depth (z).

A_2 : for the soil of Jaipur area. B_2 : for the soil of Kota area.

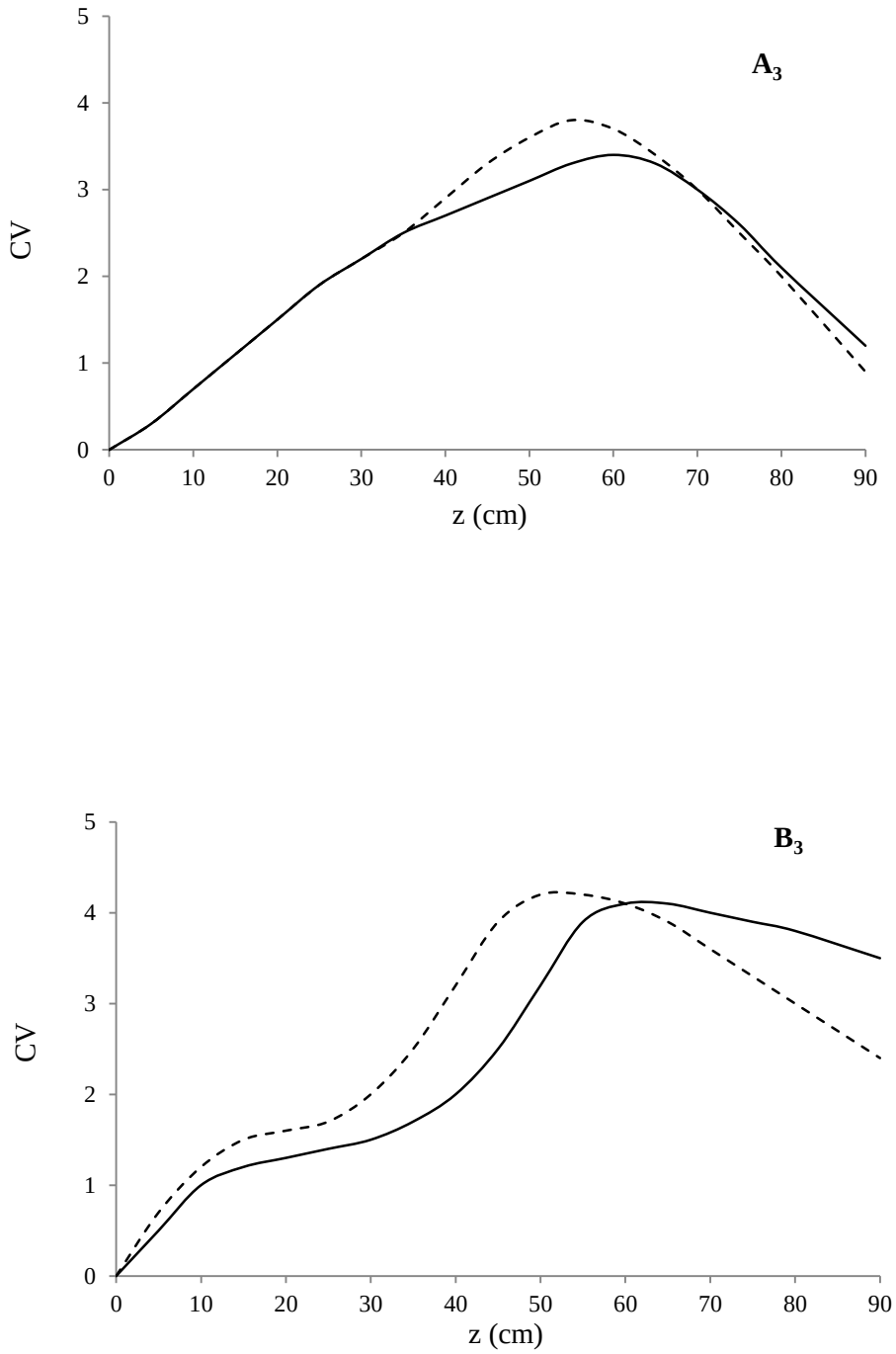

Figure 6: Coefficient of variation of C as a function of depth (z).
A_3 : for the soil of Jaipur area, B_3 : for the soil of Kota area.

It can be seen that the agreement between approximate solution is not so close. Here dotted lines show simulated results and regular lines show observed

results. The distribution of the first central moment is given in Figure 5 (A_2 and B_2) in terms of expected value of C as a function of depth (z) and that of the second moment in Figure 6 (A_3 and B_3), in terms of coefficient of variation (CV) of *C.* The agreement between the two methods of computation is enough good for the expected values as well as for the coefficient of variation of C. The results given in these figures also highlight the dissimilarities between the shapes of $E(C)$ distribution with depth from numerical computations (and approximate computations) and the shapes of deterministic $C(z,t)$.

References:

1. Bresler, E., McNeal, B.L., and Carter, D.L. 1982. Saline and Sodic Soils. Springer-Verlag, New York.
2. Saffman, P.G. 1959. A theory of dispersion in a porous medium. J. Fluid Mech. 6: 321-349.
3. Saffman, P.G. 1960. Dispersion due to molecular diffusion and macroscopic mixing in flow through a network of capillaries. J. Fluid Mech. 7: 194--208.
4. Bresler, E. 1973. Simultaneous transport of solute and water under transient unsaturated flow conditions. Water Resour. Res. 9: 975-986.
5. Segol, G. 1977. A three-dimensional Galerkin finite element model for the analysis of a contaminant transport in saturated unsaturated porous media. In: Grey, W.G., Pinder, G.F., and Brebbia, CA. (eds.). Finite Element in Water Resources. Penetech Press, London, pp. 2123-2144.
6. Bresler, E., and Laufer, A. 1974. Anion exclusion and coupling effects in non-steady transport through unsaturated soils: II Laboratory and numerical experiments. Soil Sci. Soc. Am. Proc. 38: 213-218.
7. Biggar, J.W., and Nielsen, D.R. 1976. Spatial variability of leaching characteristics of a field soil. Water Resour. Res. 12: 78-84.
8. Russo, D., and Bresler, E. 1981b. Effect of field variability in soil hydraulic properties on unsaturated water and salt flows. Soil Sci. Soc. Am. J. 45(4): 675-681.
9. Reiniger, P., and Bolt, G.A. 1972. Theory of chromatography and its applications to cation exchange in soils. N eth. J. Agric. Sci. 20: 301-313.
10. Dagan, G., and Bresler, E. 1979. Solute dispersion in unsaturated heterogeneous soil at field scale: 1. Theory. Soil Sci. Soc. Am. J. 43: 461-467.
11. Nielsen, D.R, Biggar, J.W., and Erh, K.T. 1973. Spatial variability of field measured soil-water properties. Hilgardia. 42: 215-260.
12. Warrick, A.W., Mullen, G.J., and Nielsen, D.R. 1977. Scaling field measured soil hydraulic properties using a similar media concept. Water Resour. Res. 13: 355-362.

13. Carslaw, H.S., and Jaeger, H.C. 1959. Conduction of Heat in Solids. Oxford University Press, New York.
14. Bresler, E., and Dagan, G. 1983b. Unsaturated flow in spatially variable fields: 3. Solute transport models and their application to two fields. Water Resour. Res. 19: 429-435.

Chapter 4

Transport of Solutes Under Transient Flow Conditions

4.1 INTRODUCTION

In arid and semi-arid regions the imbalance between incoming and outgoing salt has resulted in accumulation of salts in the irrigated soils. Since, the salt tolerance of crops is often based on the concentration of salts in the saturated extracts; it would be useful to have a method to predict the salt concentration throughout the soil profile under field conditions. In order to estimate the magnitude of the hazard posed by salinity, it is important to understand and identify the processes that control salt movement from the soil surface.

The transport of reactive chemicals in porous media undergoes various chemical changes through advection, diffusion and dispersion. In addition, it involves other mechanisms like rate-limited sorption and desorption, biodegradation, and chemical reaction. To understand the process of transport of heavy metals through soil layers and porous media, several mathematical models have been developed [1-7].

The impact of agricultural activities on ground water quality is closely related with the quality of water from precipitation and irrigation water. Soil-Water systems in the unsaturated zone are highly complex. Firstly, it is seldom in stable equilibrium and is in constant flux. The degree of saturation of soil–water (θ) varies both in time and space. This in turn affects flow parameters namely the suction head $h(\theta)$ and the hydraulic conductivity K (θ) which are not unique functions of θ, but exhibits hysteresis. In addition, there is the effect of air-flow through the soil and the compressibility of air, which may have some effect on unsaturated flow. Water quality problems of all kinds stem from the lack of awareness of these processes. Fertilizers are applied to agricultural fields to increase the crop yields. However, a part of the chemical constituents present in the fertilizer may percolate down to reach the ground water table thereby polluting the fresh water aquifers. It is therefore important to limit the application of fertilizers and monitor their movement in the unsaturated zone. The solute transport process has been modeled using the SWIM (Soil-Water-Infiltration-Movement) model. Saturated hydraulic conductivity was measured in the field using Guelph permeameter.

4.2 ESTIMATION OF SOIL HYDRAULIC PROPERTIES

Saturated hydraulic conductivity was determined by using disc permeameter and Guelph permeameter. Saturated moisture content was estimated by gravimetric method and soil moisture retention characteristics were determined by using pressure plate apparatus. Detailed methodology is given below.

Disc permeameter-

The disc permeameter [8] is used for the determination of soil hydraulic conductivity at the surface. The instrument allows a constant supply potential, either positive or negative, in a manner analogous to ponded ring devices. Based on the expression developed by [9], for three dimensional flow from a circular disc, the steady state infiltration (q_∞) is expressed as:

$$q_\infty = K + \frac{4b(S_0)^2}{(\theta_0 - \theta_n)\pi r}$$

(where b is a constant and taken as 0.55), θ_0 is the saturated moisture content and θ_n is the *in situ* moisture content, r is the radius of the disc (0.1 m). When the disc permeameter test is run, data are collected to obtain cumulative infiltration at various times after the start of the test. S_0 can be found from the slope of early-time plot of q_∞ vs. $St^{1/2}$ and q_∞ from the slope of the late time plot of q_∞ vs. t. The water content is measured before and after the experiment (by taking soil samples for gravimetric water content multiplied by dried bulk density determinations) to obtain the saturated moisture content (θ_0) and *in situ* moisture content (θ_n). The disc permeameter is a portable equipment, which can be used for the measurement of infiltration, hydraulic conductivity and pore characteristics.

Guelph permeameter-

The Guelph permeameter [10] was used to determine the depth-wise field saturated hydraulic conductivity. The method involves measuring the steady state rate of water recharge into unsaturated soil from a cylindrical well hole, in which a constant depth (head) of water is maintained. Constant head level in the well hole is established and maintained by regulating the level of the bottom of the air tube which is located in the center of the permeameter. As the water level in the reservoir falls, a vacuum is created in the air space above the water. The vacuum

can only be relieved when air, which enters at the top of the air tube, bubbles out of the air inlet tip and rises to the top of the reservoir. Whenever the water level in the well begins to drop below the air inlet tip, air bubbles emerge from the tip and rise into reservoir air space. The vacuum is then partially relieved and water from the reservoir replenishes the water in the well. The size of opening and geometry of the air inlet tip is designed to control the size of air bubbles in order to prevent the well water level from fluctuating.

The steady state discharge from a cylindrical well in unsaturated soil, as measured by the Guelph permeameter technique accounts for all the forces that contribute to three dimensional flow of water into soils, the hydraulic push of water into soil, the gravitational pull of liquid out through bottom of the well, and the capillary pull of water out of the well into the surrounding soil. The Richard analysis is the basis for the calculation of field saturated hydraulic conductivity. The following formulae are used to determine field saturated hydraulic conductivity, K_{fs} and matric flux potential, φ_m when following the standardized procedure

$$K_{fs} = (0.0041)(X)(R_2) - (0.0054)(X)(R_1),$$

$$\varphi_m = (0.0572)(X)(R_1) - (0.0237)(X)(R_2),$$

where,

$X =$ Reservoir constant used when the combined reservoir of the equipment is used;

$R_1 =$ Steady state rate of fall of water in the reservoir at first well height (always 5 cm in the standardized procedure);

$R_2 =$ Steady state rate of fall of water in the reservoir at second well height.

4.3 SOIL MOISTURE RETENTION CURVES

The graph between soil moisture tension and soil moisture content is referred to as soil moisture retention curve or soil moisture characteristic. If the tension is expressed as the logarithmic value, the graph is represented as pF-curve. To construct the moisture retention curve of a soil sample, the moisture content of the sample must be measured. This is done by equilibrating the moist soil sample at a succession of known pF values and each time determining the

amount of moisture that is retained. If the equilibrium moisture content (expressed preferably as volume percentage) is plotted against the corresponding tension (pF), the moisture retention curve (pF-curve) can be drawn. The pressure plate apparatus is used for the determination of pF curves in the pF range of 2.0 to 4.2 (0.1–15 bar of suction). Soil moisture is removed from the soil samples by raising air pressure in an extractor. A porous ceramic plate serves as a hydraulic link for water to move from the soil to the exterior of the extractor. The high pressure air will not flow through the pores in the plate since the pores are filled with water. The smaller the pore size, the higher the pressure that can be exerted before air passes through. During an experimental run, at any set pressure in the extractor, soil moisture will flow around each of the soil particles and out through the ceramic plate and outflow tube. Equilibrium is reached when water flow from the outflow tube ceases. At equilibrium, there is an exact relationship between the air pressure in the extractor and the soil suction (and hence the moisture content) in the samples. Accuracy of equilibrium values will be no more accurate than the regulation of air supply; therefore, the pressure control panel has independent double regulators.

4.4 SOIL WATER INFILTRATION AND MOVEMENT (SWIM) MODEL

SWIM is based on a numerical solution of the Richards equation and the advection–dispersion equation. The model has been applied to simulate the movement of solute in the unsaturated zone. The physical system and the associated flows addressed by the model are shown schematically in figure 1. Soil water and solute transport properties, initial conditions, and time dependent boundary conditions (e.g., precipitation, evaporative demand, solute input) are supplied in order to run the model [11].

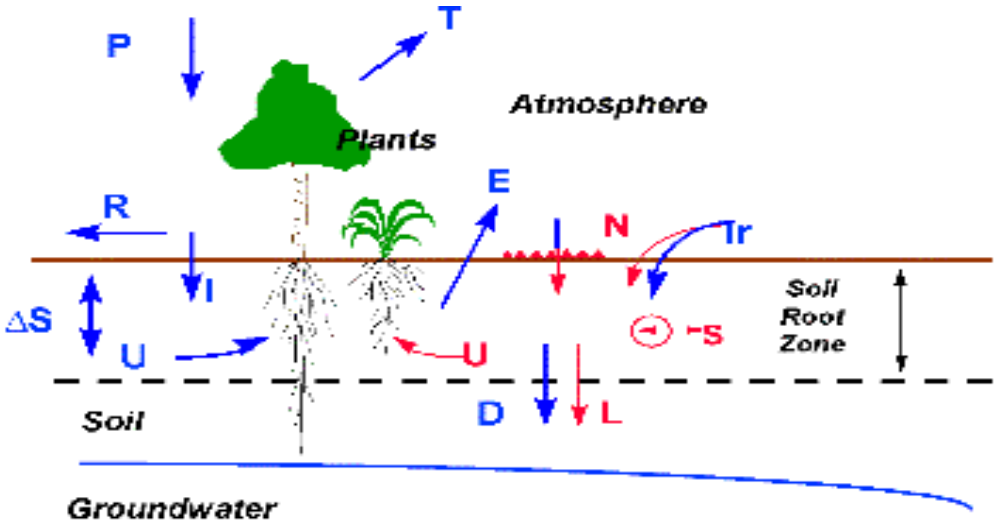

Figure 1: Schematic representation of SWIM model with components of soil water and solute balances.

Components of the soil water balances addressed by SWIM

$P =$ Precipitation, $R =$ Runoff, $I =$ Infiltration, $U_w =$ Water uptake, $U_s =$ Solute uptake, $T =$ Transpiration, $E =$ Evaporation, $D =$ Drainage, $L =$ Solute leaching, $I_r =$ Irrigation/Fertigation, $N =$ Nutrients/Fertiliser, $\Delta S =$ Storage, $S =$ Solute source/Sink [11].

4.4.1 Theoretical Development

Assuming a homogeneous and isotropic porous medium, the one-dimensional partial differential equation describing the transport of an interacting, degrading solute can be written as

$$\frac{\partial \theta C_i}{\partial t} + \frac{\partial (\rho S_i)}{\partial t} = D\left\{\frac{\partial^2 \theta C_i}{\partial z^2}\right\} - q\left\{\frac{\partial C_i}{\partial z}\right\} \pm \phi_i \qquad (1)$$

Where $C_i =$ concentration of solute (Parent material or metabolite, i), in the solution phase; $S_i =$ concentration of species I in the adsorbed phase; $\theta =$ volumetric water content; $q =$ Darcy's flux; $\phi =$ source-sink term denoting the rate of species i transformation in the degradation pathway; $D =$ apparent dispersion coefficient dependent on θ and q ; $\rho =$ soil bulk density; $z =$ vertical coordinate measured vertically down-ward' and $t =$ time In Equation (1), the apparent dispersion coefficient, d, represents the combined effects of molecular diffusion and mechanical dispersion (velocity-dependent). This combined expression can be written as

$$D = D_m + \alpha|V| \quad (2)$$

Where $D_m =$ molecular diffusion coefficient dependent on the moisture content, $\theta; V = q/\theta =$ effective pore-water velocity; and $\alpha =$ dispersivity. In laboratory experiments using relatively homogeneous porous media, values of dispersivity α, determined from breakthrough curves of conservative non interacting solutes such as chloride, are known to be of order of 0.01 to 1.0 cm. In contrast, field modeling studies use values of the dispersivity in the range of 10 to 100m, which are three to six orders of magnitude larger than typical laboratory studies. This wide difference in field and laboratory dispersivity estimates may be due to the nonhomogeneous and anisotropic nature of the field flow system compared to homogeneous, isotropic conditions of laboratory tests [12].

Given that Equation (2) is valid for defining the apparent dispersion coefficient for saturated and partially saturated flow conditions and that the mechanical dispersion term is analogous to molecular diffusion in effect, but not in mechanism, assumption of steady flow $(\partial\theta/\partial t = 0)$ reduces Equation (1) to

$$\frac{\partial C_i}{\partial t} + \frac{\rho}{\theta}\frac{\partial S_i}{\partial t} = D\left\{\frac{\partial^2 C_i}{\partial z^2}\right\} - V\left\{\frac{\partial C_i}{\partial z}\right\} \pm \frac{1}{\theta}\phi_i \quad (3)$$

Equation (3) is a generalized expression representing transport, adsorption, and transformation of a single solute species i. The source-sink term ϕ_i in Equation (3) represents the sequential steps in the degradation pathway from the parent material to the first-step product, from the first-step product to the second-step, and so on to the end of the N^{th} product. The term ϕ_i does not reflect either adsorption to the soil matrix of a degradable chemical or its metabolites. The term S_i represents the amount of parent material or metabolite adsorbed to the soil. If, for simplicity, one assumes an existence of a local equilibrium and linear adsorption isotherm solution and adsorbed phases, then

$$S_i = K_{pi}C_i \quad (i = 1,2, \ldots \ldots, N) \quad (4)$$

Where K_{pi} is the distribution or partition coefficient for the solute species i. Taking the derivative of Equation (4) with respect to time t, yields

$$\frac{\partial S_i}{\partial t} = K_{pi}\left(\frac{\partial C_i}{\partial t}\right) \quad (5)$$

Transformation process determines the fate and persistence of chemicals in the unsaturated and saturated zones. Principal among these processes are

microbiological degradation (biodegradation), hydrolysis (chemical degradation) and volatilization. For nonvolatile organic chemicals for instance, biodegradation and hydrolysis are the main attenuation mechanisms. Biodegradation is the microbiological decomposition of chemicals in the solution phase through enzymatically mediated reactions. The driving force behind these reactions is the micro-organism's need for energy, carbon, and other essential nutrients. Thus, the rate of biodegradation depends on both the concentration of the chemical and the size of the microbial population. Hydrolysis is a transformation process that changes the chemical speciation of an organic contaminant. It is the reaction of the chemical with water resulting in an exchange of some functional group from the organic molecules with a hydroxyl (OH^-) group. Like bio degradation, the extent of contaminant attenuation depends on both the chemical properties of the contaminant and the aqueous medium. Both transformation processes can be mathematically represented by first-order kinetic reactions [13]. In this study the degradation pathway of the solute can be represented in a manner similar to [14] as

$$\begin{array}{ccccc} [C_i] & \xrightarrow[k_1]{} & [C_{i+1}] & \xrightarrow[k_2]{} & [C_{i+2}] \\ \downarrow k'_1 & & \downarrow k'_2 & & \downarrow k'_3 \\ \text{Product} & & \text{Product} & & \text{Product} \end{array} \tag{6}$$

Where $k_i (i = 1,2,)$ denotes the first-order rate constants of the ith degradation step; and $k_i' (i = 1,2,3)$ denotes the rate of constants for hydrolysis. Based on Equation (6) and assuming that hydrolysis processes produce innocuous products which can be neglected in the analysis, the sequential transformations for the parent material and its two metabolites can be expressed as

$$\phi_1 = \left\{ \frac{\partial C_1}{\partial t} \right\} = -\left(k_1 + k'_1\right)\theta C_1 \tag{7a}$$

$$\phi_2 = \left\{ \frac{\partial C_2}{\partial t} \right\} = \theta k_1 C_1 - \left(k_2 + k'_2\right)\theta C_2 \tag{7b}$$

$$\phi_3 = \left\{ \frac{\partial C_3}{\partial t} \right\} = \theta k_2 C_2 - \left(k_3 + k'_3\right)\theta C_3 \tag{7c}$$

Where the subscripts 1, 2 and 3 represent the parent material and its two metabolites, respectively. Substituting Equation (5) and Equations (7a), (7b) and

(7c) into Equation (3) and upon simplification yields the following expressions for the parent material ($i = 1$) and its two metabolites ($i = 2,3$)

$$R_1\left\{\frac{\partial C_1}{\partial t}\right\} = D\left\{\frac{\partial^2 C_1}{\partial z^2}\right\} - V\left\{\frac{\partial C_1}{\partial z}\right\} - (k_1 + k'_1)C_1 \quad (8a)$$

$$R_2\left\{\frac{\partial C_2}{\partial t}\right\} = D\left\{\frac{\partial^2 C_2}{\partial z^2}\right\} - V\left\{\frac{\partial C_2}{\partial z}\right\} + k_1 C_1 - (k_2 + k'_2)C_2 \quad (8b)$$

$$R_3\left\{\frac{\partial C_3}{\partial t}\right\} = D\left\{\frac{\partial^2 C_3}{\partial z^2}\right\} - V\left\{\frac{\partial C_3}{\partial z}\right\} - k_2 C_2 - k_3 C_3 \quad (8c)$$

Where R_1, R_2 and R_3 are the retardation factors for the parent material and its first and second metabolites, respectively. These retardation factors represent the extent to which the movement of the parent material or its metabolites are retarded relative to the water movement in the soil. The retardation factors R_1, R_2 and R_3 can be defined as

$$R_1 = \left\{1 + \rho\frac{Kp^1}{\theta}\right\} \quad (9a)$$

$$R_2 = \left\{1 + \rho\frac{Kp^2}{\theta}\right\} \quad (9b)$$

$$R_3 = \left\{1 + \rho\frac{Kp^3}{\theta}\right\} \quad (9c)$$

Where Kp^1, Kp^2 and Kp^3 are the partition coefficients of the parents material, first metabolite and second metabolites, respectively.

In solving Equations (8a), (8b) and (8c) the initial and boundary conditions to be applied are

$$C_i = 0 \qquad t = 0 \qquad z \geq 0 \quad (10a)$$

$$C_i = C_i^0 \qquad 0 < t \leq t_1 \qquad z = 0 \quad (10b)$$

$$C_i = 0 \qquad t > t_1 \qquad z = 0 \quad (10c)$$

$$C_i = 0 \qquad t \geq 0 \qquad z = \infty \quad (10d)$$

$$\frac{\partial C_i}{\partial z} = 0 \qquad t \geq 0 \qquad z = \infty \quad (10e)$$

Where $C_i^0 (i = 1,2,3)$ is the initial concentration of the parent material or its two metabolites and t_1 is the time for pulse application of the chemical.

Rearranging Equations (8a), (8b) and (8c) on obtains

$$D\left\{\frac{\partial^2 C_1}{\partial z^2}\right\} - V\left\{\frac{\partial C_1}{\partial z}\right\} - (\mathrm{k}_1 + k'_1)C_1 - R_1\frac{\partial C_1}{\partial t} = 0 \qquad (11a)$$

$$D\left\{\frac{\partial^2 C_2}{\partial z^2}\right\} - V\left\{\frac{\partial C_2}{\partial z}\right\} + \mathrm{k}_1 C_1 - k_2 C_2 - R_2\frac{\partial C_2}{\partial t} = 0 \qquad (11b)$$

$$D\left\{\frac{\partial^2 C_3}{\partial z^2}\right\} - V\left\{\frac{\partial C_3}{\partial z}\right\} + \mathrm{k}_2 C_2 - k_3 C_3 - R_3\frac{\partial C_3}{\partial t} = 0 \qquad (11c)$$

Values of the transformation rate constants k_i and k_i' $(i = 1,2,3)$ given in Equations (11a), (11b) and (11c) are assumed to be constants, although it is well known that microbiologically mediated reactions are functions of many environmental variables [15]. The lack of adequate information on the functional nature of these relationships prevents representation, at present of k_i values as other than constants. However, the value of k_i can be changed with depth and time in a manner similar to [16]. In obtaining closed-form analytical solutions of Equations (11a), (11b) and (11c) the initial and boundary conditions given by Equations (10d) and (10e) are changed to

$$C_i = 0 \qquad t \geq 0 \qquad z = L \qquad (12a)$$

And

$$\frac{\partial C_i}{\partial t} = 0 \qquad t \geq 0 \qquad z = L \qquad (12b)$$

$(i = 1,2,3)$ so as to adequately describe the lower boundary of a finite column of soil of length L.

4.5 ANALYTICAL SOLUTION

A finite-difference procedure for solving a solute transport equation has been presented by [14] .However, the finite difference method, in general, requires extensive data input (data that may be sparse and uncertain) and detailed familiarity with the numerical code (a process that can be tedious and time consuming). Furthermore, the method is complicated by the dominating convective term $(V\,\partial c\,\partial z)$ which can give rise to considerable numerical oscillations or dispersion. Therefore, the closed form analytical method of solution of solute transport equation offers a useful means for an initial estimation of order of magnitude of the extent and concentration of the contaminant, Data

input are relatively simple and results compare reasonably well with those obtained Numerically [17].

The standard Laplace transform technique are used to obtain analytical solutions of Equations (11a),(11b), and (11c) subject to initial and boundary conditions given in Equations (10a),(10b),(10c),(12a), and (12b). Because this technique has been presented in detail by several investigators [18-20], only some pertinent steps in the solution procedure are outlined . Additionally, since Equations (11a), (11b) and (11c) are structurally similar, only the solution procedure for Equation (11a) is described. For the parent compound ($i = 1$), the Laplace transformation of Equation (11a) with its associated boundary condition given by Equation (10a) may be written as

$$\frac{d^2\bar{C}_1}{dz^2} - \frac{V}{D}\frac{d\bar{C}_1}{dz} - \frac{1}{D}\{(k_1 + k_1') + s\}\bar{C}_1 = 0 \tag{13}$$

Where

$$\bar{C}_1 = \int_0^\infty \bar{C}_1 \exp(-st)\, dt \tag{14}$$

Utilizing Equations (10a), (10b) and (10c) the solution of Equation (13) is

$$\bar{C}_1(z,s) = \frac{C_1^0}{s}\exp(r_1 z)\,(1 - \exp(st_1)) \tag{15}$$

Where

$$r_1 = \frac{1}{2D}\left\{V - (V^2 + 4DR_1((k_1 + k_1') + s))^{1/2}\right\} \tag{16}$$

Recognizing that

$$\lambda^{-1}\exp(r_1 z) = \frac{z}{(4\pi D t^3)^{1/2}}\, exp\left(\frac{Vz}{2D}\right).exp\left(\frac{V^2}{4D} + (k_1 + k_1')t - \frac{z^2}{4Dt}\right) \tag{17}$$

And applying the convolution theorem to obtain the Laplace inverse of Equation (15) yields.

$$C_1(z,t) = H_1(z,t) \qquad 0 < t \le t_1 \tag{18}$$

$$C_1(z,t) = H_1(z,t) - H_1(z,t - t_1) \qquad t > t_1 \tag{19}$$

Where

$$H_1(z,t) = C_1^0(P_1(\omega)) \tag{20}$$

In Which

$$P_1(\omega) = 0.5exp\left\{\frac{z(V-\omega)}{2D}\right\} erfc\left\{\frac{R_1 z - \omega t}{(4DR_1 t)^{\frac{1}{2}}}\right\} +$$

$$0.5exp\left\{\frac{z(V-\omega)}{2D}\right\}erfc\left\{\frac{R_1 z-\omega t}{(4DR_1 t)^{1/2}}\right\} \quad (21)$$

And

$$\omega = [V^2 + 4DR_1(k_1 + k_1')]^{1/2} \quad (22)$$

A procedure similar to that outlined above for $C_1(z,t)$ are adopted to obtain analytical solution for the second metabolite denote by Equation (11b).Thus, for a pulse application of c_1^0 at the soil surface for a duration t_1, analytical solution of Equation (11b) yields

$$C_2(z,t) = G_1(z,t) + G_2(z,t) \quad 0 < t < t_1 \quad (23)$$

$$C_2(z,t) = G_1(z,t) - G_1(z,t-t_1) + G_2(z,t) - G_2(z,t-t_1) \;\; t > t_1 \quad (24)$$

Where

$$G_1(z,t) = \frac{k_1 C_1^0}{k_{12}}\{\exp(-k_1 t)\, p_2(\omega_{22}) - exp[-(k_2 + k_2^1)t]p_2(\omega_{21})\} \quad (25)$$

$$G_2(z,t) = \frac{k_1 C_1^0}{k_{12}}\left\{\frac{R_1}{R_2}\right\}\times$$

$$\{\exp(-k_1 t)\,[p_1(\omega_{11}) - p_2(\omega_{22})] + \exp(-\beta_{12})\,(p_2(\omega_{23}) - p_2(\omega_{12}))\} \quad (26)$$

In which

$$k_{12} = (k_2 + k_2') - \; k_1 \quad (27)$$

$$\beta_{12} = \frac{k_1 R_1 - (k_2 + k_2')R_2}{R_1 - R_1} \quad (28)$$

$$p_i(\omega_{ij}) = 0.5exp\left\{\frac{z(V-\omega_{ij})}{2D}\right\}erfc\left\{\frac{R_j z-\omega_{ij} t}{4DR_j t^{1/2}}\right\} +$$

$$0.5exp\left\{\frac{z(V-\omega_{ij})}{2D}\right\}erfc\left\{\frac{R_j z-\omega_{ij} t}{4DR_j t^{1/2}}\right\} \quad (29)$$

Where $(i = 1,2; j = 1,2,3)$

$$\omega_{11} = \omega_{21} = V \quad (30)$$

$$\omega_{11} = (V^2 + 4DR_1(k_1 - (k_2 + k_2')))^{1/2} \quad (31)$$

$$\omega_{22} = (V^2 + 4DR_2[(k_2 + k_2') - k_1))^{1/2} \quad (32)$$

$$\omega_{23} = (V^2 + 4DR_1[(k_2 + k_2') - k_1))^{1/2} \quad (33)$$

A similar analytical procedure to that outlined above for $C_2(z,t)$ can be adopted to obtain the solution of Equation (11c).

4.6 RESULTS

Solutions of $C_1(z,t)$ and $C_2(z,t)$ for application of C_1^0 at the soil surface for a duration of t_1 were obtained using the superposition principle for $t > t_1$ as given by Equations (19) and (24). From Equations (19) and (24), it can be easily verified that $C_1(z,t) \to 0$ as $z \to 0$ and/or $t \to \infty$ for small values of t_1. Also, for continuous application of C_1^0 at the soil surface, a steady-state concentration distribution can be obtained for given z values and $t \to \infty$.

Also, comparison between observed and simulated heavy metal profiles are given in figure 2. Graph (i) is showing comparison for the soil of Jaipur area and Graph (ii) show is showing comparison for the soil of Kota area. Average concentration of heavy metals is taken in mg/cm^3 and depth is calculated in centimetre. The result indicate that in both area (Jaipur and Kota), there is an accumulation of heavy metals in the top layers of soil, Which will ultimately lead to soil and water contamination.

(i)

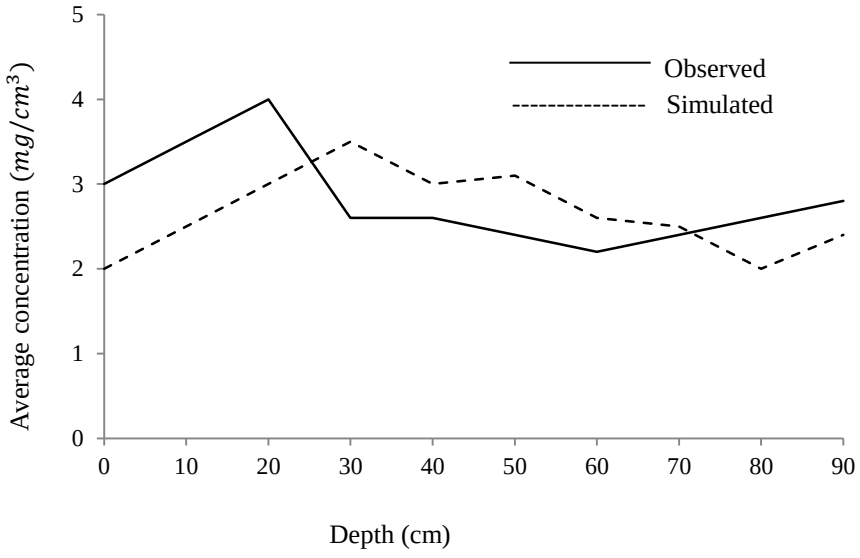

(ii)

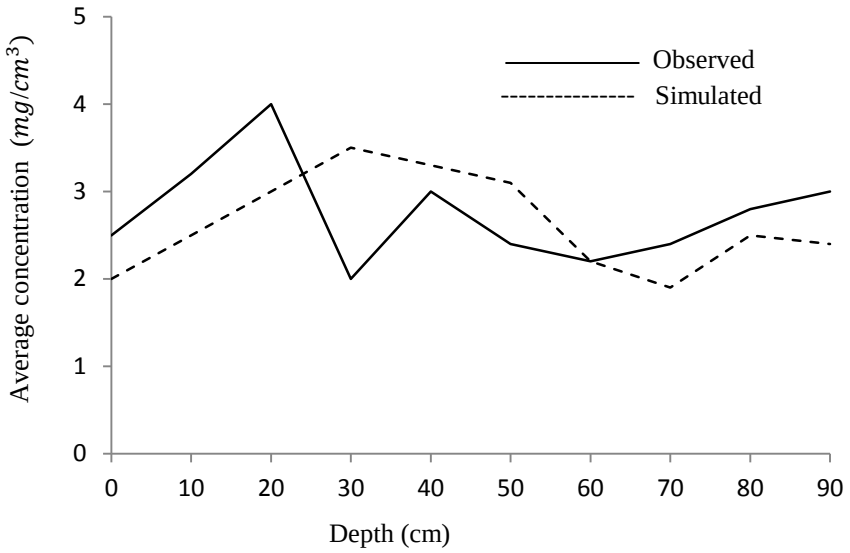

Figure 2: Comparison of observed and simulated heavy metal profiles: (i) for the soil of Jaipur area (ii) for the soil of Kota area

References:

1. Valocchi, J. 1985. Validity of the local equilibrium assumption for modeling sorbing solute transport through homogeneous soils. Water Resources Research. 21(6): 808–820.
2. Evans, L., and Stagnitti, F. 1996. Nutrient transport through basaltic agricultural soils near Australian and New Zealand National Soils Conference: Soil Science–Raising the profile, Vol.2, Oralpapers, University of Melbourne.
3. Srivastava, R., and Brusseau, M.L. 1996. Non-deal transport of reactive solutes in heterogeneous porous media:1. Numerical model development and moments analysis. Journal of Contaminant Hydrology. 24(2): 117–143.
4. Xu, L., and Brusseau, M.L. 1996. Semi analytical solution for solute transport in porous media with multiple spatially variable reaction processes. Water Resources Research. 32(7): 1985–1991.
5. Stagnitti, F.,& Li, L. 1999. A mathematical model for estimating the extent of solute and water-flux heterogeneity in multiple sample percolation experiments. Journal of Hydrology. 215(1–4): 59–69.
6. De Rooij, G.H., and Stagnitti, F. 2000. Spatial variability of solute leaching: Experimental validation of a quantitative parameterization. Soil Science Society of America Journal. 64(2): 499–504.
7. Rajmohan, N., and Elango, L. 2001. Modelling the movement of chloride and nitrogen in the unsaturated zone, New Dehli: UNESCO-IHP. Allied Publishers. 209–223.
8. Perroux, K.M., and White, I. 1988. Designs for disc permeameters. Soil Science Society of America Journal. 52(5): 1205–1215
9. Wooding, R.A. 1968. Steady infiltration from a shallow circular pond. Water Resources Research. 4(6): 1259–1273
10. Reynolds, W.D., and Elrick, D.E. 1985. *In situ* measurement of field-saturated hydraulic conductivity, sorptivity, and the (alpha)-parameter using the Guelph Permeameter. Soil Science. 140(4): 292–302.

11. Verburg, Kirsten, Ross, P.J., and Bristow, K.L. 1996. SWIMv2.1 user manual. Divisional report No.130. Australia: CSIRO.
12. Reddell, D.L., and Sunada, D.K. 1970. Numerical simulation of dispersion in groundwater aquifers. Fort Collins, Colorado: Colorado State University.
13. Smith, D.B., and Johnson, K.S. 1988. Single-step purification of polypeptides expressed in Escherichia coli as fusions with glutathione S-transferase. Gene. 67(1): 31–40.
14. Wagenet, R.J., and Hutson, J.L. 1986. Predicting the fate of nonvolatile pesticides in unsaturated zone. Journal of Environment Quality. 15(4): 315–322.
15. Ou, J.A., and Penman, S.H. 1989. Financial statement analysis and the prediction of stock returns. Journal of Accounting and Economics. 11(4): 295–329.
16. Tillostson, W.R., Robbins, C.W., and Wagnet, R.J. 1980. Soil water, solute and plant growth simulation. Utah State University, Logan, Utah Agric. Exp. Stn. Bull. No. 502.
17. Huyakorn, P.S., Mercer, J.W., and Ward, D.S. 1985.Finite element matrix and mass balance computational schemes for transport in variably saturated porous media. Water Resources Research. 21(3): 346–358.
18. Ames, W.F. 2014. Numerical methods for partial differential equations. Academic Press.
19. Bieniasz, L.K. 2015. Analytical Solution Methods. Berlin Heidelberg: Springer. 249–268.
20. Gökdoğan, A., Merdan, M., and Yildirim, A. 2012. The modified algorithm for the differential transform method to solution of Genesio systems. Communications in Nonlinear Science and Numerical Simulation. 17(1): 45–51.

Chapter 5

Kinetic Multireaction Approach for Leaching of Heavy Metals

5.1 INTRODUCTION

The soil gets contaminated with leaching of chemicals like pesticides, heavy metals, waste water released from the industries, garbage and leakage through sewage lines. Such harmful substances including heavy metals, organic chemicals ruin the layers of the soil and it is equally harmful to surface water bodies. So it has aroused the curiosity to understand the process of solute reaction pertaining to soil and water.

To trace out the transport of heavy metals, certain models are established related to absorption and release with the mould of the soil. The process of leaching in soils in terms of reactions includes precipitation/dissolution, ion exchange, and adsorption/desorption reactions [1]. The above mentioned process of absorption and release are affected by several characteristics of soil including texture, bulk density, pH, Eh, organic matter, and type and amount of clay minerals. The method of leaching and absorption of particular level of soil emanate in connection with firmly gripping the soil to the surface to form outer or inner sphere solute-surface site complexes and ion exchange is the process of substituting ions on soil particles. The composition of absorption and ion exchange is such that it has the capacity to form a surface complex and may substitute another ionic solute species already on the surface gripping site.

Equilibrium models and kinetic or time dependent models are possessed with such ingredients that explain solute leaching and released by soil matrix surfaces and equilibrium model retains the tendency of reacting faster and accurately with soil matrix. Common approaches are Langmuir-type models which describe maximum sorption term and linear and non-linear Freundlich-type models. Leaching of chemicals explained by ‘Kinetic models’ as a function of time.

5.1.1 A Simplified approach-

The easiest technique for quantifying the tendency of heavy metals in soils is given by the Freundlich equation. And there is no doubt it can be considered as one of the oldest method of non linear sorption equations. It has been given

weightage to explain solute leaching by soil [2-5]. The nonlinear Freundlich equation is

$$S = K_d c^b \tag{1}$$

where S is the quantity of solute retained by the soil ($mg\ Kg^{-1}$), c is the solute concentration in solution ($mg\ L^{-1}$), K_d is the distribution coefficient ($cm^3\ \ kg^{-1}$), and parameter b is dimensionless and has a value of $b < 1$. With reference to the equation cited above the distribution coefficient explains the separating of solute species between solid and liquid in relation to concentration range. And it is cosidered as comparable state of the balanced unchanging phase for a chemical reaction.

However the Freundlich equation has been considered accurate equation [6], and its reliability does not exhibit the exact information concerned with actual processes involved in it and it is observed that equation has the capacity to give solution to the leaching processes. Furthermore typical leaching process can be explained at least in part comparing with the Freundlich equation. Hence, K_d and b are assumed as the best models for explaining parameters in the absence of independent evidence pertaining to leaching mechanism.

The vast body of literature also explains leaching of several elements by soils [4]. The study based on [7] reveals that leaching of a single element is the part of a few soils. In this context some researchers, such as Harter [8] made a comparable study regarding different elements. To draw the estimates in connection with leaching parameters in regard to the relationship between the characteristics of soils and leaching parameters, when retention data for a particular and specific element and soil type are lacking but soil property data are available. The elements can be grouped in case when the leaching characteristics of heavy metals are same enough. In terms of regression equation an estimated b value for any one of them could be anticipated from soil pH data. Such an estimate would prove to be advantageous in explaining the leaching properties of the soil. This Simplified approach also provide characteristics of leaching properties of the soil specially when data are rarely available and it is useful for leaching parameters for the purpose of study in future.

5.2 KINETIC MULTIREACTION APPROACH

In the following process two conceptual models known as MRTM and MRM were devised and updated to explain the fortune of heavy metals in soil. And the main characteristic of both the models is that they rely on number of leaching reactions of the reversible and irreversible type. The procedure of leaching involve non-linear balanced state and at the same time linear and non-linear kinetic reactions. The pattern of functioning of these models are explained here. The MRTM agrees with the transport and possession of heavy metals in soil in relation to time and depth. The MRM explains kinetic type leaching and in such a situation no water flow is considered.

Further, in this context, it is assumed that two models MRTM and MRM as mentioned above are solved on the basis of numerical approximation techniques in connection with their equations.

5.3 FORMULATION OF MODELS

5.3.1 Multireaction model (MRM)-

Consider that the solute in the soil domain is present in the soil solution (c) and in numerous phases signifying heavy metal retained by the soil ($s_e, s_1, s_2,$ and s_{irr}) where *c* and *s* are taken in mgL^{-1} and $mgkg^{-1}$, respectively. Moreover, we assume that the leaching release procedures are run by many concurrent as well as sequential type reactions.

The sorbed phase s_e is assumed as the quantity of heavy metals which is sorbed reversibly and is in local equilibrium with that in soil solution phase (c) at all times (Figure 1). Hence, we consider that the local equilibrium hypothesis between c and s_e is useable [9]. The governing equilibrium reaction mechanism is that of the Freundlich equation by [2],

$$s_e = K_d c^b \tag{2}$$

Where K_d is the associated distribution coefficient and b is a Freundlich parameter. The value of parameter b based on batch studies, found to be consistently less than unity for various elements [10].

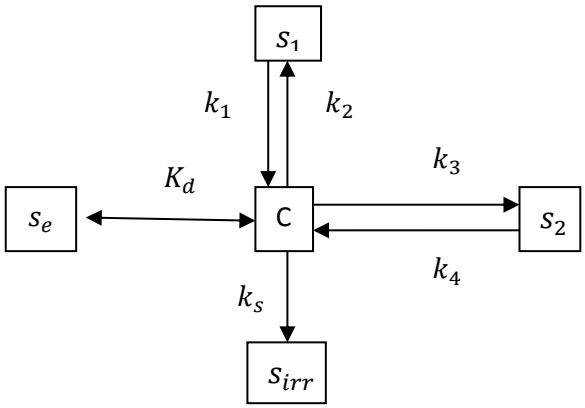

Figure 1: Schematic diagram of the multireaction retention model.

The heavy metal present in the soil solution phase (c) is considered to react kinetically (i.e., it is time dependent) and reversibly with s_1, s_2 and irreversibly with s_{irr}. The kinetic reaction between *C* and s_1 can be expressed by [11-12],

$$\rho\left(\frac{\partial s_1}{\partial t}\right) = \theta k_1 c^n - \rho k_2 s_1 \tag{3}$$

Where k_1 and k_2 are the forward and reverse rate coefficients (hr^{-1}), ρ is the soil bulk density ($g\ cm^{-3}$) and θ is the water content ($cm^3 cm^{-3}$). Parameter *n* (dimensionless) is the reaction order, where for $n \neq 1$, the reaction is nonlinear. Since it is considered that *c* and s_1 react rapidly and reversibly, k_1 and k_2 are taken relatively large in magnitude. If *c* and s_1 attains equilibrium almost instantaneously, the ratio k_1/k_2 is the equilibrium constant for that reaction.

The kinetic reaction between *c* and s_2 can be expressed by

$$\rho\left(\frac{\partial s_2}{\partial t}\right) = \theta k_3 c^m - \rho k_4 s_2 \tag{4}$$

Where k_3 and $k_4\,(hr^{-1})$ are the forward and reverse rate coefficients, respectively, and *m* is the reaction order. Equation (4) is similar to Equation (3), except that reaction (4) is considered to be more kinetic than reaction (3). As a result the magnitudes of rate coefficients k_3 and k_4 are smaller than k_1 and k_2 in Equation (3). Moreover, the reaction are assumed to be nonlinear, where in $m \neq 1$ and *m* and *n* need not be the same.

The reaction between *c* and s_{irr} may be expressed by

$$\rho\left(\frac{\partial s_{irr}}{\partial t}\right) = \theta k_s c \tag{5}$$

Where k_s is the rate coefficient for the irreversible retention reaction. Hence, s_{irr} represents an irreversible sink term.

An extension of the existing multireaction model involves a serial reaction (Figure 1). The concurrent-consecutive multireaction model involves an extra leaching stage. This stage signifies the quantity of solute strongly contained by the soil that reacts slowly and reversibly with s_2. Therefore, the model allows the description of the frequently observed very slow release of solute from the soil [13].

If a continuous reaction is involves in the model, then Equation (4) must be changed to incorporate the reversible reaction.

The MRM is required for the explanation of kinetic and equilibrium leaching behavior of sorption-desorption isotherms for heavy metals in soils. Isotherms that represent the quantity sorbed or contained by the soil vs the quantity in soil solution, that are often obtained using batch-type experiments for a range of initial (or applied) solute concentrations and for a given soil-to-solution ratio. However, for heavy metals that interact slowly, a set of isotherms with every representing one reaction time can be derived. The MRM is capable of explaining such isotherms for a given initial concentration with time as required. Detail explanation on kinetic heavy metal isotherms given by [1].

5.3.2 Multireaction and transport model (MRTM)-

This model characterizes an extension of the multireaction model (MRM) to involve transport in addition to leaching behavior of heavy metals in the soil environment. To explain the movement of heavy metals in the soil profile, the classic convective-dispersive transport equation is used. For one-dimensional, steady-state water flow conditions, the transport equation for reactive solutes may be explained as [14-15]

$$\rho \frac{\partial s}{\partial t} + \theta \frac{\partial c}{\partial t} = \theta D \frac{\partial^2 c}{\partial x^2} - v \frac{\partial c}{\partial x} - Q \qquad (6)$$

Where c is solute concentration in solution ($mg\ L^{-1}$). θ is the soil water content ($cm^3 cm^{-3}$), ρ is the soil bulk density ($g\ cm^{-3}$), D is the hydrodynamic dispersion coefficient ($cm^2 hr^{-1}$), v is Darcy's water flux density ($cm\ hr^{-1}$), x is soil depth (cm), and t is time (hr). In addition, s is the solute concentration connected with the solid phase of the soil ($mg\ kg^{-1}\ soil$), and Q is the rate of

solute removal (or supply) from soil solution ($mg\ cm^{-3}hr^{-1}$) and is not involved in s. In a fashion equal to the multireaction model explained by [11], we assume the $\partial s/\partial t$ term to explain fully reversible method between the solution and the solid phases. In particular, we assume that the reversible retention to be of the multireaction (multisite) equilibrium-kinetic type where *s* is comprised of three stages:

$$s = s_e + s_1 + s_2 \tag{7}$$

Here we consider s_e as the quantity of solute metal ($mg\ kg^{-1}$ soil) that is sorbed reversibly and is in equilibrium with that in soil solution phase (c) at all times. The governing equilibrium leaching-release mechanism is that of the nonlinear Freundlich type as explained in the MRM,

$$s_e = K_d c^b \tag{8}$$

Where K_d is the associated distribution coefficient ($cm^3 kg^{-1}$), and b is a dimensionless Freundlich parameter ($b < 1$).

The leaching-release reactions associated with s_1, s_2 are concurrent- or consecutive-type kinetic reactions (Figure 1). Where, the s_1 and s_2 phases are assumed to be in direct contact with c, and reversible processes of the (nonlinear) kinetic type govern their reactions [11-13]

$$\frac{\partial s_1}{\partial t} = k_1(\theta/\rho)c^n - k_2 s_1 \tag{9}$$

$$\frac{\partial s_2}{\partial t} = k_3(\theta/\rho)c^m - k_4 s_2 \tag{10}$$

where k_1 and k_2 are the forward and backward rate coefficients (hr^{-1}), respectively, and *n* is the reaction order connected with s_1. Also, k_3, k_4, and *m* are the reaction parameters associated with s_2. These sorbed stages may be considered as the quantity sorbed on surfaces of soil particles and chemically bound, although it is not essential to have a priori knowledge of the accurate leaching mechanisms for these reactions. In particular, these phases are considered by their release tendency and kinetic sorption to the soil solution and therefore they are susceptible to leaching in the soil. In addition, the primary difference between these two phases lies not only in the difference in their kinetic reference but also in the degree of nonlinearity as pointed by parameters *n* and *m*.

The sink-source term Q of Equation (6) is generally used to account for irreversible reactions such as precipitation-dissolution, mineralization, and immobilization. We took the sink term as a first-order kinetic process:

$$Q = \rho \frac{\partial S_s}{\partial t} = \theta k_s C \tag{11}$$

where k_s is the connected rate coefficient (hr^{-1}). This sink term is calculated in terms of a first-order irreversible reaction for reductive sorption or precipitation or interior diffusion as defined by [1, 11]. Equation (11) is similar to that for a diffusion-controlled precipitation reaction if one accepts that the equilibrium concentration for precipitation is very small [16].

The leaching-release reactions of Equation (9) through (11) include equilibrium and kinetic processes. The multireaction model is given by [11], on which this transport and leaching procedure is based, where local equilibrium with the solution phase is not implicitly assumed. It is noticed that it is important in this study to include a Freundlich-type equilibrium reaction Equation (8) into the transport model to forecast the transport behavior. In the two-site model developed by [17-18], a linear or nonlinear kinetic reaction and an equilibrium reaction are combined with the convection-dispersion transport Equation (6).

5.4 INITIAL AND BOUNDARY CONDITIONS

The retention reactions connected with the MRM seek to provide a solution for solute concentration in soil solution and sorbed phases as a function of time. To solve the MRM, the proper initial conditions are to be identified [19-20]. The initial constraints are that of a given initial solute concentration in solution and considered no solute leaching at time zero, as is the case for batch kinetic tests. Specifically, the essential conditions are as follows:

$$c = C_i, \qquad t = 0 \tag{12}$$

$$c = C_0, \qquad t > 0 \tag{13}$$

$$s_e = s_1 = s_2 = 0, \qquad t = 0 \tag{14}$$

Where C_i and C_0 are the initial and applied (input) solute concentrations, respectively. The model can include other restrictions if the concentration for every sorbed solute species (s_e, s_1, s_2) is changed from zero at the initial time for simulation $(t = 0)$.

To calculate the transport and leaching-release equations connected with the MRTM, the proper initial and boundary conditions must be identified. Here we confine to steady-state water flow conditions in a homogeneous soil with uniform moisture distribution. Hence, water flux *v* and soil moisture content Q are assumed time-invariant. It is also considered that a solute solution of known concentration (C_0) was applied at the soil surface for a given duration *t* and was thereafter followed by a solute-free solution. The conditions connected with such a pulse are normally evaluated as [17-19]

$$c = C_i, \qquad t = 0, 0 < x < L \tag{15}$$

$$s_e = s_1 = s_2 = 0, \qquad t = 0, 0 < x < L \tag{16}$$

$$vC_0 = -\theta D \frac{\partial c}{\partial x} + vc, \qquad x = 0, \mathrm{t} < \mathrm{t_p} \tag{17}$$

$$0 = -\theta D \frac{\partial c}{\partial x} + vc, \qquad x = 0, \mathrm{t} > \mathrm{t_p} \tag{18}$$

$$\frac{\partial c}{\partial x} = 0, \qquad x = L, \mathrm{t} > 0 \tag{19}$$

Equations (15) and (16) signify initial conditions for a soil profile of length *L* (cm) with uniform initial concentration C_i in the solution and devoid of sorbed phases along the soil outline at time zero. However, this model is not confined to uniform conditions; rather, nonuniform initial distributions of c, s_e, s_1, s_2 can be included. Equations (17) and (18) displays a third type of boundary condition of solute convection and dispersion at the soil surface, where C_0 is the applied solute concentration. These conditions simulate a solute input for a duration t_p(hr) that is preceded and followed by a solute-free solution. Equation (20) describe a flux- or Newman-type boundary condition at the bottom (x=L) of the soil profile at all times *t.* For a conversation of boundary conditions that explained solute transport problems [17].

The convection-dispersion solute transport Equation (6) subject to the initial and boundary conditions elaborated above is calculated using finite-difference explicit-implicit methods [22-23]. Finite-difference solutions provide distributions of solution and sorbed phase concentrations at incremental distances Δx and time steps Δt as required. In a finite difference form a variable such as c is explained as

$$c(x, t) = c(i\Delta x, j\Delta t) \tag{20}$$

Where $i = 1,2,3, \ldots N$ and $j = 1,2,3, \ldots$

$$x = i\Delta x, \qquad \text{and } t = j\Delta t \tag{21}$$

For simplicity, the concentration $c(x,t)$ is abbreviated as

$$c(x,t) = C_{i,j} \tag{22}$$

Where written letter *i* indicates incremental distance in the soil and *j* denotes the time step. Here it is considered that the concentration distribution at all incremental distances Δx is known for time *j*. Now, extract a numerical approximation of the concentration distribution at time *j+1*. The convection-dispersion Equation (6) must be explained in a finite difference form. For the dispersion and convection terms, the finite difference forms used are

$$\theta D\,\partial^2 c/\partial x^2 = \theta D\big(C_{i+1,j+1} - 2C_{i,j+1} + C_{i-1,j+1}\big)/2(\Delta x)^2 + \theta D\big(C_{i+1,j} - 2C_{i,j} + C_{i-1,j}\big)/2(\Delta x)^2 + O(\Delta x)^2 \tag{23}$$

and

$$v\frac{\partial c}{\partial x} = v\big(C_{i+1,j+1} - C_{i,j+1}\big)/\Delta\xi + O\Delta x \tag{24}$$

Where $O\Delta x$ and $O(\Delta x)^2$ are the error terms connected with the above finite-difference approximations, respectively. In the above derivations, the second-order derivative (the dispersion term) is explained in an explicit-implicit form generally known as the Crank-Nickolson or central approximation method [24]. This is extracted by using Taylor series expansion and is divided equally for time *j* (known) and time *j+1* (unknown). Such an approximation has a truncation error, as derived from the Taylor series expansion, in the order of $(\Delta x)^2$, which is elaborated as $O(\Delta x)^2$. Moreover, in the above approximations, the convection term is explained in a fully implicit form, which resulted in a truncation error of $O\Delta x$. In this numerical solution, for small values of Δx and Δt, these truncation errors are regarded to be sufficiently small and therefore they are neglected [25].

The time dependent term of Equation (6) is explained as

$$R\frac{\partial c}{\partial t} = R_{i,j}\big(C_{i,j+1} - C_{i,j}\big)/\Delta t + O\Delta t \tag{25}$$

Where the retardation term R is solved explicitly as

$$R = 1 + (b\rho K_d/\theta)c^{b-1} \tag{26}$$

It is included in a finite difference form using iteration method due to the nonlinearity of the equilibrium leaching reactions. Particularly, the retardation term is given as

$$R = \left(R_{i,j}\right)_r = 1 + (b\rho K_d/\theta)(Y^{b-1})_r \quad (27)$$

where *Y* represents the average concentration over time step *j* (known) and that at time step *j+1* for which solution is being required, such that

$$Y_r = \left(\left|C_{i,j+1}\right|_r + C_{i,j}\right)/2$$

where *r* refers to the iteration steps.

For the kinetic retention equations, the time derivative for s_1 and s_2 are explained in their finite-difference forms in an exact manner to the above equations. Therefore, neglecting the error terms and including the iteration technique, we have

$$\rho\, \partial s_1/\partial t = k_1\theta c^n - k_2\rho s_1$$
$$= k_1\theta\left\{\left[\left(C_{i,j+1}\right)_r + C_{i,j}\right]/2\right\}^n - k_2\rho\left[(s_1)_{i,j}\right]_r \quad (28)$$

$$\rho\, \partial s_2/\partial t = k_3\theta\left\{\left[\left(C_{i,j+1}\right)_r + C_{i,j}\right]/2\right\}^m - k_4\rho\left[(s_2)_{i,j}\right]_r \quad (29)$$

Moreover, the irreversible term Q was described in an implicit-explicit fashion as

$$Q = k_s Q\left(C_{i,j+1} + C_{i,j}\right)/2 \quad (30)$$

For each time step *(j+1)*, after rearrangement and incorporation of the initial and boundary conditions in their finite difference form, the finite difference of the solute transport equation can be expressed by a set of *N* equations having *N* unknown concentrations,. The form of the *N* equations is

$$a_{i,1}C_{i-1,j+1} + b_{i,j}C_{i,j+1} + u_{i,j}C_{i+1,j+1} = e_{i,j} \quad (31)$$

Where *N* is the number of incremental distances in the soil $\left(N = \frac{L}{\Delta x}\right)$. The coefficients *a,b,u* and *e* are the connected set of equation parameters. The above *N* equations are calculated simultaneously for every time step using the Gaussian elimination method [24] to find concentration *C* at all nodal points along the soil profile. In particular, MRTM gives a solution for a set of linear equations using the Thomas algorithm for tridiagonal matrix-vector equations [23]. The newly evaluated *C* values are used as input parameters in the solution for the leaching Equation (28) through (30). The solution of these equations provides the quantity of sorbed phases due to the irreversible and reversible reactions at the same time *(j+1)* and incremental distances along the soil profile.

The numerical approximation system given above for the MRTM is also used in calculating the solute leaching equations connected with the MRM. The study is based on the hypothesis that, for any given time step *j***,** the quantity in soil solution c and in the sorbed phase s_e, are in local equilibrium [9] and their amounts are associated by the K_d value according to the nonlinear Freundlich Equation (2). Therefore, for any given time step, the total amount in the solution and sorbed phases is

$$H = \theta c + \rho s_e \tag{32}$$

Or

$$H = \theta c + \rho K_d c^b \tag{33}$$

As a result, in the calculation process, from c and s_e the amount H is evaluated for time step j. To evaluate these variables at time step $j+1$ following the derivation of all other variables (i.e., s_1, s_2 etc.), we find a new value for H and partition such a value between c and s_e (based on the Freundlich equation) using the following implicit equation:

$$c = H/(\theta + \rho K_d c^{b-1}) \tag{34}$$

Which is calculated directly from Equation (37) and is based on the newly derived for the sum of concentration and equilibrium sorbed phases, *H.* Equation (38) is an implicit equation for c and where iteration is essential. In particular, a solution for concentration *C* or specifically $C_{i,j}$ at each time step is calculated as:

$$C_r = H/(\theta + \rho K_d |c^{b-1}|_{r-1}) \tag{35}$$

5.5 RESULTS

For the MRTM and MRM, the above equations are calculated in a serial manner for each time step, until the required time for simulation is achieved. To explain kinetic behaviour of heavy metal leaching as obtained by multireaction and transport model (MRTM), simulation figures are given. This explains the sensitivity of heavy metal concentration results to a wide range of model parameters necessary for the MRTM with emphasis on the governing leaching mechanism. The parameters selected for simulation analysis are $\rho = 1.25\ g\ cm^{-3}, \theta = 0.4\ cm^3, L = 90\ cm, D = 1.0\ cm^2 hr^{-1}$. It is assumed that steady water flow velocity v is constant. The influence of the distribution

coefficient K_d, which is associated with s_e of the equilibrium type reaction, on the transport of heavy metal is shown in Figure 2. Here the nonlinear parameter b is taken as 0.5 and all reaction coefficients are equal to zero. The shape of the break through curve of Figure 2 reflects the influence of a nonlinear Freundlich type sorption. A BTC is a representation of heavy metal concentration in terms of relative concentration (C/C_0) vs depth (z), where C_0 is the maximum concentration. The influence of a wide range of b values on the shape of the BTC is shown in Figure 3(A) and Figure 3(B). For values of $b < 1$, the shape of the BTCs indicates a sharp rise in concentration or a steep sorption side with an increase of the tailing of the desorption side for decreasing values of b. For values of $b > 1$, the sorption side indicates a slow increase of concentration, which is associated with a lack of tailing of the desorption side of the BTCs.

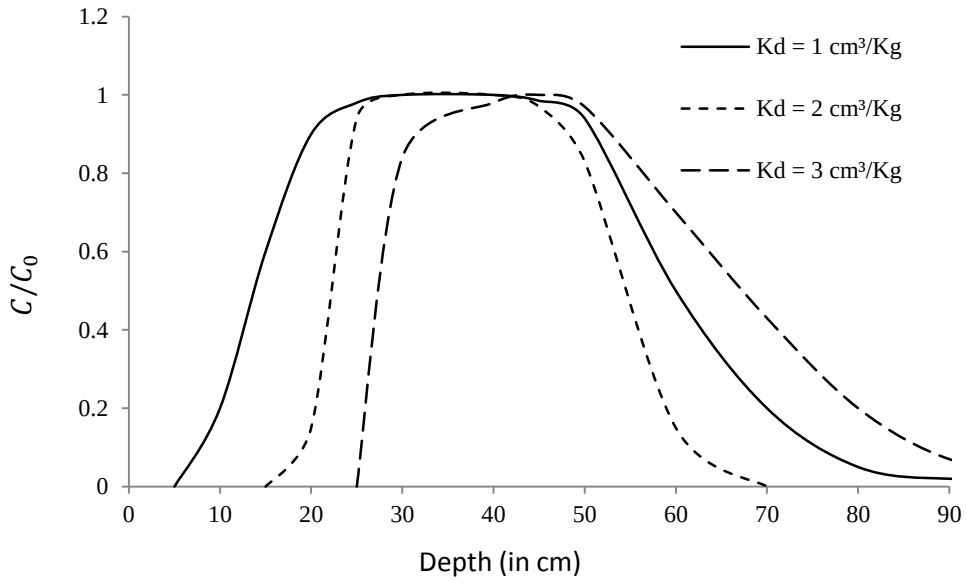

Figure 2: Breakthrough curves for several K_d values where $b = 0.5\ and\ k_1 = k_2 = k_3 = k_4 = 0$.

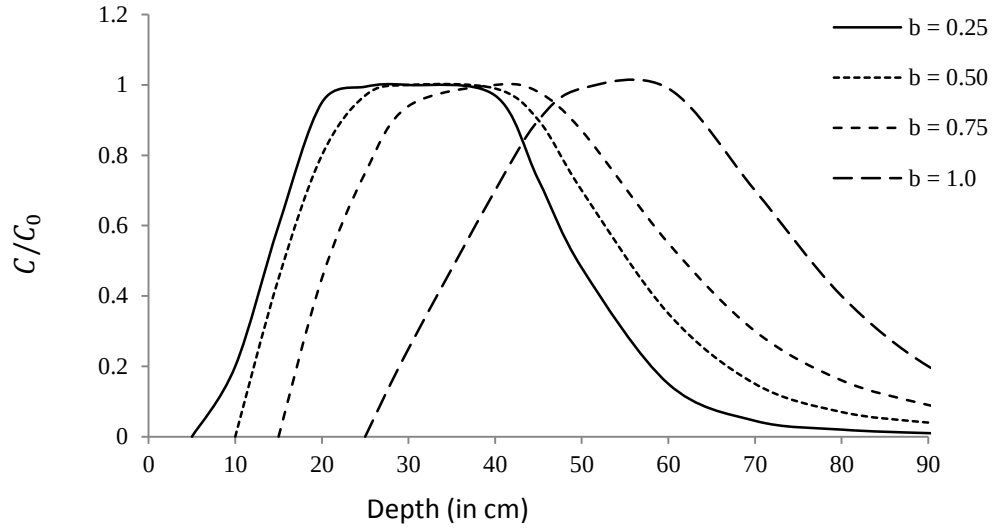

Figure 3(A): Breakthrough curves for several b values where $b \leq 1.0\ and\ k_1 = k_2 = k_3 = k_4 = 0$.

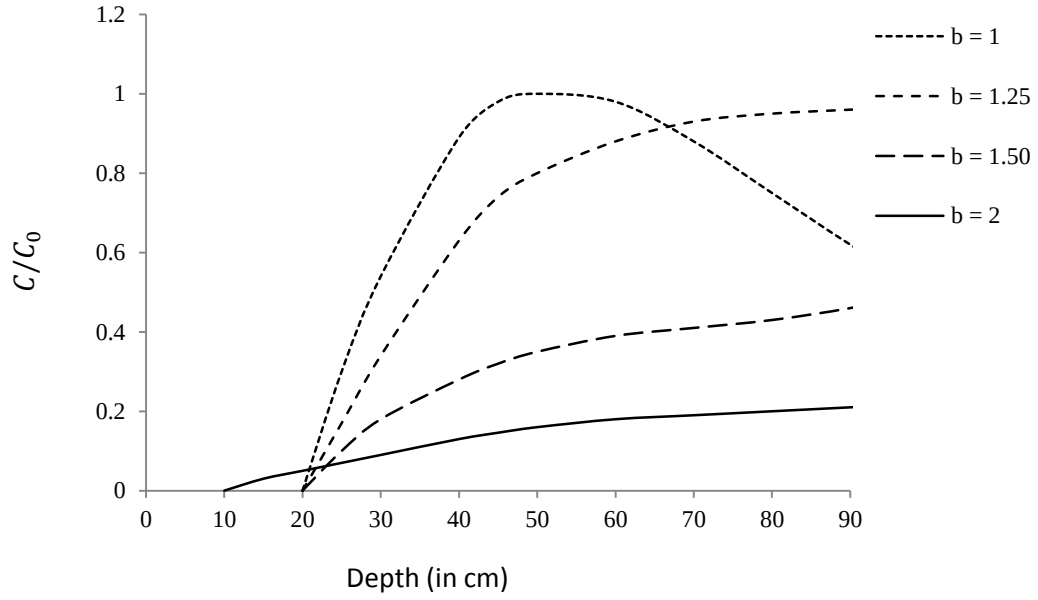

Figure 3(B): Breakthrough curves for several b values where $b \geq 1.0\ and\ k_1 = k_2 = k_3 = k_4 = 0$.

(C/C_0 is heavy metal concentration, where 0.2 units equals to $90\ mg/L$ in Figure 2, 3(A) and 3(B))

References:

1. Amacher, M.C., Kotuby-Amacher, J., Selim, H.M., and Iskandar, I.K. 1986. Retention and release of metals by soil- evaluation of several models. Geoderma. 38: 131-154.
2. Helfferich, F. 1962. Ion Exchange. New York: McGraw-Hill.
3. Sposito, G. 1984. The Surface Chemistry of Soils. New York: Oxford University Press.
4. Travis, C.C. and Etnier, E.L. 1981. A survey of sorption relationships or reactive solutes in soil. Journal of Environmental Quality. 10: 8-17.
5. Murali, V. and Aylmore, L.A.G. 1983. Competitive adsorption during solute transport in soils. Mathematical models. Soil Science. 135: 143-150.
6. Sposito, G. 1980. Derivation of the Freundlich equation for ion exchange reactions in soils. Soil Science Society of America Journal. 44: 652--654.
7. Goldberg, S. and Glaubig, R.A. 1986. Boron adsorption on California soils. Soil Science Society of America Journal. 50: 1173-1176.
8. Harter, R.D. 1983. Effect of soil pH on adsorption of lead, copper, zinc, and nickel. Soil Science Society of America Journal. 47: 47-51.
9. Rubin, J. 1983. Transport of reactive solutes in porous media, relation between mathematical nature of problem formulation and chemical nature of reactions. Water Resources Research. 9: 1231-1252.
10. Buchter, B., Davidoff, B., Amacher, M.C., Hinz, C., Iskandar, I.K., and Selim, H.M. 1989. Correlation of Freundlich K. and n retention parameters with soils and elements. Soil Science. 148: 370-379.
11. Amacher, M.C., Selim, H.M., and Iskandar, I.K. 1988. Kinetics of chromium (VI) and cadmium retention in soils, a nonlinear multireaction model. Soil Science Society of America Journal. 52: 398-408.
12. Van Genuchten, M.Th., Davidson, J.M., and Wierenga, P.J. 1974. An evaluation of kinetic and equilibrium equations for the prediction of pesticide movement in porous media. Soil Science Society of America Proceedings. 38: 29-35.

13. Selim, H.M. 1989. Prediction of contaminant retention and transport in soils using kinetic multireaction models. Environmental Health Perspectives. 83: 69-75.
14. Brenner, H. 1962. The diffusion model of longitudinal mixing in beds of finite length; numerical values. Chemical Engineering Science. 17: 220-243.
15. Nielsen, D.R., Van Genuchten, M.Th., and Biggar, J.M. 1986. Water flow and solute transport process in the unsaturated zone. Water Resources Research. 22: 89S-108S.
16. Stumm, W., and Morgan, J.J. 1981. Aquatic Chemistry. New York: Wiley Interscience.
17. Selim, H.M., and Mansell, R.S. 1976. Analytical solution of the equation of reactive solutes through soils. Water Resources Research. 12: 528-532.
18. Klute, A., and Cameron, D. 1977. Convective-dispersive solute transport with chemical equilibrium and kinetic adsorption model. Water Resources Research. 13: 183-188.
19. Selim, H.M., Davidson, J.M., and Mansell, R.S. 1976. Evaluation of a two-site adsorption-desorption model for describing solute transport in soils. In Proceedings of Summer Computer Simulation Conference. Washington. D.C. L.' Jolla. California: Simulation Councils. Inc. p. 144-448.
20. Selim, H.M. 1978. Evaluation of a multi-step model for describing phosphorus transformations and transport in soils. In Proceedings of Summer Computer Simulation Conference, Newport Beach, California. La Jolla. California: Simulation Councils. Inc. p. 647-653.
21. VanGenuchten, M.Th., and Parker, J.C. 1984. Boundary conditions for displacement experiments through short laboratory soil columns. Soil Science Society of America Journal, 40: 473-480.
22. Remson, I., Hornberger, G.M., and Molz, F.J. 1971. Numerical Methods in Subsurface Hydrology. New York: Wiley.
23. Pinder, G.F., and Gray, W. 1977. Finite Element Simulation in Surface and Subsurface Hydrology. New York: Academic Press.

24. Carnahan, P., Luther, H., and Wilkes, J.O. 1969. Applied Numerical Methods. New York: Wiley.
25. Henrici, P. 1962. Discrete Variable Methods in Ordinary Differential Equations. New York: Wiley.

Chapter 6

Assessment of Heavy Metal Contamination in Soil Sediments of Jaipur and Kota Industrial Areas

6.1 METHOD AND MATERIAL

Heavy metal contamination to soil and the environment has been accelerated in modern society due to industrialization, rapidly expanded world population, and intensified agriculture [1]. Environmental contamination is correlated with the degree of industrialization and intensities of chemical usage. The effect of heavy metals on the environment is of serious concern and threatens life in all forms [2]. Toxicity of these compounds has been reported extensively [3-5]. They accumulate over time in soils which act as a sink from which these toxicants are released to the groundwater and plants, and end up through the food chain in man thereby causing various toxicological manifestations. According to IARC [6], Cadmium (Cd) is an extremely toxic industrial and environmental pollutant classified as a human carcinogen. Human occupational exposure to chromium clearly indicates that these compounds are respiratory tract irritants, resulting in airway irritation, airway obstruction, and lung, nasal, or sinus cancer [7]. Cr compounds are teratogenic in animals and can induce mutations. Toxicity of copper is associated with abdominal pain, headache, nausea, dizziness, vomiting and diarrhea, gastrointestinal bleeding, liver and kidney failure, and death. Nickel is one of many carcinogenic metals known to be an environmental and occupational pollutant. Chronic exposure to Ni is connected with increased risk of lung cancer, cardiovascular disease, neurological deficits, and developmental deficits in childhood [8]. Lead poisoning tends to have increased risk for cardiovascular disease, nephropathy, immune suppression and liver impairment [9]. Zinc toxicity may result in nausea, vomiting, diarrhea, metallic taste, kidney and stomach damage and other side effects [10].

The main objective of the present study is to determine the level of soil pollution with respect to some heavy metals in Jaipur and Kota districts of Rajasthan.

6.1.1 Chemicals

All chemicals used in the present study were of analytical reagent grade and were purchased from reliable firms.

6.1.2 Studied area

The present study area covers Jaipur and Kota districts of Rajasthan. The soils were collected from different industrial areas that could contribute to a

higher level of heavy metals contamination. Total eight different locations were selected in the present study, Four different locations that were selected in Jaipur industrial area are: Sitapura Industrial area (location 1), Jhotwara Industrial Area (location 2), RIICO Industrial Area (location 3) and Viswakarma Industrial Area (location 4); and four different locations were selected in Kota industrial area which are: Indraprastha Industrial area (location 5), Chambal Industrial Area (location 6), RIICO Paryavaran Industrial Area (location 7) and Large scale Industrial Area (location 8).

6.1.3 Sampling

To avoid contamination of the soil sample, essential cleanness conditions were maintained. The samples were collected randomly in triplicates from different sites of industrial area. All samples were collected and put in clean polythene bags and they were sealed in double bags. Use of metal tools was avoided and a plastic spatula was used for sample collection. The soil samples consisting of three subsamples were collected at random by digging the soil at four different depths: from the surface layer (0–5 cm depth), the first feet below the surface (30 cm depth), the second feet below the surface (60 cm depth) and the third feet below the surface (90 cm depth). Samples were collected with a plastic spade during the winter of 2015, and the collected samples were placed in black polyethylene bag. All samples were labelled appropriately.

6.1.4 Analysis of the samples

The soil samples were allowed to dry for 48 h at room temperature. The dry soil sample was disaggregated in mortar pestle. The sample was finely powdered, sieved with a 2 µm sieve and stored in plastic vials. One gram of each sample was weighed and transferred into pre-washed and oven dried beakers. The dried samples were wet digested according to standard protocols and they were labelled properly.

6.1.5 pH analysis

The soil samples were collected from upper surface, first foot, second foot and third foot of sediments in triplicates. The pH was measured as described by Liza Jacob *et al*. [11]. A soil suspension was made with soil and water in the ratio 1: 2. Ten gram of soil sample was taken in a 50 ml beaker and added 20 ml of

distilled water into it. The solution was stirred immediately with glass rod for 30 minutes. It was stirred again just before taking pH reading. The pH was read using pH meter. The electrodes of the pH meter were washed with distilled water after each determination. For standardizing the pH meter, two buffer solutions of known pH values (pH-4 and pH-7) were used.

6.1.6 Heavy metal detection

The detection of heavy metals is accomplished by various methods but here the AAS technique was used, which is relatively simple, versatile, accurate and free from interferences. Heavy metals readily form complexes with organic constituents and therefore, it is necessary to destroy them by digestion with strong acids. Nitric-perchloric acid digestion method was performed for sample preparation [12]. One gram of a sample was placed in 250 ml digestion tube and 10 ml of concentrated HNO_3 was added. The mixture was boiled for 30-45 minutes to oxidize all easily oxidizable matter. After cooling, 5 ml of 70 % $HClO_4$ was added and the mixture was boiled gently till the appearance of dense white fumes. The contents were cooled and 20 ml of distilled water was added, and re-boiled to stop the release of any fumes. The solution was cooled again, filtered off through Whatman No. 42 filter paper and transferred to 25 ml volumetric flask. The volume was made up to the mark with distilled water.

All of the digested soil samples were analyzed for their total concentrations of Cd, Cr, Cu, Ni, Pb and Zn by using Atomic Absorption Spectrophotometer (Perkin Elmer A Analyst 300).

6.1.7 Statistical calculations

The S.E.M. was calculated by the following formula:

$$\text{S.E.M.} = \frac{\text{S.D.}}{\sqrt{n}}$$

Where x = individual observation

n = number of observation

The results were expressed as Mean ± S.E.M. (Standard Error of Mean).

The present study area covers the Jaipur and Kota districts of Rajasthan. Forty eight soil samples were collected from different industrial areas and

analyzed. The concentration of six heavy metals (Cd, Cr, Cu, Ni, Pb and Zn) were identified and quantified by using Atomic absorption spectrophotometer in 4 different locations. Reconnaissance survey was carried out on the surface layer (0–5 cm depth), the first foot below the surface (30 cm depth), the second foot below the surface (60 cm depth) and the third foot below the surface (90 cm depth) to determine the total metal concentration. Sampling was done according to standard procedures.

Various results obtained are tabulated and depicted below:

6.2 DISTRIBUTION OF STUDIED HEAVY METALS IN DIFFERENT LOCATIONS OF JAIPUR DISTRICT

Table and Figure 1, 2, 3 and 4 represents the heavy metal burden in soil samples of Jaipur district. Four different industrial areas were selected in the present study. The survey were carried out in Sitapura industrial area, Jhotwara industrial area, RIICO industrial area and Viswakarma industrial area, which were named location 1, 2, 3 and 4 accordingly.

Table and Figure 1-4 indicates that most of the metals were found in varying concentrations. The mean concentrations of Cd, Cr, Cu, Ni, Pb and Zn in almost all soil samples were significantly higher than background contents of these heavy metals in the soils, suggesting the industrial area are highly polluted. The maximum average concentration is showed by Zn metal (254.16 ppm) in location 4. This was followed by Pb (248.60 ppm) and Cu (227.37 ppm) mean concentrations at location 3 and 4, respectively. The maximum obtained average concentration of Cr was 200.61 ppm (location 1), which was further followed by Ni (91.87 ppm) and Cd (22.5 ppm) at location 4. The maximum obtained average concentrations of heavy metals decreased as follows- Zn > Pb > Cu > Cr > Ni > Cd.

6.2.1 Distribution of heavy metals at location 1- Sitapura Industrial Area (Table and Figure 1)

Table and Figure 1 represent the descriptive statistics of the heavy metal concentrations of Sitapura industrial area. There was a remarkable change in the content of heavy metals among the sampled soils. The concentrations of Cd, Cr,

Cu, Ni, Pb and Zn varied between 2.56 and 15.42, 56.17 and 374.83, 54.58 and 198.34, 21.65 and 134.87, 58.84 and 284.6, 12.76 and 208.54 ppm, respectively. All of the mean values of the heavy metal concentrations were significantly higher than their normal permitted values. The maximum average concentrations of Cr, Cu and Pb were found in the uppermost surface (200.61 ppm, 144.50 ppm and 184.59 ppm, respectively), while Ni was present maximally in the second foot of sediment (86.85 ppm). The average concentrations of Cd and Zn were highest in the first foot of sediment (8.78 ppm and 123.11 ppm), respectively.

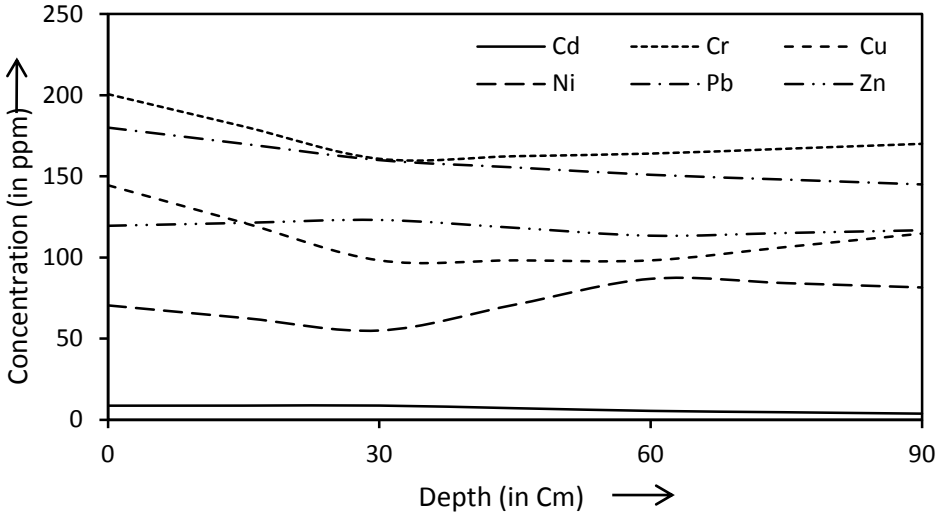

Figure 1: Heavy metals concentrations in soil samples of Sitapura Industrial area, Jaipur district.

6.2.2 Distribution of heavy metals at location 2 - Jhotwara Industrial Area (Table and Figure 2)

The ranges of the concentrations of the studied metals in Jhotwara industrial area are shown in Table and Figure 2. The Table and Figure 2 shows that the heavy metal concentrations in the upper surface sediments decreased in the following order: Pb > Zn > Cr > Cu > Ni > Cd. In the first foot of sediment sampled, the heavy metal concentrations decreased in the following order: Pb > Cr > Zn > Cu > Ni > Cd. In the second and third foot of sediment sampled, the heavy metal concentrations decreased in the following order: "Pb > Cr > Cu > Zn > Ni > Cd" and "Pb > Cu > Cr > Zn > Ni > Cd", respectively. The average concentrations of heavy metals were predominated mostly in the upper most surface having average

values of 15.79 ppm for Cd, 158.59 ppm for Cr, 139.38 ppm for Cu, 54.07 ppm for Ni, 212.41 ppm for Pb and 188.24 ppm for Zn.

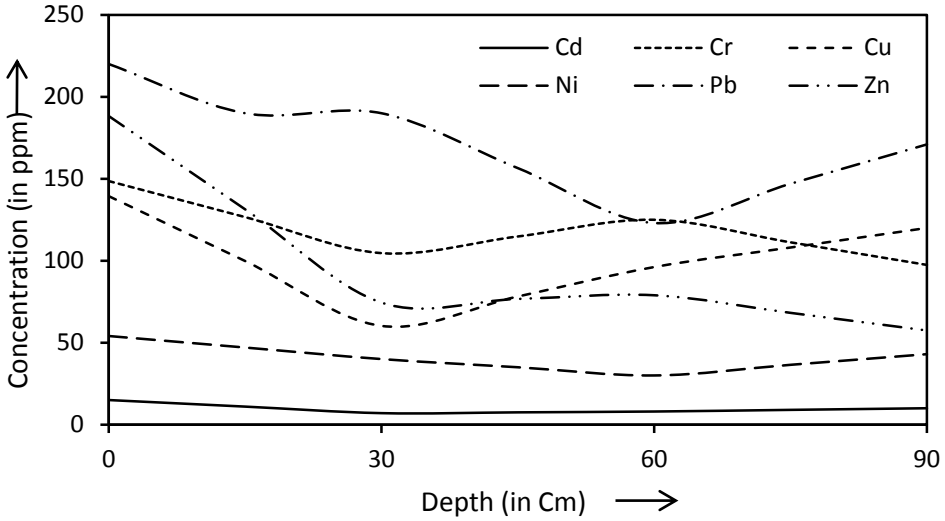

Figure 2: Heavy metals concentrations in soil samples of Jhotwara Industrial Area, Jaipur district.

6.2.3 Distribution of heavy metals at location 3 - RIICO Industrial Area (Table and Figure 3)

The spatial distribution of heavy metals (Cd, Cr, Cu, Ni, Pb and Zn) in the RIICO industrial area is shown in Table and Figure 3. In the upper surface stratum, the average concentrations of Cr (142.98 ppm), Cu (200.26 ppm) and Pb (248.60 ppm) were obtained at their highest levels. In the first foot of sediment, the average concentration of Zn was highest (210.80 ppm). Other studied metals (Cd and Ni) were highest at second foot level with average values of 14.22 ppm and 89.60 ppm, respectively. The minimum concentrations of Cd (3.95 ppm) and Ni (7.67 ppm) were found in the first foot of sediments, while third foot strata were showing minimum concentration Cr (10.36 ppm) and Cu (17.83 ppm). The lowest concentrations of Pb (19.65 ppm) and Zn (26.98 ppm) were present in the second foot strata and uppermost surface, respectively.

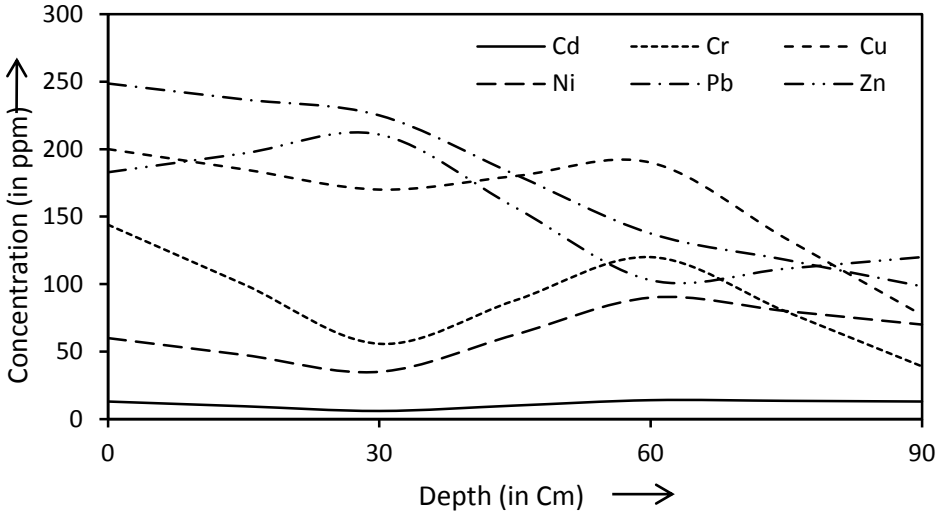

Figure 3: Heavy metals concentrations in soil samples in RIICO Industrial Area, Jaipur district.

6.2.4 Distribution of heavy metals at location 4 - Viswakarma Industrial Area (Table and Figure 4)

Table and Figure 4 show total concentrations of heavy metals in the Viswakarma industrial area. The studied heavy metals Cd, Cr, Cu, Ni, Pb and Zn concentration levels ranged between 5.87 to 37.15 ppm, 19.67 to 248.16 ppm, 34.56 to 357.78 ppm, 12.87 to 149.98 ppm, 17.84 to 439.67 ppm and 18.89 to 407.87 ppm, respectively with maximum mean values of 22.5 ppm for cadmium, 121.6 ppm for chromium, 227.37 ppm for copper, 91.87 ppm for nickel, 240.30 ppm for lead and 254.16 ppm for Zn. In this study, the following trend of heavy metal contamination was established. Excessive level of Pb was observed in the upper most soil layer (Mean value- 240.30 ppm) as compared to all the other elements. In the first, second and third foot of strata, the predominating heavy metal was mainly Cu with an average value of 206.11 ppm and 227.37 and 190.26 ppm, respectively.

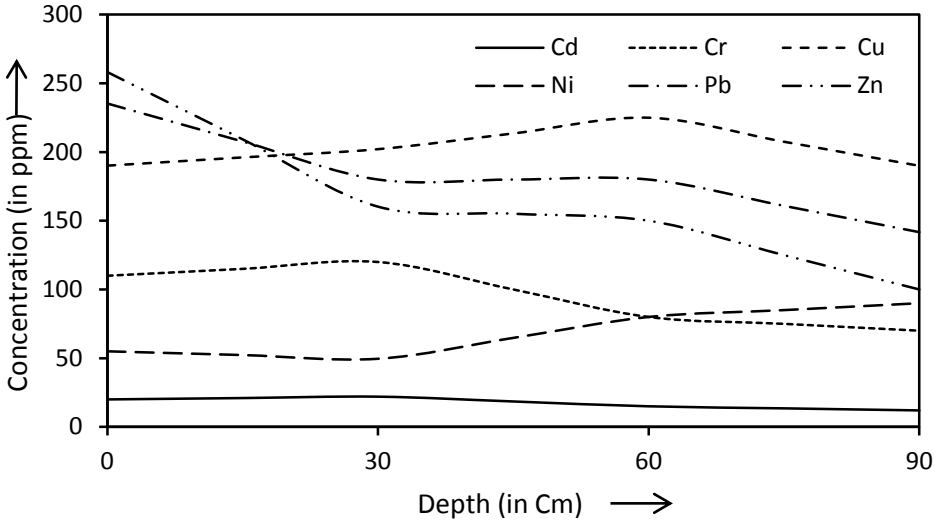

Figure 4: Heavy metals concentrations in soil samples of Viswakarma Industrial Area, Jaipur district.

6.3 DISTRIBUTION OF STUDIED HEAVY METALS IN DIFFERENT LOCATIONS OF KOTA DISTRICT

The change in the heavy metal concentrations were recorded in 4 different locations of Kota district. Soil samples were collected from the industrial region of Indraprastha, Chambal, RIICO Paryavaran and Large scale area; and these industrial areas were designated as location 5, 6, 7 and 8, respectively. The results concerning industrial areas of Kota are given in Table and Figures (5, 6, 7 and 8).

6.3.1 Distribution of heavy metals at location 5 - Indraprastha Industrial Area (Table and Figure 5)

Plumbism was evident in all the strata with maximum concentration of Pb (940 ppm) as compared to other studied heavy metals. The concentration of Pb ranges from 36.85 ppm to 940 ppm. The second most prevalent heavy metal was Zn with the average mean values of 312.21 ppm (upper surface), 301.56 ppm (first feet) and 257.56 ppm (second feet). However, in third feet of strata, Zn was predominating heavy metal with the average mean value of 275.52 ppm. Highest mean value for Cd (22.83 ppm) was observed in third foot of strata. Cr and Ni were showing elevated concentrations in second foot layer with the mean values

of 174.07 ppm and 86.85 ppm, respectively. Average concentration of Cu was present maximum at first feet of strata (222.65 ppm).

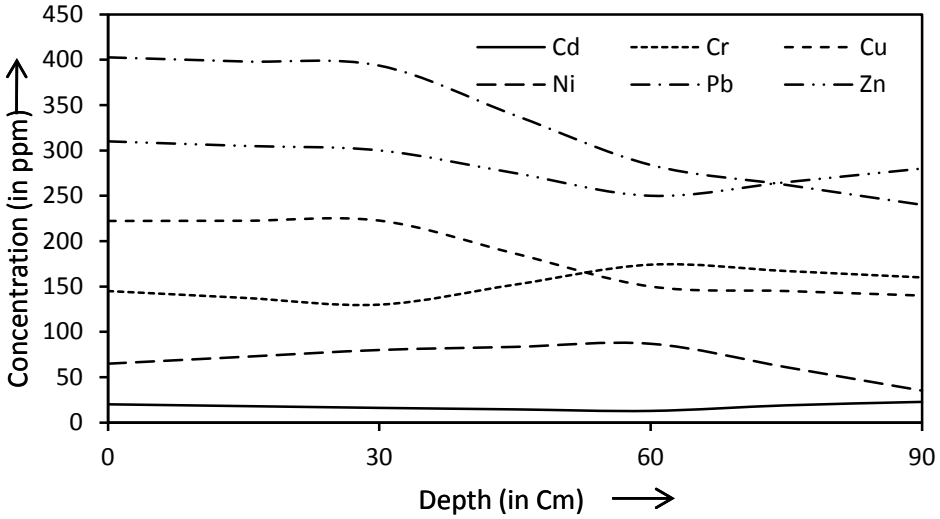

Figure 5: Heavy metals concentrations in soil samples of Indraprastha Industrial area, Kota district.

6.3.2 Distribution of heavy metals at location 6 - Chambal Industrial Area (Table and Figure 6)

Heavy metal distribution in Chambal industrial area showed elevated levels of all heavy metals in the uppermost surface. The maximum average concentrations of Cd, Cr, Cu, Ni, Pb and Zn in topmost surface were found to be 25.29 ppm, 184.74 ppm, 210.85 ppm, 51.02 ppm, 371.80 ppm and 292.64 ppm, respectively.

Minimum average concentration of Cd, Ni and Pb were present in the third feet of strata (15.06 ppm, 21.36 ppm and 269.87 ppm, respectively), while Cu mean concentration value was least in the first feet of strata (125.85 ppm). Cr and Zn in second foot of sediment were revealing lowest mean concentration values of 104.15 ppm and 169.86 ppm, consequently.

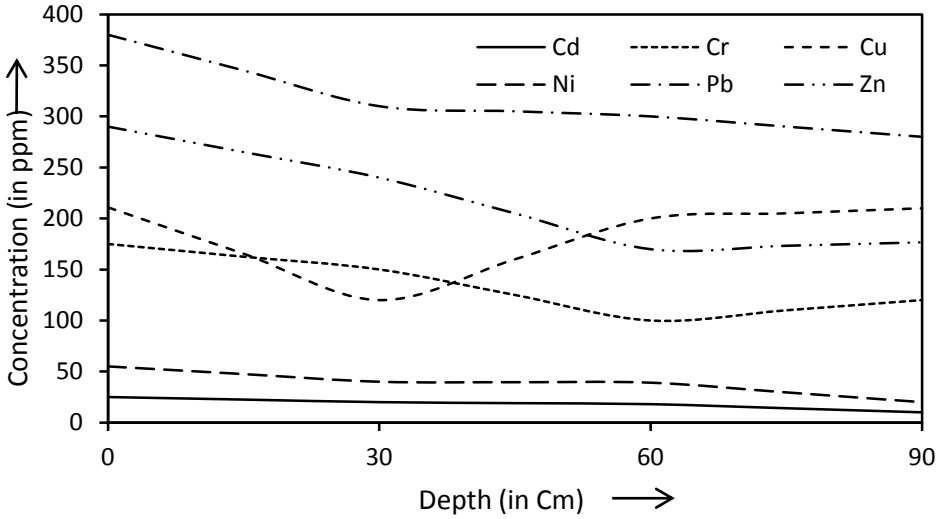

Figure 6: Heavy metals concentrations in soil samples of Chambal Industrial Area, Kota district.

6.3.3 Distribution of heavy metals at location 7 - RIICO Paryavaran Industrial Area (Table and Figure 7)

Results for Cd, Cr, Cu, Ni, Pb and Zn concentrations in the soil samples of RIICO Paryavaran Industrial Area are presented in Table 7. In the present study, level of cadmium was found in the range of 2.87 ppm to 37.89 ppm. Maximum and minimum mean concentrations of Cd were observed in the uppermost surface soil (21.64 ppm) and first feet of soil (7.27 ppm) samples, respectively. Maximum average Cr and Pb content were found in upper surface (200.11 ppm and 335.27 ppm, respectively), which is much higher than the minimum obtained mean concentration values (62.53 ppm and 221.57 ppm, respectively) from the third feet of strata. The mean concentration values of Cu and Zn were minimum in second feet of strata (174.51 ppm and 159.16 ppm, accordingly) and maximum in uppermost surface (238.23 ppm and 284.64 ppm, respectively). Ni average mean value was highest in third feet of strata (86.72 ppm) and lowest in first feet of sediments (58.22 ppm).

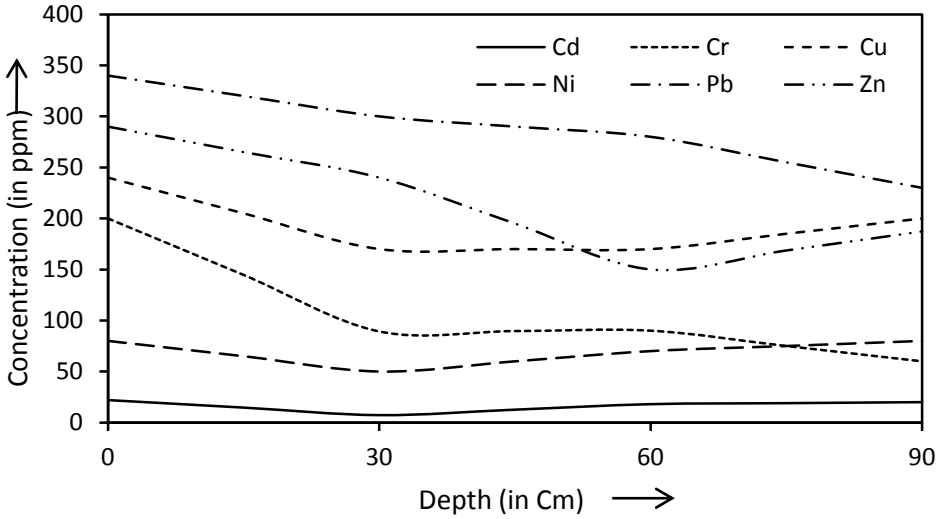

Figure 7: Heavy metals concentrations in soil samples in RIICO Paryavaran Industrial Area, Kota district.

6.3.4 Distribution of heavy metals at location 8 – Large scale Industrial Area (Table and Figure 8)

Table and Figure 8 show the content of heavy metals in the soil of the selected area. Maximum heavy metal loads of the soils in the study area are 42.78 ppm for Cd, 358.09 ppm for Cr, 423.98 ppm for Cu, 181.08 ppm for Ni, 528 ppm for Pb and 443.88 ppm for Zn, whereas minimum heavy metal load for Cd, Cr, Cu, Ni, Pb and Zn are 7.89 ppm, 15.9 ppm, 24.68 ppm, 17.95 ppm, 42.98 ppm and 34.98 ppm, respectively. Maximum average concentration of Cd, Cr, Cu Ni, Pb and Zn are present in the uppermost surface with mean values of 28.44 ppm, 177.39 ppm, 253.98 ppm, 85.38 ppm, 359.32 ppm and 272.65 ppm, respectively.

Minimum mean concentration values of Cd, Cr, Cu Ni, Pb and Zn are found to be 14.88 ppm (third feet), 74.32 ppm (first feet), 149.54 ppm (second feet), 42.37 ppm (first feet), 219.65 ppm (third feet) and 159.59 ppm (third feet), respectively.

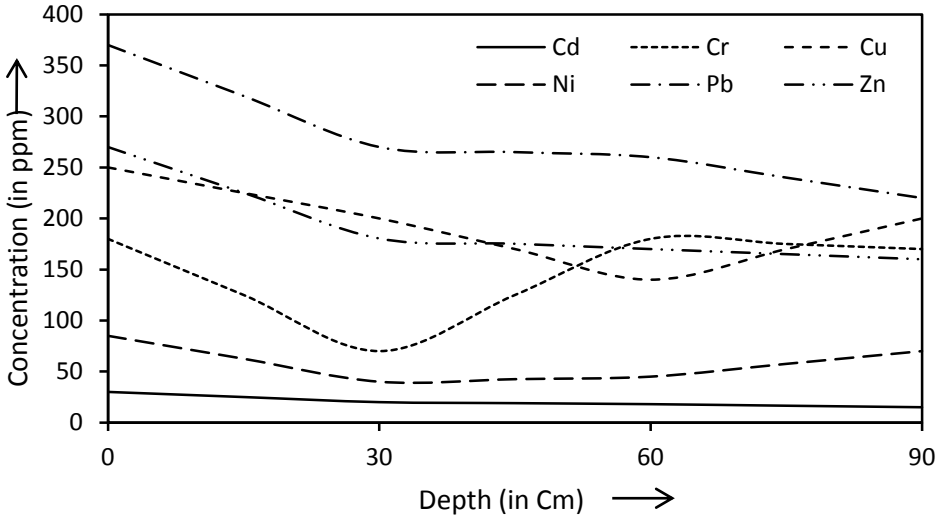

Figure 8: Heavy metals concentrations in soil samples of Large scale Industrial Area, Kota district.

Table 1. Heavy metals concentrations in soil samples of Sitapura Industrial area: Jaipur district.

	Location 1- Sitapura Industrial Area	Heavy metal concentration (ppm)					
		Cd	**Cr**	**Cu**	**Ni**	**Pb**	**Zn**
Upper surface	Maximum	12.34	374.83	198.34	120.48	284.6	206.17
	Minimum	5.67	56.71	73.18	25.87	84.18	12.76
	Mean±S.E.M.	8.71±1.94	200.61±93.07	144.50±37.17	70.49±27.44	184.59±57.85	119.52±56.73
First feet	Maximum	15.42	236.94	142.72	98.72	267.37	208.54
	Minimum	5.17	56.17	56.82	21.65	63.31	37.17
	Mean±S.E.M.	8.78±3.32	160.79±54.09	98.22±24.84	56.76±22.51	161.51±58.15	123.11±49.47
Second feet	Maximum	7.15	258.72	144.87	134.87	197.98	165.84
	Minimum	2.75	59.36	54.98	45.87	58.84	40.47
	Mean±S.E.M.	5.51±1.38	164.57±57.76	98.21±26.86	86.85±25.93	150.94±46.7	113.43±37.57
Third feet	Maximum	5.63	265.49	163.47	114.2	178.62	167.46
	Minimum	2.56	64.46	65.73	58.4	67.57	46.86
	Mean±S.E.M.	3.79±0.92	170.65±58.91	114.73±28.32	81.53±16.79	142.03±37.14	116.77±36.25

Values are Mean ± S.E.M. (Standard error of the Mean); n= 3

Table 2. Heavy metals concentrations in soil samples of Jhotwara Industrial Area: Jaipur district.

	Location 2- Jhotwara Industrial Area	Heavy metal concentration (ppm)					
		Cd	**Cr**	**Cu**	**Ni**	**Pb**	**Zn**
Upper surface	Maximum	23.87	305.91	267.48	98.78	345.67	278.84
	Minimum	10.76	42.87	25.68	17.67	72.56	45.89
	Mean±S.E.M.	15.79±4.24	158.59±79.96	139.38±70.17	54.07±23.78	212.41±76.95	188.24±72.05
First feet	Maximum	11.62	228.43	148.31	72.78	317.52	126.67
	Minimum	5.08	28.46	10.56	15.73	55.78	16.67
	Mean±S.E.M.	7.54±1.94	105.93±62.38	64.95±42.31	42.83±16.52	186.92±75.66	74.14±31.56
Second feet	Maximum	13.67	253.82	184.87	48.87	247.97	134.38
	Minimum	6.14	35.78	18.67	9.87	26.18	21.67
	Mean±S.E.M.	8.56±2.47	126.46±68.7	94.15±46.08	30.85±10.93	127.68±65.27	78.84±32.18
Third feet	Maximum	16.87	185.76	228.4	89.78	292.8	89.46
	Minimum	9.78	24.6	25.46	19.38	32.17	7.87
	Mean±S.E.M.	10.88±3.07	97.45±47.20	121.54±57.49	45.78±21.89	170.99±67.89	57.44±25.13

Values are Mean ± S.E.M. (Standard error of the Mean); n= 3

Table 3. Heavy metals concentrations in soil samples in RIICO Industrial Area: Jaipur district.

	Location 3- RIICO Industrial Area	Heavy metal concentration (ppm)					
		Cd	**Cr**	**Cu**	**Ni**	**Pb**	**Zn**
Upper surface	Maximum	20.75	281.7	295.92	114.20	380.87	310.67
	Minimum	7.27	37.36	49.85	23.78	87.97	26.98
	Mean±S.E.M.	12.32±4.16	142.98±72.52	200.26±72.16	57.19±28.66	248.60±85.73	182.85±83.08
First feet	Maximum	11.17	125.28	268.58	78.43	336.54	393.48
	Minimum	3.95	13.35	38.37	7.67	56.42	28.47
	Mean±S.E.M.	6.24±2.23	59.77±33.57	164.95±67.32	37.06±22.13	221.62±85.42	210.80±105.37
Second feet	Maximum	24.67	258.48	284.18	156.48	219.78	192.7
	Minimum	8.89	27.68	47.48	32.96	19.65	36.88
	Mean±S.E.M.	14.22±5.38	122.52±67.24	188.61±71.26	89.60±35.69	137.47±60.44	102.91±46.52
Third feet	Maximum	21.87	78.94	194.69	143.78	187.57	238.67
	Minimum	6.72	10.36	17.83	23.37	39.67	42.78
	Mean±S.E.M.	12.65±4.71	39.02±20.58	77.06±58.81	72.01±36.70	98.33±45.35	124.08±58.46

Values are Mean ± S.E.M. (Standard error of the Mean); n= 3

Table 4. Heavy metals concentrations in soil samples of Viswakarma Industrial Area: Jaipur district.

	Location 4- Viswakarma Industrial Area	Heavy metal concentration (ppm)					
		Cd	**Cr**	**Cu**	**Ni**	**Pb**	**Zn**
Upper surface	Maximum	31.63	235.78	278.67	103.51	439.67	407.87
	Minimum	11.89	27.87	34.56	17.67	52.58	74.51
	Mean±S.E.M.	20.74±5.00	114.77±63.53	189.11±77.29	53.65±27.54	240.30±117.62	254.16±97.27
First feet	Maximum	37.15	248.16	319.27	87.16	324.78	256.76
	Minimum	14.18	35.48	48.17	12.87	38.65	56.84
	Mean±S.E.M.	22.5±7.75	121.6±64.23	206.11±76.31	49.59±19.46	181.99±82.25	160.25±57.81
Second feet	Maximum	27.86	178.87	357.78	124.15	317.89	245.89
	Minimum	6.78	23.73	56.19	24.63	41.64	42.78
	Mean±S.E.M.	15.80±4.95	84.52±47.78	227.37±88.95	78.97±29.0	175.8±78.46	151.48±61.17
Third feet	Maximum	19.13	155.58	278.68	149.98	285.67	184.12
	Minimum	5.87	19.67	47.98	34.87	17.84	18.89
	Mean±S.E.M.	11.55±3.09	72.41±38.54	190.26±72.89	91.87±33.58	141.72±77.96	97.33±49.82

Values are Mean ± S.E.M. (Standard error of the Mean); n= 3

Table 5. Heavy metals concentrations in soil samples of Indraprastha Industrial Area: Kota district.

	Location 5- Indraprastha Industrial Area	Heavy metal concentration (ppm)					
		Cd	**Cr**	**Cu**	**Ni**	**Pb**	**Zn**
Upper surface	Maximum	35.73	195.65	401.67	124.89	940	386.78
	Minimum	1.07	68.98	54.78	12.89	36.85	195.89
	Mean±S.E.M.	20.13±10.15	145.51±60.04	222.25±100.31	64.91±32.57	402.61±274.48	312.21±64.27
First feet	Maximum	34.12	230.09	398.09	160.98	681.98	508.98
	Minimum	1.56	48.78	12.97	12.68	98.56	150.71
	Mean±S.E.M.	16.19±9.54	128.28±58.04	222.65±112.48	80.98±47.25	393.51±168.45	301.56±103.70
Second feet	Maximum	29.86	270.12	230.87	134.87	430.89	440.82
	Minimum	1.87	76.95	70.98	45.87	130.84	114.89
	Mean±S.E.M.	12.86±8.61	174.07±55.76	147.21±46.86	86.85±25.93	284.57±63.66	257.56±98.71
Third feet	Maximum	56.8	290.42	270.56	87.78	389.98	458.68
	Minimum	1.07	46.27	16.84	1.97	50.89	106.89
	Mean±S.E.M.	22.83±66.70	170.09±70.71	149.13±73.24	35.21±26.58	234.29±98.61	275.52±105.15

Values are Mean ± S.E.M. (Standard error of the Mean); n= 3

Table 6. Heavy metals concentrations in soil samples of Chambal Industrial Area: Kota district.

	Location 6- Chambal Industrial Area	Heavy metal concentration (ppm)					
		Cd	**Cr**	**Cu**	**Ni**	**Pb**	**Zn**
Upper surface	Maximum	58.18	380.75	418.86	84.63	572.67	477.91
	Minimum	2.46	25.85	67.73	18.96	81.84	86.94
	Mean±S.E.M.	25.29±17.87	184.73±104.73	210.85±106.42	51.02±19.07	371.80±101.61	292.64±109.83
First feet	Maximum	52.89	288.81	227.85	67.76	526.89	428.98
	Minimum	2.14	32.84	37.78	17.85	78.67	82.98
	Mean±S.E.M.	19.53±13.80	156.75±73.81	125.85±55.36	38.13±15.91	309.48±129.97	237.95±106.22
Second feet	Maximum	42.78	214.87	347.87	69.87	457.98	356.87
	Minimum	7.9	30.78	56.87	18.46	76.78	37.84
	Mean±S.E.M.	19.85±11.28	104.15±55.05	200.61±89.90	39.06±15.03	296.54±113.92	169.86±99.42
Third feet	Maximum	32.67	230.98	377.86	48.65	451.87	250.98
	Minimum	5.45	35.87	63.86	1.78	116.98	78.87
	Mean±S.E.M.	15.06±7.88	122.54±56.06	209.86±91.42	21.36±13.80	269.87±92.93	176.61±51.04

Values are Mean ± S.E.M. (Standard error of the Mean); n= 3

Table 7. Heavy metals concentrations in soil samples in RIICO Paryavaran Industrial Area: Kota district.

	Location 7- RIICO Paryavaran Industrial Area	Heavy metal concentration (ppm)					
		Cd	**Cr**	**Cu**	**Ni**	**Pb**	**Zn**
Upper surface	Maximum	37.89	417.81	397.87	182.87	488.87	459.98
	Minimum	8.16	40.87	45.86	36.86	147.98	112.98
	Mean±S.E.M.	21.64±7.13	200.11±112.42	238.23±105.38	86.57±48.66	335.27±102.79	284.64±100.86
First feet	Maximum	13.98	156.87	284.98	143.9	435.98	438.87
	Minimum	2.87	12.87	40.87	17.87	69.97	98.89
	Mean±S.E.M.	7.27±3.40	89.27±41.80	175.31±77.02	58.22±42.40	297.64±117.49	249.87±102.93
Second feet	Maximum	28.81	172.65	286.57	158.98	410.08	372.56
	Minimum	5.87	20.98	42.98	20.87	61.98	47.95
	Mean±S.E.M.	18.95±15.65	94.20±43.31	174.51±48.36	73.31±41.40	280.01±108.32	159.16±103.43
Third feet	Maximum	34.98	130.76	310.98	173.09	371.85	397.87
	Minimum	7.78	12.87	56.98	40.98	42.98	69.98
	Mean±S.E.M.	20.91±7.11	62.53±31.07	198.64±69.17	86.72±44.22	221.57±91.18	187.24±101.42

Values are Mean ± S.E.M. (Standard error of the Mean); n= 3

Table 8. Heavy metals concentrations in soil samples of Large scale Industrial Area: Kota district.

	Location 8- Large scale Industrial Area	Heavy metal concentration (ppm)					
		Cd	**Cr**	**Cu**	**Ni**	**Pb**	**Zn**
Upper surface	Maximum	42.78	358.09	423.98	181.08	528.98	443.88
	Minimum	13.78	32.62	56.98	35.98	157.96	103.89
	Mean±S.E.M.	28.44±8.98	177.39±93.01	253.98±104.44	85.38±42.21	359.34±107.35	272.65±95.49
First feet	Maximum	34.98	156.98	367.98	90.07	468.52	338.52
	Minimum	9.1	15.9	43.89	17.95	77.98	47.57
	Mean±S.E.M.	21.66±7.18	74.32±42.35	205.98±92.45	42.37±23.63	276.35±113.32	180.38±84.94
Second feet	Maximum	26.89	342.89	312.98	97.89	443.71	328.87
	Minimum	8.67	34.87	24.68	19.98	58.78	41.98
	Mean±S.E.M.	18.88±5.98	175.61±89.81	149.54±89.99	46.98±25.71	260.82±117.76	169.25±84.06
Third feet	Maximum	21.98	327.98	365.09	127.09	397.9	316.9
	Minimum	7.89	27.98	37.98	32.89	42.98	34.98
	Mean±S.E.M.	14.88±4.70	169.01±84.74	193.65±94.05	70.98±30.95	219.65±105.58	159.59±82.85

Values are Mean ± S.E.M. (Standard error of the Mean); n= 3

6.4 pH ANALYSIS

The results of pH analysis are shown in Table and Figure 9. In the present study, soil samples were collected from four zones of Jaipur and four zones of Kota industrial areas. In all the location, when we moved from surface to deep soil area, the acidic nature of soil decreased. In the present study, the soil samples from the industrial area showed an acidic pH. The acidic behavior of soil is responsible for heavy metal leaching, which in turn increases the amount of heavy metals in soil. An acidic soil can free many toxic metals from its combined state which in turn can make the soil toxic.

In Jaipur industrial areas (location 1, 2, 3 and 4), the pH of location 1 ranged from 6.2 (acidic) to 7.2 (alkaline). The upper surface of location 2 was found to be maximally acidic (pH-5.8) and this pH restored near to neutral at third feet (pH-6.8). In location 3, same behavior was observed. On the other hand, in location 4, pH range was 6.1 to 7.3. Maximum alkaline condition was found in the third foot of strata (pH-7.3) at location 4.

Industrial areas of Kota (location 5, 6, 7 and 8) are also showing similar results. In location 5, the uppermost surface is showing maximum acidic condition with a pH value of 5.8. At third feet of strata, the pH become near to neutral with a pH value of 6.8. In location 6, pH values ranges from 5.9 (uppermost layer) to 7.1 (third feet of strata). Location 7 is also showing maximum acidic condition in topmost layer (pH- 6.4) and pH becomes slightly alkaline at third feet of strata (pH-7.2). In the location 8, pH value ranges from 6.3 (uppermost layer) to 7.1 (third foot of sediments).

Location	Upper surface(0 Cm)	First feet(30 Cm)	Second feet(60 Cm)	Third feet(90 Cm)
1	6.2	6.4	6.9	7.2
2	5.8	6.2	6.3	6.8
3	5.9	6.2	6.6	6.9
4	6.1	6.6	6.8	7.3
5	5.8	6.3	6.4	6.8
6	5.9	6.7	6.8	7.1
7	6.4	6.7	6.7	7.2
8	6.3	6.6	6.8	7.1

Table 9: pH values at different locations of Jaipur and Kota district.

6.5 CORRELATION BETWEEN HEAVY METALS

Correlation analyses have been widely applied in environmental studies. They provide a useful way to disclose the relationships between multiple variables and thus have been helpful for understanding the influencing factors as well as the sources of chemical components. Heavy metals in soil usually have complex relationships among them. The high correlations between heavy metals in soil may reveal that the accumulated concentrations of these heavy metals come from similar pollution sources. The results of the Pearson's correlation matrix of heavy metals in the surface soils of Jaipur and Kota Industrial Area are shown in Table 10 (A) and 10 (B) respectively.

Table 10 (A): Pearson's Correlation matrix of heavy metals in the surface soils of Jaipur.

	Cd	Cr	Cu	Ni	Pb	Zn
Cd	1					
Cr	-0.19	1				
Cu	0.62	-0.11	1			
Ni	-0.05	0.10	0.22	1		
Pb	0.29	0.17	0.45	-0.41	1	
Zn	0.47	-0.03	0.52	-0.15	0.71	1

Table 10 (B): Pearson's Correlation matrix of heavy metals in the surface soils of Kota.

	Cd	Cr	Cu	Ni	Pb	Zn
Cd	1					
Cr	0.01	1				
Cu	-0.14	-0.001	1			
Ni	-0.25	0.11	0.35	1		
Pb	-0.18	0.27	0.51	0.22	1	
Zn	0.25	0.47	0.26	0.29	0.74	1

The correlation coefficient between Pb and Zn are 0.71 and 0.74, which indicates a strong linear correlation and a common origin of these metals. Cu and Zn, Cu and Pb formed another correlated pair with a correlation coefficient of 0.52 and 0.51, suggesting they probably originated from the same common sources. From Table 10 (A), Cd exhibited strong positive correlations with both Cu (0.62) and Zn (0.47). Cu and Zn occur naturally at abundant levels and are thus barely affected by human activities, which explain their apparent correlation in the surface soils. Cd is also widely scattered in the Earth's crust, and its correlations indicate that its occurrence in the surface soils was mainly due to natural sources. Zn and Cr formed another correlated pair with a correlation coefficient of 0.47 from Table 10 (B). The lack of significant linear correlation between, Cr and Ni with other heavy metals from Table 10 (A) and Cd with other heavy metals from Table 10 (B), suggests that its sources were quite different from those of the others.

References:

1. He Z., Shentu, J., Yang, X., Baligar, V.C., Zhang, T., Stoffella, P.J. 2015. Heavy Metal Contamination of Soils: Sources, Indicators, and Assessment. Journal of Environmental Indicators. 9: 17-18.
2. Chimezie Anyakora, Teddy Ehianeta and Oghenetega Umukoro. 2013. Heavy metal levels in soil samples from highly industrialized Lagos environment. African Journal of Environmental Science and Technology. 7(9): 917-924.
3. Dupler, D. 2001. Heavy metal poisoning. Gale Encyclopedia of Alternative Medicine. Farmington Hills, MI: Gale Group.
4. Momodu, M., Anyakora, C. 2010. Heavy metal contamination of groundwater: the Surulere case study. Res. J. Environ. Earth Sci. 2(1): 29-43
5. Anyakora, C., Nwaeze, K., Awodele, O., Nwadike, C., Arbabi, M., Coker, H. 2011. Concentrations of Heavy Metals in some Pharmaceutical Effluents in Lagos, Nigeria. J. Environ. Chem. Ecotoxicol. 3(2): 25- 31.
6. (IARC) International Agency for Research on Cancer. 1993. Beryllium, cadmium, mercury and exposures in the glass manufacturing industry, vol. 58. IARC, Lyon, France. 119-238.
7. EPA. 1998. "Toxicological Review of Trivalent Chromium. CAS No. 16065-83-1. In support of Summary Information on the Integrated Risk Information System (IRIS). U.S. Environmental Protection Agency, Washington, D.C.
8. Chervona, Y., Arita, A., Costa, M. 2012. Carcinogenic metals and the epigenome: understanding the effect of nickel, arsenic, and chromium. Metallomics. 4(7): 619-27.
9. Veena Sharma, Arti Sharma, Leena Kansal. 2010. The effect of oral administration of *Allium sativum* extracts on lead nitrate induced toxicity in male mice. Food and chemical toxicology. 48(3): 928-936.
10. *Fosmire, GJ. 1990. Zinc toxicity. Am. J. Clin. Nutr. 51 (2): 225–227.*

11. Liza Jacob, Romilly Margaret Mendez, Bindu Antony. 2015. Analysis of the soil properties of an industrial area in Kerala. International journal of scientific & technology research. 4(12): 139-140.
12. Sharma, R.K., Agarwal, M., and Marshall, F. 2007. Heavy Metals Contamination of Soil and Vegetables in suburban Areas of Varanasi, India. Ecotoxicology and Environmental Safety. 66: 258-266.

HOSTED BY

ELSEVIER

Available online at www.sciencedirect.com

ScienceDirect

International Soil and Water Conservation Research ▮ (▮▮▮▮) ▮▮▮–▮▮▮

www.elsevier.com/locate/iswcr

Transport of solutes under transient flow conditions – A case study – Yamuna river sub basin (Kosi Kalan to Agra)

Arun Kumar[a,*], Ajay Kumar Sharma[a], Ashu Rani[b]

[a]*Department of Mathematics, Government College Kota (Raj.), India*

[b]*Department of Pure & Applied Chemistry, University of Kota, Kota, India*

Received 10 April 2015; received in revised form 16 June 2015; accepted 17 June 2015

Abstract

The imbalance between incoming and outgoing salt causes salinization of soils and sub-soils that result in increasing the salinity of stream-flows and agriculture land. This salinization is a serious environmental hazard particularly in semi-arid and arid lands. In order to estimate the magnitude of the hazard posed by salinity, it is important to understand and identify the processes that control salt movement from the soil surface through the root zone to the ground water and stream flows. In the present study, Yamuna sub-basin (both sides of Gokul dam site) has been selected which has two distinct climatic zones, sub-humid (upstream of Mathura) and semi-arid region (downstream of Mathura). In the upstream, both surface and ground waters are used for irrigation, whereas in the downstream mostly groundwater is used. Both soils and ground waters are more saline in downstream parts of the study area. In this study we characterized the soil salinity and groundwater quality in both areas. An attempt is also made to model the distribution of potassium concentration in the soil profile in response to varying irrigation conditions using the Soil-Water Infiltration and Movement (SWIM) model. Fair agreement was obtained between predicted and measured results indicating the applicability of the model.

© 2015 International Research and Training Center on Erosion and Sedimentation and China Water and Power Press. Production and Hosting by Elsevier B.V. This is an open access article under the CC BY-NC-ND license (http://creativecommons.org/licenses/by-nc-nd/4.0/).

Keywords: SWIM; Disc permeameter; Guelph permeameter; Hydrolysis; Soil moisture

1. Introduction

In arid and semi-arid regions the imbalance between incoming and outgoing salt has resulted in accumulation of salts in the irrigated soils. Since, the salt tolerance of crops is often based on the concentration of salts in the saturated extracts; it would be useful to have a method to predict the salt concentration throughout the soil profile under field conditions. In order to estimate the magnitude of the hazard posed by salinity, it is important to understand and identify the processes that control salt movement from the soil surface through the root zone to the ground waters and stream flows.

Modeling and monitoring transport of water and solutes is further complicated owing to temporal variation resulting from chemical non-equilibrium and the structure of the soil. The most challenging problem confronting mathematical modeling of solute transport in field soils is how to effectively characterize and quantify the geometric,

*Corresponding author.

E-mail address: arunkr71@gmail.com (A. Kumar).

Peer review under responsibility of IRTCES and CWPP.

http://dx.doi.org/10.1016/j.iswcr.2015.06.004

2095-6339/© 2015 International Research and Training Center on Erosion and Sedimentation and China Water and Power Press. Production and Hosting by Elsevier B.V. This is an open access article under the CC BY-NC-ND license (http://creativecommons.org/licenses/by-nc-nd/4.0/).

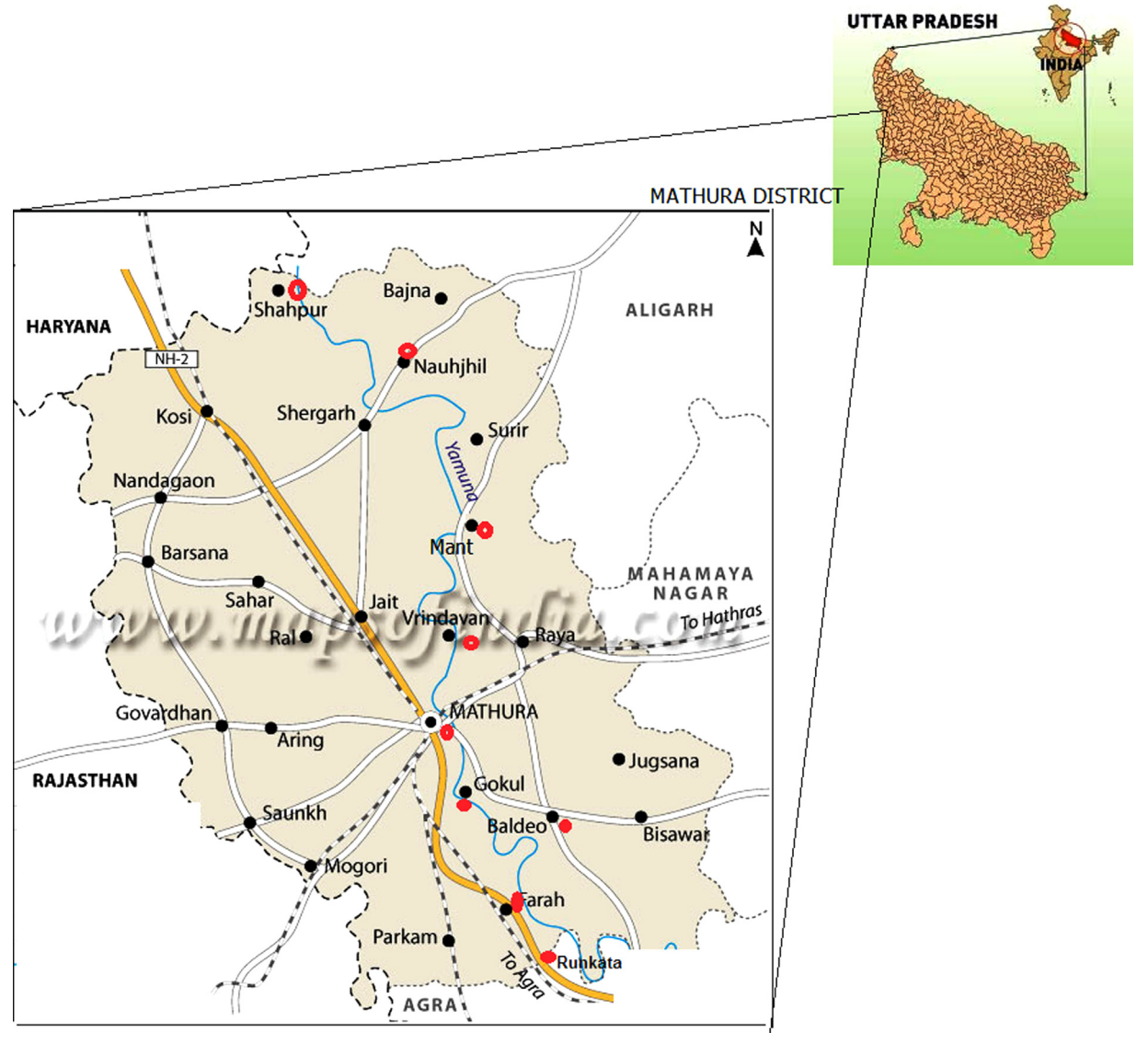

Fig. 1. Index map of the study area (Yamuna sub-basin) with groundwater sampling.

hydraulic, and chemical properties of porous media. The process can be explained through several mathematical models based on Convective Diffusion Equations, Soil Water Infiltration and Movement (SWIM) etc. (De Rooij & Stagnitti, 2000; Evans & Stagnitti, 1996; Rajmohan & Elango, 2001; Srivastava & Brusseau, 1996; Stagnitti & Li, 1999, 2001; Valocchi, 1985; Xu & Brusseau, 1996).

The impact of agricultural activities on ground water is closely related to the quality of water from precipitation and irrigation. Soil-water systems in the unsaturated zone are highly complex. Firstly, it is seldom in stable equilibrium and is in constant flux. The degree of saturation of soil-water (θ) varies both in time and space. This in turn affects flow parameters namely the suction head $h(\theta)$ and the hydraulic conductivity $K(\theta)$, which are not unique functions of θ but exhibits hysteresis.

Water quality issues originated through leaching of water soluble contaminants stems from the lack of understanding related to soil transport phenomenon, as an example fertilizer application in an agricultural field results in leaching of fertilizer ions in ground water unplanned during irrigation. Thus it is important to understand and develop a suitable transport model addressing simultaneous transport phenomenon of soil water and dissolved salts.

Please cite this article as: Kumar, A., et al. *International Soil and Water Conservation Research* (2015), http://dx.doi.org/10.1016/j.iswcr.2015.06.004

In this study, the solute transport process in two agricultural zones representing sub-humid (Mathura to Kosi) and semi-arid (Mathura to Agra) conditions in Yamuna sub-basin has been modeled using the Soil-Water-Infiltration-Movement (SWIM) model (Ross, 1990). Saturated hydraulic conductivity was measured in the field using a Guelph permeameter and soil sampling was done before and after application of fertilizer (N–P–K). Soil moisture retention characteristics were obtained in the laboratory using the Pressure Plate Apparatus.

2. Study area

The study area extends between 74°20 and 75°E longitude and 15°20 and 15°40 N latitude in the Mathura district of Uttar Pradesh (Fig. 1). To harness the waters of the Yamuna River, a dam has been constructed at Gokul, Mathura district to impound 1377 million cubic meter of water. There are three seasons prevailing in the catchment, the summer from March to May, the monsoon from June to November, and the winter from December to February. The Yamuna river sub basin has two distinct rainfall regimes, i.e., the area upstream of Mathura to Kosi has an annual average rainfall of 1200 mm, whereas downstream of Mathura to Agra, the average rainfall is 700 mm. The major soil groups in the catchment are clay loam soil (Ultisols), black soil (vertisols) in upstream and sandy loam soils (mainly Alfisols), black soil in downstream. The land use pattern of the Yamuna sub-basin shows that 15.4% is covered by forests, 10.5% shrub, 7.9% waste land, 38.1% cropped area, 24.2% fallow land, and the remaining 4.0% is occupied by water bodies.

2.1. Materials and methods

Ground water samples were collected from selected wells (locations are shown in Fig. 1) during pre-monsoon and post-monsoon seasons and analysed for various chemical parameters such as, electrical conductivity (EC_e), total alkalinity (Carbonate CO_3 and bicarbonate HCO_3), total dissolved solids (TDS), chloride (Cl), sulfate (SO_4), sodium (Na), potassium (K), calcium (Ca) and magnesium (Mg) using APHA methods (Carter, 1993). Soil samples were collected from agriculture fields located at Mathura to Kosi (upstream) and also from Mathura to Agra (downstream). Soil extracts were prepared by stirring 20gm of soil sample into 50 ml water, and analysed for chemical parameters.

The cation exchange capacity (CEC) of a soil is the total negative charge of the soil measured under specific conditions. Its determination involves the saturation or all the charges by one cation. Conventionally, for soils with less than 7.0 pH. Ammonium (NH_4) is the cation of choice, and the determination is done at pH 7.0 by leaching the soil with NH_4OAc solution buffered at that pH. Kjeldahl distillation apparatus was used for the estimation of calcium and magnesium. Sodium and potassium were determined by analyzing the ammonium acetate extract directly for sodium and potassium using Flame photometer.

2.2. Estimation of soil hydraulic properties

Saturated hydraulic conductivity was determined by using a disc permeameter and a Guelph permeameter. Saturated moisture content was estimated by the gravimetric method (Hillel, 2012). Soil moisture retention characteristics were determined by using pressure plate apparatus. Detailed methodology is given below.

2.2.1. Disc permeameter

The disc permeameter (Perroux & White, 1988) was used for the determination of soil hydraulic conductivity at the surface. The instrument allows a constant supply potential, either positive or negative, in a manner analogous to ponded ring devices. Based on the expression developed by Wooding (1968), for three dimensional flow from a circular disc, the steady state infiltration (q_∞) is expressed as Eq. (1)

$$q_\infty = K + \frac{4b(S_0)^2}{(\theta_0 \quad -\theta_n)\pi r} \tag{1}$$

where b is a constant taken as 0.75 (Smettem, Parlange, Ross, & Haverkamp, 1994), θ_0 is the saturated moisture content and θ_n is the in situ moisture content, r is the radius of the disc (0.1 m). When the disc permeameter test is run, data are collected to obtain cumulative infiltration at various times after the start of the test. S_0 can be found from the slope of early-time plot of q_∞ vs. $St^{1/2}$ and q_∞ from the slope of the late time plot of q_∞ vs. t. The water content

Please cite this article as: Kumar, A., et al. *International Soil and Water Conservation Research* (2015), http://dx.doi.org/10.1016/j.iswcr.2015.06.004

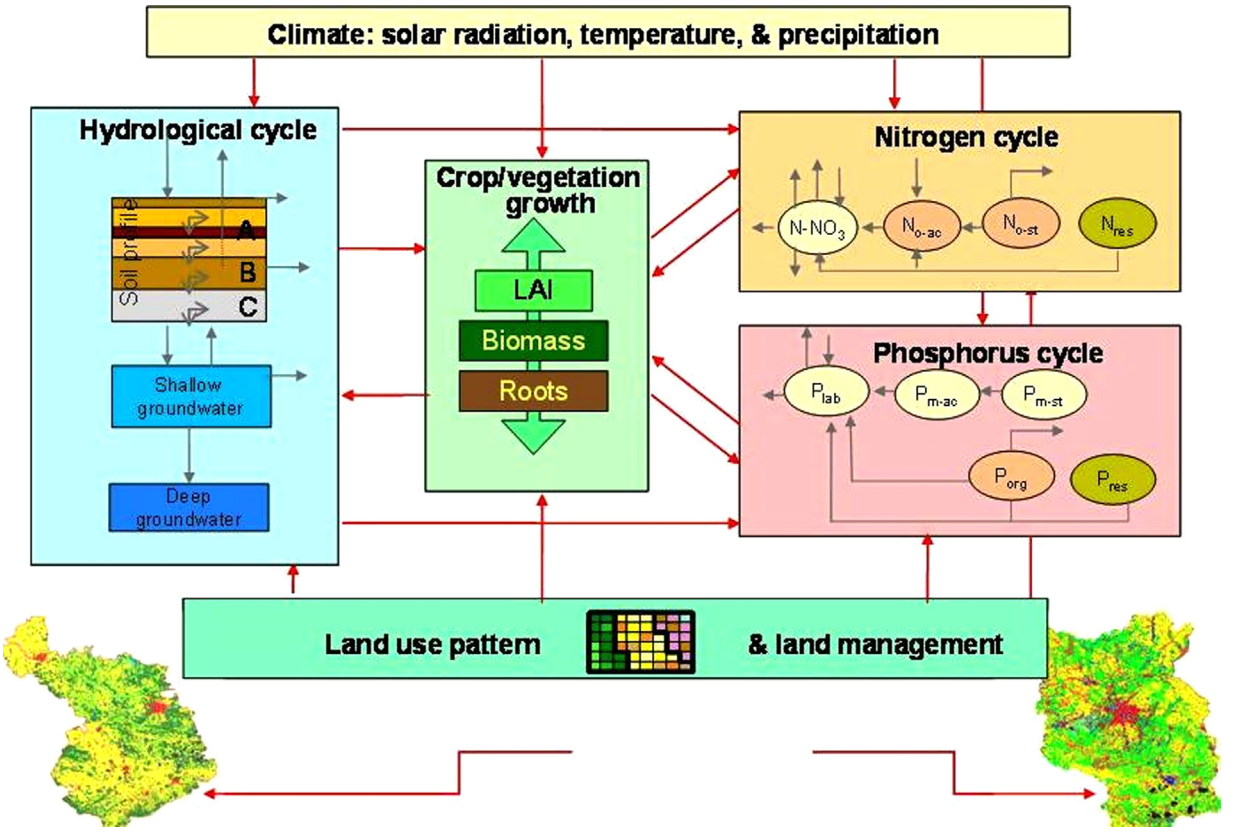

Fig. 2. Framework of SWIM Model.

is measured before and after the experiment (by taking soil samples for gravimetric water content multiplied by dried bulk density determinations) to obtain the saturated moisture content (θ_0) and in situ moisture content (θ_n). Thus K can then be calculated from Eq. (1). The disc permeameter is portable and can be used for the measurement of infiltration, hydraulic conductivity, and pore characteristics, although only the hydraulic conductivity is reported here.

2.2.2. *Guelph permeameter*

The Guelph permeameter (Reynolds & Elrick, 1985) was used to determine the depth-wise field saturated hydraulic conductivity. The method involves measuring the steady state rate of water recharge into unsaturated soil from a cylindrical well hole, in which a constant depth (head) of water is maintained. Constant head level in the well hole is established and maintained by regulating the level of the bottom of the air tube which is located in the center of the permeameter. As the water level in the reservoir falls, a vacuum is created in the air space above the water. The vacuum can only be relieved when air, which enters at the top of the air tube, bubbles out of the air inlet tip and rises to the top of the reservoir. Whenever the water level in the well begins to drop below the air inlet tip, air bubbles emerge from the tip and rise into reservoir air space. The vacuum is then partially relieved and water from the reservoir replenishes the water in the well. The size of opening and geometry of the air inlet tip is designed to control the size of air bubbles in order to prevent the well water level from fluctuating.

The steady state discharge from a cylindrical well in unsaturated soil, as measured by the Guelph permeameter technique accounts for all the forces that contribute to three dimensional flow of water into soils, the hydraulic push of water into soil, the gravitational pull of liquid out through bottom of the well, and the capillary pull of water out of the well into the surrounding soil. The Richard analysis is the basis for the calculation of field saturated hydraulic conductivity (Carter,1993).

Please cite this article as: Kumar, A., et al. *International Soil and Water Conservation Research* (2015), http://dx.doi.org/10.1016/j.iswcr.2015.06.004

3. Soil Water Infiltration and Movement (SWIM) model

Ross (1990) proposed the SWIM model which is based on a numerical solution of the Richards equation and the advection–dispersion equation. In the present study, the model has been applied to simulate the movement of solute in the unsaturated zone. The physical system and the associated flows addressed by the model are shown schematically in Fig. 2. Soil water and solute transport properties, initial conditions, and time dependent boundary conditions (e.g., precipitation, evaporative demand, solute input) were provided in order to run the model (Verburg, Ross, & Bristow, 1996).

3.1. Theoretical development

Assuming a homogeneous and isotropic porous medium, the one-dimensional partial differential equation describing the transport of an interacting, degrading solute can be written as

$$\frac{\partial \theta C_i}{\partial t} + \frac{\partial (\rho s_i)}{\partial t} = D\left\{\frac{\partial^2 \theta C_i}{\partial z^2}\right\} - q\left\{\frac{\partial C_i}{\partial z}\right\} \pm \phi_i \tag{2}$$

where C_i is concentration of solute (parent material or metabolite, i), in the solution phase; s_i is concentration of species i in the adsorbed phase; θ is volumetric water content; q is Darcy's flux; ϕ source-sink term denoting the rate of species i transformation in the degradation pathway; D is apparent dispersion coefficient dependent on θ and q; ρ is soil bulk density; z is vertical coordinate measured vertically down-ward' and t is time.

The apparent dispersion coefficient represents the combined effects of molecular diffusion and mechanical dispersion (velocity-dependent). This combined expression can be written as

$$D = D_m + \alpha \left| V \right| \tag{3}$$

where D_m is molecular diffusion coefficient dependent on the moisture content θ; $V = q/\theta$ is effective pore-water velocity; and α is dispersivity. In laboratory experiments using relatively homogeneous porous media, values of dispersivity α, determined from breakthrough curves of conservative non interacting solutes such as chloride, are known to be of order of 0.01–1.0 cm. In contrast, field modeling studies use values of the dispersivity in the range of 10–100 m, which are three to six orders of magnitude larger than typical laboratory studies. This wide difference in field and laboratory dispersivity estimates may be due to the non-homogeneous and anisotropic nature of the field flow system compared to homogeneous, isotropic conditions of laboratory tests (Reddell & Sunada, 1970).

Given that Eq. (3) is valid for defining the apparent dispersion coefficient for saturated and partially saturated flow conditions and that the mechanical dispersion term is analogous to molecular diffusion in effect, but not in mechanism, assumption of steady flow ($\partial\theta/\partial t = 0$) reduces Eq. (2) to

$$\frac{\partial C_i}{\partial t} + \frac{\rho}{\theta}\frac{\partial S_i}{\partial t} = D\frac{\partial^2 C_i}{\partial z^2} - V\frac{\partial C_i}{\partial z} \pm \frac{1}{\theta}\phi_i \tag{4}$$

Eq. (3) is a generalized expression representing transport, adsorption, and transformation of a single solute species i. The source-sink term ϕ_i in Eq. (4) represents the sequential steps in the degradation pathway from the parent material to the first-step product, from the first-step product to the second-step, and so on to the end of the nth product. The term ϕ_i does not reflect either adsorption to the soil matrix of a degradable chemical or its metabolites, nor plant uptake and volatilization. The term S_i represents the amount of parent material or metabolite adsorbed to the soil. If, for simplicity, one assumes an existence of a local equilibrium and linear adsorption isotherm solution and adsorbed phases, then.

$$S_i = K_{pi} C_i \quad (i = 1, 2, \ldots\ldots, N) \tag{5}$$

where K_{pi} is the distribution or partition coefficient for the solute species i. Taking the derivative of Eq. (4) with respect to time, t, yields

$$\frac{\partial S_i}{\partial t} = K_{pi}\left(\frac{\partial C_i}{\partial t}\right) \tag{6}$$

Transformation process determines the fate and persistence of chemicals in the unsaturated and saturated zones. Principal among these processes are microbiological degradation (biodegradation), hydrolysis (chemical degradation) and volatilization. The driving force behind these reactions is the microorganism's need for energy, carbon, and other essential nutrients. Thus, the rate of biodegradation depends on both the concentration of the chemical and the size of the microbial population. Hydrolysis is a transformation process that changes the chemical speciation of an organic contaminant. It is the reaction of the chemical with water resulting in an exchange of some functional group from the organic molecules with a hydroxyl (OH^-) group. Like bio degradation, the extent of contaminant attenuation depends on both the chemical properties of the contaminant and the aqueous medium. Both transformation processes can be mathematically represented by first-order kinetic reactions (Smith & Johnson, 1988). In this study the degradation pathway of the solute can be represented in a manner similar to Wagenet and Hutson (1986) as

$$\begin{array}{ccccc} [C_i] & \underset{k_1}{\Longrightarrow} & [C_{i+1}] & \underset{k_2}{\Longrightarrow} & [C_{i+2}] \\ \downarrow k_1' & & \downarrow k_2' & & \downarrow k_3' \\ \text{product} & & \text{product} & & \text{product} \end{array} \tag{7}$$

where k_i($i=1,\ 2,\ 3$) denotes the first-order rate constants of the ith degradation step; and k'_i ($i=1,\ 2$) denotes the rate of constants for hydrolysis. Based on Eq. (7) and assuming that hydrolysis processes produce innocuous products which can be neglected in the analysis, the sequential transformations for the parent material and its two metabolites can be expressed as

$$\phi_1 = \left\{\frac{\partial C_1}{\partial t}\right\} = -(k_1 + k'_1)\theta C_1 \tag{8a}$$

$$\phi_2 = \left\{\frac{\partial C_2}{\partial t}\right\} = \theta k_1 C_1 - (k_2 + k_2')\theta C_2 \tag{8b}$$

$$\phi_3 = \left\{\frac{\partial C_3}{\partial t}\right\} = \theta k_2 C_2 - (k_3 + k'_3)\theta C_3 \tag{8c}$$

where the subscripts 1, 2 and 3 represent the parent material and its two metabolites, respectively. Substituting Eq. (6) and Eqs. (8a)–(8c) into Eq. (4) and upon simplification yields the following expressions for the parent material ($i=1$) and its two metabolites ($i=2,\ 3$)

$$R_1\left\{\frac{\partial C_1}{\partial t}\right\} = D\left\{\frac{\partial^2 C_1}{\partial z^2}\right\} - V\left\{\frac{\partial C_1}{\partial z}\right\} - (k_1 + k'_1)C_1 \tag{9a}$$

$$R_2\left\{\frac{\partial C_2}{\partial t}\right\} = D\left\{\frac{\partial^2 C_2}{\partial z^2}\right\} - V\left\{\frac{\partial C_2}{\partial z}\right\} + k_1 C_1 - (k_2 + k'_2)C_2 \tag{9b}$$

$$R_3\left\{\frac{\partial C_3}{\partial t}\right\} = D\left\{\frac{\partial^2 C_3}{\partial z^2}\right\} - V\left\{\frac{\partial C_3}{\partial z}\right\} - k_2 C_2 - k_3 C_3 \tag{9c}$$

where R_1, R_2 and R_3 are the retardation factors for the parent material and its first and second metabolites, respectively. These retardation factors represent the extent to which the movement of the parent material or its metabolites are retarded relative to the water movement in the soil. The retardation factors R_1, R_2 and R_3 can be defined as

$$R_1 = \left\{1 + \rho\frac{Kp^1}{\theta}\right\} \tag{10a}$$

$$R_2 = \left\{1 + \rho\frac{Kp^2}{\theta}\right\} \tag{10b}$$

$$R_3 = \left\{1 + \rho\frac{Kp^3}{\theta}\right\} \tag{10c}$$

where Kp^1, Kp^2 and Kp^3 are the partition coefficients of the parents material, first metabolite and second metabolites,

Please cite this article as: Kumar, A., et al. *International Soil and Water Conservation Research* (2015), http://dx.doi.org/10.1016/j.iswcr.2015.06.004

respectively. In solving Eqs. (9a)–(9c) the initial with boundary conditions

$$C_i = 0 \quad t = 0 \quad z \geq 0 \tag{11a}$$

$$C_i = C_i^0 \quad 0 < t \leq t_1 \quad z = 0 \tag{11b}$$

$$C_i = 0 \quad t > t_1 \quad z = 0 \tag{11c}$$

$$C_i = 0 \quad t \geq 0 \quad z = \infty \tag{11d}$$

$$\frac{\partial C_i}{\partial z} = 0 \quad t \geq 0 \quad z = \infty \tag{11e}$$

where C_i^0 $(i = 1, 2, 3)$ is the initial concentration of the parent material or its two metabolites and t_1 is the time for pulse application of the chemical. Rearranging Eqs. (9a), (9b) and (9c) one obtains

$$D\left\{\frac{\partial^2 C_1}{\partial z^2}\right\} - V\left\{\frac{\partial C_1}{\partial z}\right\} - (k_1 + k'_1)C_1 - R_1\frac{\partial C_1}{\partial t} = 0 \tag{12a}$$

$$D\left\{\frac{\partial^2 C_2}{\partial z^2}\right\} - V\left\{\frac{\partial C_2}{\partial z}\right\} + k_1 C_1 - k_2 C_2 - R_2\frac{\partial C_2}{\partial t} = 0 \tag{12b}$$

$$D\left\{\frac{\partial^2 C_3}{\partial z^2}\right\} - V\left\{\frac{\partial C_3}{\partial z}\right\} + k_2 C_2 - k_3 C_3 - R_3\frac{\partial C_3}{\partial t} = 0 \tag{12c}$$

Values of the transformation rate constants k_i and k'_i $(i = 1,2,3)$ given in Eqs. (12a), (12b) and (12c) are assumed to be constants, although it is well known that microbiologically mediated reactions are functions of many environmental variables (Ou & Penman, 1989). Inadequate information on the functional nature of these relationships prevents representation, at present of k_i values as other than constants. However, the value of k_i can be changed with depth and time in a manner similar to Tillostson, Robbins, and Wagnet (1980). In obtaining closed-form analytical solutions of Eqs. (12a), (12b) and (12c) the initial and boundary conditions given by Eqs. (11d) and (11e) are modified to

$$C_i = 0 \quad t \geq 0 \quad z = L \tag{13a}$$

and

$$\frac{\partial C_i}{\partial t} = 0 \quad t \geq 0 \quad z = L \tag{13b}$$

$(i = 1,2,3)$ so as to adequately describe the lower boundary of a finite column of soil of length L.

3.2. Analytical solution

A finite-difference procedure for solving a solute transport equation similar to that developed in this study has been presented by Wagenet and Hutson (1986). However, the finite difference method, in general, requires extensive data input (data that may be sparse and uncertain) and detailed familiarity with the numerical code (a process that can be tedious and time consuming). Furthermore, the method is complicated by the dominating convective term $V\frac{\partial C}{\partial z}$ which can give rise to considerable numerical oscillations or dispersion. Therefore, the closed form analytical method of solution of the solute transport equation offers a useful means for an initial estimation of order of magnitude of the extent and concentration of the contaminant, Data input is relatively simple and results compare reasonably well with those obtained numerically (Huyakorn, Mercer, & Ward, 1985).

The standard Laplace transform technique is used to obtain analytical solutions of Eqs. (12a), (12b) and (12c) subject to initial and boundary conditions given in Eqs. (11a), (11b), (11c), (13a), and(13b). Because this technique has been presented in detail by several investigators (Ames, 2014; Bieniasz, 2015; Gökdoğan, Merdan, & Yildirim, 2012), only some pertinent steps in solving are outlined in this paper. Additionally, since Eqs. (12a), (12b) and (12c) are structurally similar, only the solving procedure for Eq. (12a) is described. For the parent compound $(i = 1)$, the

Please cite this article as: Kumar, A., et al. *International Soil and Water Conservation Research* (2015), http://dx.doi.org/10.1016/j.iswcr.2015.06.004

Laplace transformation of Eq. (12a) with its associated boundary condition given by Eq. (11a) may be written as

$$\frac{d^2\overline{C_1}}{dz^2} - \frac{V}{D}\frac{d\overline{C_1}}{dz} - \frac{1}{D}\{(k_1+k'_1)+s\}\overline{C_1} = 0 \tag{14}$$

where

$$\overline{C_1} = \int_0^\infty C_1 \exp(-st)dt \tag{15}$$

Using Eqs. (11a), (11b) and (11c) the solution of Eq. (14) is

$$\overline{C_1}(z,s) = \frac{C_1^0}{s}\exp(r_1 z)[1-\exp(st_1)] \tag{16}$$

where

$$r_1 = \frac{1}{2D}\{V-(V^2+4DR_1[k_1+k'_1)+s])^{1/2}\} \tag{17}$$

Recognizing that

$$\lambda^{-1}\exp(r_1 z) = \frac{z}{(4\pi Dt^3)^{1/2}}\exp\left(\frac{Vz}{2D}\right).\exp\left(\frac{V^2}{4D}+(k_1+k'_1)t-\frac{z^2}{4Dt}\right) \tag{18}$$

and applying the convolution theorem to obtain the Laplace inverse of Eq. (16) yields

$$C_1(z,t) = H_1(z,t) \quad o < t \le t_1 \tag{19}$$

$$C_1(z,t) = H_1(z,t) - H_1(z,t-t_1) \quad t > t_1 \tag{20}$$

where

$$H_1(z,t) = C_1^0[P_1(\omega)] \tag{21}$$

in which

$$P_1(\omega) = 0.5\exp\left\{\frac{z(V-\omega)}{2D}\right\}erfc\left\{\frac{R_1 z-\omega t}{(4DR_1 t)^{1/2}}\right\} + 0.5\exp\left\{\frac{z(V-\omega)}{2D}\right\}erfc\left\{\frac{R_1 z-\omega t}{(4DR_1 t)^{1/2}}\right\} \tag{22}$$

and

$$\omega = [V^2+4DR_1(k_1+k'_1)]^{1/2} \tag{23}$$

A procedure similar to that outlined above for $C_1(z,t)$ can be adopted to obtain an analytical solution for the second metabolite denote by Eq. (12b). Thus, for a pulse application of c_1^0 at the soil surface for a duration t_1, analytical solution of Eq. (12b) yields

$$C_2(z,t) = G_1(z,t)+G_2(z,t) \quad 0 < t < t_1 \tag{24}$$

$$C_2(z,t) = G_1(z,t) - G_1(z,t-t_1)+G_2(z,t)-G_2(z,t-t_1)t > t_1 \tag{25}$$

where

$$G_1(z,t) = \frac{k_1 C_1^0}{k_{12}}\left\{\exp(-k_1 t)p_2(\omega_{22}) - \exp\left[-(k_2+k_2^1)t\right]p_2(\omega_{21})\right\} \tag{26}$$

$$G_2(z,t) = \frac{k_1 C_1^0}{K_{12}}\left\{\frac{R_1}{R_2}\right\}\left\{\exp(-k_1 t)\left[P_1(\omega_{11})-P_2(\omega_{22})\right]+\exp(-\beta_{12})[P_2(\omega_{23})-P_2(\omega_{12})]\right\} \tag{27}$$

In which

$$K_{12} = (k_2+k'_2)-k_1 \tag{28}$$

$$\beta_{12} = \frac{k_1 R_1-(k_2+k_2')R_2}{R_1-R_1} \tag{29}$$

Please cite this article as: Kumar, A., et al. *International Soil and Water Conservation Research* (2015), http://dx.doi.org/10.1016/j.iswcr.2015.06.004

$$P_i(\omega_{ij}) = 0.5\exp\left\{\frac{z(V-\omega_{ij}}{2D}\right\} erfc\left\{\frac{R_j z-\omega_{ij} t}{4DR_j t^{1/2}}\right\} + 0.5\exp\left\{\frac{z(V-\omega_{ij}}{2D}\right\} erfc\left\{\frac{R_j z-\omega_{ij} t}{4DR_j t^{1/2}}\right\} \quad (30)$$

where $[i=1, 2; j=1, 2, 3]$

$$\omega_{11} = \omega_{21} = V \quad (31)$$

$$\omega_{12} = \left(V^2 + 4DR_1[k_1 - (k_2 + k'_2]\right)^{1/2} \quad (32)$$

$$\omega_{22} = \left(V^2 + 4DR_2[(k_2 + k'_2) - k_1]\right)^{1/2} \quad (33)$$

$$\omega_{23} = \left(V^2 + 4DR_1[(k_2 + k'_2) - k_1]\right)^{1/2} \quad (34)$$

A similar analytical procedure to that outlined above for $C_2(z, t)$ can be adopted to obtain the solution of Eq. (12c). Solutions of $C_1(z, t)$ and $C_2(z, t)$ for application of C_1^0 at the soil surface for a duration of t_1 were obtained using the superposition principle for $t > t_1$ as given by Eqs. (20) and (25). From Eqs. (20) and (25), it can be easily verified that $C_1(z, t) \to 0$ as $z \to 0$ and/or $t \to \infty$for small values of t_1. Also, for continuous application of C_1^0at the soil surface, a steady-state concentration distribution can be obtained for given z values and $t \to \infty$. A FORTRAN computer program was used to evaluate the solutions for $C_1(z, t)$ and $C_2(z, t)$ and all computations were carried out in double precision.

3.3. Model conceptualization

The SWIM model was applied to the Yamuna sub-basin to understand the solute transport characteristics that pass through the unsaturated zone. This solute enters the soil profile with the irrigation water. Therefore, to account for the spatial variation of saturated hydraulic conductivity, twelve in situ field experiments were conducted on the soil surface (top layer) and also at the bottom layer (45–60 cm depth) at different locations with different soil types. Logarithmic mean value was considered as the model input parameter. The model was run under two conditions, one in the clay loam soil area (Mathura to Kosi) with single vegetation (Jowar) and the second run is for the downstream area, dominated by medium to sandy loam soil (Mathura to Agra), where wheat is the type of vegetation. Solute was included in the simulation through application of fertilizer (N–P–K) at the surface. The model was simulated for 30 days comprising two irrigations of 6 cm each on 3rd and 20th day and one initial application of fertilizer (solute). Exponential root growth with depth and linear interpolation with time was considered. The profile is 150 cm deep with surface at 0 cm and bottom boundary condition applying at 150 cm. There is also some solute present initially. Solute production and first order decay processes are active. In the model, solute production/uptake and first order decay processes are expressed in terms of source or sink terms. There was no solute exclusion from plant water uptake, i.e., all solute dissolved in the uptake water was also taken up by the plant. Plant uptake of solute is assumed to take place only by mass flow. In this case, vapor conductivity is not taken into account nor is the effect of osmotic potential. There are two hydraulic property sets (for upper and lower soil layers) that are applied at 16 depth nodes of the 150 cm deep profile. Initially, there is no water ponded on the surface. Runoff is governed by a simple power law function. A matric potential gradient of 0, i.e., 'unit gradient', has been applied as a bottom boundary condition throughout the simulation. Runoff in SWIMv2.1 is based on the assumption that the soil has a certain surface roughness, which can detain water and prevent it from running off.

3.3.1. Data acquisition

3.3.1.1. Rainfall. Daily rainfall data for the period 1995–2005 were collected from the statistical department (Uttar Pradesh State) for rain gauges located within the catchment of Yamuna sub-basin.

3.3.1.2. Evaporation. Daily evaporation data of Mathura to Kosi and Gokul dam site (1995–2003) were obtained from the Uttar Pradesh State Irrigation Department.

3.3.1.3. Saturated hydraulic conductivity. Saturated hydraulic conductivity was measured at 9 stations using disc permeameter and Guelph permeameter. The saturated hydraulic conductivity near Mathura to Kosi is taken as

Please cite this article as: Kumar, A., et al. *International Soil and Water Conservation Research* (2015), http://dx.doi.org/10.1016/j.iswcr.2015.06.004

ARTICLE IN PRESS

2.1 cm/h (surface) and at a depth of 45–60 cm, it is 0.9 cm/h. In areas, dominated by clay loam soil, the values considered are 0.6 cm/h at the surface and 0.01 cm/h at the bottom layer.

3.3.1.4. Van Genuchten parameters. Soil samples were analyzed in the laboratory for soil moisture retention characteristics by using pressure plate apparatus. The averaged van Genuchten parameters for the soil layer were obtained by non-linear regression analysis. The van Genuchten parameter α_v varies between 0.0083 cm^{-1} and 0.0560 cm^{-1} and the n parameter varies between 1.4046 and 1.5037.

3.3.1.5. Vegetation. Two types of vegetation (Jowar/Gram) showing exponential root growth with depth and sigmoid with time were assumed for the study. Data pertaining to vegetation type was not available; therefore, it is adopted from the study carried out by Kumar and Shilpa (2002) for the Dharwad district.

Jowar	
Root radius (rad)	0.08 cm
Root conductance (groot)	1.2×10^{-7}
Minimum xylem potential (psi_{min})	−15,000 cm
Root depth constant (x_c)	30 cm
Grams	
Maximum root length density (rld_{max})	4 cm/cm^3
Root radius (rad)	0.12 cm
Root conductance (groot)	1.0×10^{-7}
Minimum xylem potential (psi_{min})	−15,000 cm
Root depth constant (x_c)	20 cm
Maximum root length density (rld_{max})	3 cm/cm^3

4. Results and discussion

4.1. Soil salinity

Soil salinization has been observed in the downstream part of the Yamuna sub-basin. Presently, it is noticed that only about 15–20% of the study area (out of the total irrigated land) are salt affected (i.e., $EC_e > 4$ ds/m). Although soil salinity was generally low, it tended to increase with depth, due to the accumulation of salt in the deeper layer which could be attributed to the presence of higher clay content and low permeability as observed in the soil profile.

Thus, the percentage of the irrigated area with EC_e values higher than 4 ds/m was 6.8% for the 0–30 cm soil depth and increased to 15.7% for the 60–90 cm soil depth. The EC_e values being greater than 4 ds/m in the soil horizons of downstream region indicate a high level of salinity particularly in deep to medium black soils from Mathura to Agra. Calcium is the dominant base on exchange complex with Ca/Mg ranging from 3.2 to 3.6 for black soils and for red soil it varies between 1.83 and 3.57.

4.2. Hydrochemistry of anions and cations

Acid-base reactions are important in groundwater because of their influence on pH and the ion chemistry. A pH value of 7.5–8.0 usually indicates the presence of carbonates of calcium and magnesium, and a pH value of 8.5 or above shows appreciable exchangeable sodium. The results of the present study (Tables 1 and 2) show clearly the dominance of bicarbonate, sodium and chloride towards down-stream as compared to upstream.

The total concentration of soluble salts expressed as electrical conductivity in ground water of Yamuna sub-basin varied from 0.36 to 29.6 ds/m. However, it is observed that in most of the cases (42%), the EC_e was more than 4 ds/m, and 28% of the samples had EC_e less than 2.5 ds/m, thereby indicating that salinity is more prevalent than sodicity

Please cite this article as: Kumar, A., et al. *International Soil and Water Conservation Research* (2015), http://dx.doi.org/10.1016/j.iswcr.2015.06.004

Table 1
Measured chemical properties of the water samples collected from bore well (BW) during pre-monsoon (*) and post-monsoon (**) (unit; mg/l).

Stations	pH	EC_e, ds/m	TDS	CO_3	HCO_3	Cl	SO_4	Hardness as $CaCO_3$	Ca	Mg	Na	K
Shahpur (upstream)												
*	7.00	0.0599	36.00	NIL	63.68	7.10	50.00	10.00	3.20	0.50	3.90	1.00
**	8.10	0.1848	111.00	NIL	134.40	12.40	295.0	154	25.60	22.0	3.40	0.40
Nauhjhil (upstream)												
*	8.05	0.3980	239.00	NIL	290.10	7.10	92.50	94.00	28.80	5.37	29.50	2.70
**	7.50	0.4540	272.00	NIL	297.20	8.86	92.50	110.0	28.80	9.27	48.00	7.45
Mant (upstream)												
*	8.70	0.2700	161.90	NIL	198.13	28.36	78.00	60.00	12.80	6.83	15.50	3.25
**	8.20	0.3130	187.60	NIL	212.30	12.40	85.00	90.00	23.20	7.80	9.00	1.75
Vrindavan (upstream)												
*	8.10	0.3350	201.00	NIL	84.90	62.04	92.50	54.00	15.20	3.90	27.00	17.50
**	7.50	0.3410	205.00	NIL	92.00	63.80	485.00	72.00	16.80	7.32	11.00	6.50
Mathura (upstream)												
*	8.90	0.4610	276.00	6.96	141.50	58.50	97.00	82.00	16.00	10.25	22.50	1.95
**	7.90	0.6450	387.00	NIL	198.12	90.40	106.50	126.00	24.80	15.60	22.50	4.50
Gokul (downstream)												
*	8.30	0.8590	515.00	NIL	283.04	108.1	83.00	190.0	40.80	21.47	36.50	2.70
**	6.90	1.198	719.00	NIL	325.50	186.1	90.00	268.0	52.80	33.18	203.0	6.10
Baldeo (downstream)												
*	7.65	3.510.	2100.0	NIL	367.95	758.6	260.00	780.0	184.0	78.10	184.0	2.00
**	7.00	3.800	2280.0	NIL	460.00	753.3	275.00	828.0	201.6	79.06	396.0	6.00
Farah (downstream)												
*	7.60	2.0400	1222.0	NIL	495.30	402.36	65.00	488.0	97.60	59.54	119.00	84.00
**	7.10	2.450	1472.0	NIL	707.60	432.5	40.00	564.0	126.4	60.50	284.0	146.0
Runakta (downstream)												
*	9.10	1.037	622.00	69.6	35.38	134.7	95.00	50.00	8.00	7.32	67.50	189.0
**	7.60	1.892	1135.0	13.9	353.80	237.5	295.00	166.0	44.80	13.17	40.00	120.0

in the study area. Studies carried out by Jain, Bhatia, Kumar, and Purandara (2001) also reported a similar trend in the area. EC_e was found to be highly correlated with *Na* ($r=0.88$), *Cl* ($r=0.96$) and also with sulfate ($r=0.71$). The soluble carbonates and bicarbonates in the water samples analyzed varied from 1.04 to 8.1 me L^{-1} during pre-monsoon and 0.58 to 12.53 me L^{-1} during post-monsoon. The concentrations of carbonate and bicarbonate are important because these affect the precipitation of calcium and thereby result in excessive saturation in soil. The Residual Sodium Carbonate (RSC) of waters indicates that about 71% samples had RSC between 2.5 me L^{-1} and 5 me L^{-1}.

The results indicated that the continuous and indiscriminate use of these ground waters is expected to build up excessive sodium in the soil solution and exchange complex and will also clog the soil pores which may lead to drainage problems (Sood, Verma, Thomas, Sharma, & Brar, 1998). Soluble sodium is the dominant cation varying in concentration from 0.39 to 17.5 me L^{-1} in these waters. However, the Sodium Adsorption Ratios (SAR) values of all samples are less than 10. It was observed that waters of high EC_e values are predominant with sodium and chloride ions. Further it was observed that saline waters also have relatively high calcium, magnesium and bicarbonate ions. This was observed specially at downstream (Runakta). Potassium and carbonate ions, if present, are mostly confined up to a range of 5% of the total salt concentration. It is quite difficult to draw a general conclusion on the ionic composition of the water in relation to geographical conditions. In general, waters in areas of high rainfall, i.e., above 1000 mm per annum and with good drainage are of good quality. It is clear from the present study that, in the upstream where there is more rainfall (above 1000–3000 mm) the quality of water is good whereas in the

Please cite this article as: Kumar, A., et al. *International Soil and Water Conservation Research* (2015), http://dx.doi.org/10.1016/j.iswcr.2015.06.004

ARTICLE IN PRESS

Table 2
Measured chemical properties of the water samples collected from open well (OW) during pre-monsoon (*) and post-monsoon (**) (unit; mg/l).

Stations	pH	EC_e, ds/m	TDS	CO_3	HCO_3	Cl	SO_4	Hardness as $CaCO_3$	Ca	Mg	Na	K
Shahpur (upstream)												
*	9.40	0.1483	89.00	NIL	84.90	8.86	52.00	28.00	7.20	2.44	5.25	1.40
**	5.90	0.0361	21.60	NIL	35.38	7.10	48.00	20.00	2.40	3.42	4.80	1.00
Nauhjhil (upstream)												
*	8.30	0.2000	120.20	NIL	77.84	10.64	80.50	50.00	11.20	5.37	5.50	0.60
**	7.10	0.1463	87.80	NIL	84.90	12.40	71.00	44.00	7.20	6.34	20.00	1.20
Mant (upstream)												
*	8.60	0.0394	237.00	NIL	106.14	46.10	113.50	46.00	12.80	3.42	25.00	36.50
**	7.60	0.6080	366.00	NIL	92.00	90.40	100.00	76.00	16.00	8.80	25.00	31.00
Vrindavan (upstream)												
*	8.80	0.1776	106.50	14.0	77.84	14.20	83.00	32.00	7.20	3.42	11.00	2.70
**	8.25	0.1686	101.20	NIL	106.14	19.50	85.00	42.00	8.00	5.37	11.05	2.15
Mathura (upstream)												
*	8.50	0.3510	210.00	6.96	155.67	33.68	36.50	72.00	18.40	6.34	20.00	2.30
**	7.30	0.3410	205.00	NIL	169.82	37.22	52.00	78.00	20.80	6.34	69.00	8.50
Gokul (downstream)												
*	8.50	1.068	641.00	14.0	120.30	226.9	106.50	218.0	27.20	36.60	66.50	6.10
**	6.70	1.448	869.00	NIL	389.20	216.3	106.50	312.0	68.80	34.16	110.0	9.00
Baldeo (downstream)												
*	9.60	0.7800	468.00	69.6	42.45	109.9	95.00	48.00	8.00	6.83	62.00	46.00
**	7.50	1.330	798.00	NIL	460.00	131.2	100.00	246.0	61.60	22.45	188.0	149.0
Farah (downstream)												
*	9.70	0.3420	205.00	41.8	28.30	37.22	71.00	48.00	8.00	6.83	20.00	40.00
**	7.60	0.6160	369.00	NIL	162.75	69.12	83.00	98.00	30.40	5.37	108.0	168.0
Runakta (downstream)												
*	7.90	2.6200	1570.	NIL	438.7	290.7	415.0	218.00	60.80	16.10	45.00	180.0
**	7.00	2.4900	1792.	6.96	396.2	358.0	415.0	274.00	55.20	33.20	60.00	195.0

downstream area, various water quality parameters exceed the acceptable limits (Adhikary, Dash, Kumar, & Chandrasekharan, 2014; Phocaides, 2000).

The distribution of anions and cations with total ion concentration, indicate that bicarbonates and sulfate ions are the dominating anions in the upstream, whereas towards downstream, concentration of chloride increases over bicarbonates indicating salinity problems in black soil (vertisol). Similarly among cations calcium and magnesium are the predominant ones. This is attributed to rock types and clay minerals rich in potassium. In the downstream of Yamuna sub-basin (from dam site to Farah) it is expected that, the most important exchange reactions involved are the removal of Ca^{2+} and Mg^{2+} out of water and to replace them with Na^{+}. The main requirement for this process is a large reservoir of exchangeable Na^{+}, which is most often provided by clay minerals deposited (mostly montmorillonite and smectite group). This is evident in the present study as HCO_3^{-} and Na^{+} are the ions, which indicate the presence of ion-exchanged waters.

SAR of all the samples in the study area can be grouped under the low-sodium hazard zone; however, the hydraulic conductivity varies considerably from low to very high. Further, the ground water samples collected from the deep black soil areas showed a shift towards medium hazard zone due to continuous use of poor quality ground water. This indicates the future trend of soil and ground water salinization in these areas and therefore proper measures should be taken to control the possible impacts.

Please cite this article as: Kumar, A., et al. *International Soil and Water Conservation Research* (2015), http://dx.doi.org/10.1016/j.iswcr.2015.06.004

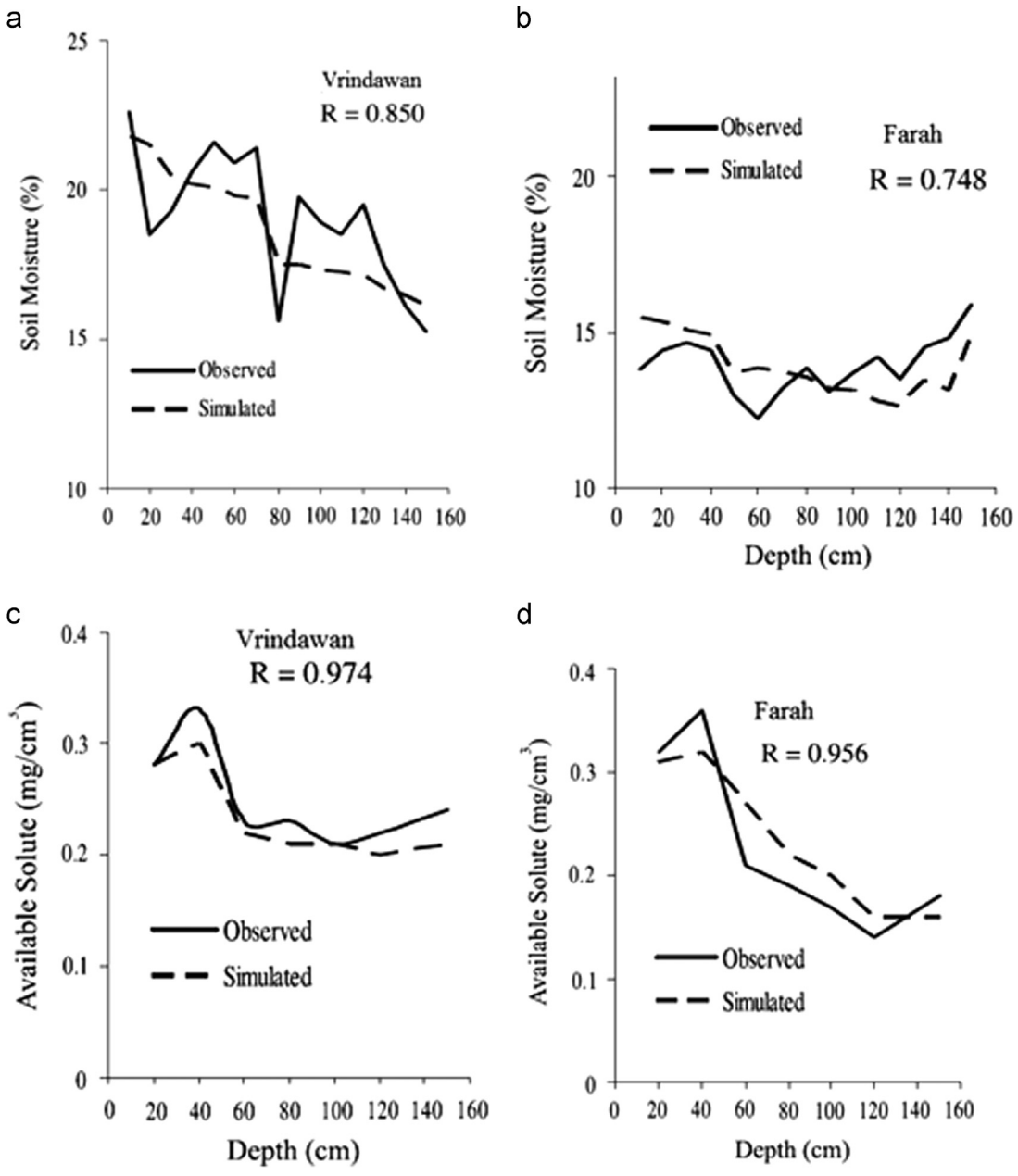

Fig. 3. Comparison of observed and simulated soil moisture profiles: (a) upstream (Vrindawan) and (b) downstream (Farah); and solute profiles: (c) upstream (Vrindawan) and (d) downstream (Farah) in Yamuna sub-basin.

4.3. Simulation of soil moisture

The model was calibrated by using soil moisture profiles available for the Yamuna sub-basin. In the present study, the moisture observed during the study period was compared with the simulated profile for both upstream and downstream parts of the study area (Fig. 3a and b). The profiles showed a reasonable match between the actual data and simulated results with exception at a few depths.

In the case of solute profiles (Fig. 3c and d), both observed and simulated profiles follow a similar trend of downward movement. The results indicate that in the upstream area rich in black soil, due to the very low permeability, the ions move very slowly and remain mostly in the unsaturated zone leading to water quality

Please cite this article as: Kumar, A., et al. *International Soil and Water Conservation Research* (2015), http://dx.doi.org/10.1016/j.iswcr.2015.06.004

ARTICLE IN PRESS

problems, particularly in open wells. However, in the downstream areas covered by red loamy soils (alfisols), due to the presence of highly porous rocks and better flow conditions, ions remain in continuous movement without affecting the water quality.

Further, during the rainy season, there is an increase in water level due to which the deposited salts move in the ground water and during the sunny days the salts are accumulated in the sub-soil layers. Apart from this, in cultivated lands, plants absorb only part of each of the nutrients present in soluble forms in soils. As the concentration of the nutrients in the soil water increases, it results in greater total nutrient absorption and greater crop yields. If fertilizers are added to supplement the supplies of particular nutrients that are deficient in soils, greater residues of the nutrients remain in the soils. Part of the excess may be lost to the groundwater if it remains in soil-water. Most of the chemical ions added in fertilizers are retained to some degree by soils as a result of chemical inter-actions, and this reduces their potential for loss to groundwater. As a consequence of such a process both soil and water get contaminated. This could be the reason for accumulation of salts in the downstream area as reported by Varadarajan (2000). The present observation also indicated that there is an accumulation of salts in the top layers of black soil (vertisol), which will ultimately lead to soil and water contamination.

5. Conclusion

Ground water quality and solute transport investigations have revealed that there is deterioration in chemical quality of both soil and water at various locations of Yamuna sub-basin, particularly in the downstream region. The cause for deterioration of chemical quality is attributed to the unstable equilibrium between various ions such as carbonate, silicate and alumino-silicate minerals. These constituents will continue to dissolve in the saturated zone. The source of cations and anions may vary from place to place. However, the higher concentration of bicarbonates is attributed to the release of carbon dioxide by plant roots and the decomposing organic matter present in soils. The weathering of primary minerals can be described as a breakdown of silicate with the release of cations which will appear as bicarbonates.

Soil salinity and groundwater quality deterioration also depend on the rainfall. They increase during the summer and are considerably reduced during the monsoon due to dilution by rainwater. In the downstream area, rainfall is significantly less than in the upstream area and the climate varies from sub-humid to semi-arid, due to which there is a considerable change in ground water quality and soil salinity. Further, the variation in salinity and its ionic composition depend upon the depth of water table, infiltration capacity of the soil, and the rainfall characteristics of the area concerned. The quality of groundwater in many regions shows wide variations with depth of the aquifer.

The study revealed the fact that there are soil and water salinization problems in the study area particularly in black soils. One of the major reasons as observed that non-utilization of the available ground water due to which the salinization problem worsens further. So it is important to pump out the water regularly and conjunctive use practice of surface- and ground-water should be adopted in such areas where the soils are affected by soil salinity and the rainwater harvesting structures and sub-surface drainage should be constructed at appropriate locations. Apart from this, certain salt tolerant crops should be grown which have already given some good results in certain areas, to reduce the intensity of salinization in the study area.

References

Adhikary, P. P., Dash, C. J., Kumar, G., & Chandrasekharan, H. (2014). Characterization of groundwater quality for irrigation and drinking purposes using a modified groundwater quality index. *Indian Journal of Soil Conservation*, *42*(3), 260–267.

Ames, W. F. (2014). *Numerical methods for partial differential equations*. Academic Press.

Bieniasz, L. K. (2015). *Analytical Solution Methods* (pp. 249–268)Berlin Heidelberg: Springer249–268.

Carter, M. R. (Ed.). (1993). *Soil sampling and methods of analysis*. CRC Press: CRC Press, 1993.

De Rooij, G. H., & Stagnitti, F. (2000). Spatial variability of solute leaching: Experimental validation of a quantitative parameterization. *Soil Science Society of America Journal*, *64*(2), 499–504.

Evans, L., & Stagnitti, F. (1996). *Nutrient transport through basaltic agricultural soils near Australian and New Zealand National Soils Conference: Soil Science – Raising the profile*, Vol. 2, Oral papers, University of Melbourne.

Gökdoğan, A., Merdan, M., & Yildirim, A. (2012). The modified algorithm for the differential transform method to solution of Genesio systems. *Communications in Nonlinear Science and Numerical Simulation*, *17*(1), 45–51.

Hillel, D. (2012). *Soil and water: Physical principles and processes*. Elsevier.

Please cite this article as: Kumar, A., et al. *International Soil and Water Conservation Research* (2015), http://dx.doi.org/10.1016/j.iswcr.2015.06.004

ARTICLE IN PRESS

Huyakorn, P. S., Mercer, J. W., & Ward, D. S. (1985). Finite element matrix and mass balance computational schemes for transport in variably saturated porous media. *Water Resources Research*, *21*(3), 346–358.

Jain, C. K., Bhatia, K. K.S., Kumar, C. P., & Purandara, B. K. (2001). Irrigation water quality in Malaprabha Sub-basin, Karnataka. *Indian Journal of Environment Protection*, *21*(4), 348–354.

Kumar, C. P., & Shilpa, S. R. (2002). Modeling of solute transport in agricultural fields using SWIM. *Journal of Hydrology*, *25*(2–3), 21–32.

Ou, J. A., & Penman, S. H. (1989). Financial statement analysis and the prediction of stock returns. *Journal of Accounting and Economics*, *11*(4), 295–329.

Perroux, K. M., & White, I. (1988). Designs for disc permeameters. *Soil Science Society of America Journal*, *52*(5), 1205–1215.

Phocaides, A. (2000). *Technical handbook on pressurized irrigation techniques*. Rome: FAO.

Rajmohan, N., & Elango, L. (2001). *Modelling the movement of chloride and nitrogen in the unsaturated zone* (pp. 209–223)New Dehli: UNESCO-IHP, Allied Publishers209–223.

Reddell, D. L., & Sunada, D. K. (1970). *Numerical simulation of dispersion in groundwater aquifers*. Fort Collins, Colorado: Colorado State University.

Reynolds, W. D., & Elrick, D. E. (1985). In situ measurement of field-saturated hydraulic conductivity, sorptivity, and the [alpha]-parameter using the Guelph Permeameter. *Soil Science*, *140*(4), 292–302.

Ross, P. J. (1990). *SWIM: a simulation model for soil water infiltration and movement: refereNce manual*. CSIRO Division of Soils.

Smettem, K. R.J., Parlange, J. Y., Ross, P. J., & Haverkamp, R. (1994). Three-dimensional analysis of infiltration from the disc infiltrometer: 1. A capillary-based theory. *Water Resources Research*, *30*(11), 2925–2929.

Smith, D. B., & Johnson, K. S. (1988). Single-step purification of polypeptides expressed in Escherichia coli as fusions with glutathione S-transferase. *Gene*, *67*(1), 31–40.

Sood, A., Verma, V. K., Thomas, A., Sharma, P. K., & Brar, J. S. (1998). Assessment and management of underground water quality in Talwandi sabo Tehsil of Bathinda District (Punjab). *Journal of the Indian Society of Soil Science*, *46*(3), 421–426.

Srivastava, R., & Brusseau, M. L. (1996). Non-ideal transport of reactive solutes in heterogeneous porous media: 1. Numerical model development and moments analysis. *Journal of Contaminant Hydrology*, *24*(2), *117–143*.

Stagnitti, F., & Li, L. (1999). A mathematical model for estimating the extent of solute and water-flux heterogeneity in multiple sample percolation experiments. *Journal of Hydrology*, *215*(1–4), 59–69.

Stagnitti, F., & Li, L. (2001). Modelling solute transport in structured soils: Performance evaluation of the ADR and TRM models. *Mathematical and Computer Modelling*, *34*(3–4), 433–440.

Tillostson, W. R., Robbins, C. W., & Wagnet, R. J. (1980). *Soil water*, *solute and plant growth simulation*. Utah State University, Logan, Utah Agric. Exp. Stn. Bull. No. 502.

Valocchi, A. J. (1985). Validity of the local equilibrium assumption for modeling sorbing solute transport through homogeneous soils. *Water Resources Research*, *21*(6), 808–820.

Varadarajan, N. (2000). *Groundwater Quality Evaluation and Modelling (M.E. thesis)*. Dharwad, India: Karnataka University.

Verburg, Kirsten, Ross, P. J., & Bristow, K. L. (1996). SWIMv2.1 user manual. *Divisional report No. 130.* Australia: CSIRO.

Wagenet, R. J., & Hutson, J. L. (1986). Predicting the fate of nonvolatile pesticides in unsaturated zone. *Journal of Environment Quality*, *15*(4), 315–322.

Wooding, R. A. (1968). Steady infiltration from a shallow circular pond. *Water Resources Research*, *4*(6), 1259–1273.

Xu, L., & Brusseau, M. L. (1996). Semi analytical solution for solute transport in porous media with multiple spatially variable reaction processes. *Water Resources Research*, *32*(7), 1985–1991.

Please cite this article as: Kumar, A., et al. *International Soil and Water Conservation Research* (2015), http://dx.doi.org/10.1016/j.iswcr.2015.06.004

International Journal of Engineering, Management & Sciences (IJEMS)
ISSN-2348 –3733, Volume-3, Issue-10, October 2016

Assessment of Heavy Metal Contamination in Soil Sediments of Jaipur and Kota Industrial Areas, Rajasthan, India

Ajay Sharma, Arun Kumar

***Abstract*— Intense industrialization and urbanization had lead to a serious environmental problem due to increased heavy metal pollution in soils, air and water. Soil is a major reservoir for contaminants as it possesses an ability to bind various chemicals. In this study, the soil samples from upper surface sediments and the first, second and third one-foot-thick strata were investigated. Soil samples were collected from the industrial areas of Jaipur and Kota districts of Rajasthan and analyzed for their heavy metal contents.**

The results of present finding indicate that the soils are characterized by high concentrations of Cd, Cr, Cu, Ni, Pb and Zn. The maximum obtained concentrations of Cd, Cr, Cu, Ni, Pb and Zn are 58.18 ppm, 417.81 ppm, 423.98 ppm, 182.87 ppm, 940 ppm and 508.98 ppm, respectively. The mean values of all the heavy metal concentrations were higher than the background values. The pollution level of the industrial areas soil was also higher, which clearly indicate the significant need for the development of heavy metal pollution prevention occurring due to industrial processing.

***Index Terms*— Soil properties, Heavy metals (Cd, Cr, Cu, Ni, Pb, Zn), industrial soil pollution, Correlation analysis.**

I. INTRODUCTION

Heavy metal contamination to soil and the environment has been accelerated in modern society due to industrialization, rapidly expanded world population, and intensified agriculture [1]. Environmental contamination is correlated with the degree of industrialization and intensities of chemical usage. The effect of heavy metals on the environment is of serious concern and threatens life in all forms [2]. Toxicity of these compounds has been reported extensively [3, 4, 5]. They accumulate over time in soils which act as a sink from which these toxicants are released to the groundwater and plants, and end up through the food chain in man thereby causing various toxicological manifestations. The According to IARC [6], Cadmium (Cd) is an extremely toxic industrial and environmental pollutant classified as a human carcinogen. Human occupational exposure to chromium clearly indicates that these compounds are respiratory tract irritants, resulting in airway irritation, airway obstruction, and lung, nasal, or sinus cancer [7]. Cr compounds are teratogenic in animals and can induce mutations. Toxicity of copper is associated with abdominal pain, headache, nausea, dizziness, vomiting and diarrhea, gastrointestinal bleeding, liver and kidney failure, and death. Nickel is one of many carcinogenic metals known to be an environmental and occupational pollutant. Chronic exposure to Ni is connected with increased risk of lung cancer, cardiovascular disease, neurological deficits, and developmental deficits in childhood [8]. Lead poisoning tends to have increased risk for cardiovascular disease, nephropathy, immune suppression and liver impairment [9]. Zinc toxicity may result in nausea, vomiting, diarrhea, metallic taste, kidney and stomach damage and other side effects [10].

The main objective of the present study is to determine the level of soil pollution with respect to some heavy metals in Jaipur and Kota districts of Rajasthan.

Manuscript received October 20, 2016

Ajay Sharma, Department of Mathematics, Government College Kota (Raj.), India

Arun Kumar, Department of Mathematics, Government College Kota (Raj.), India

II. METHOD AND MATERIALS

A. Studied area

The present study area covers Jaipur and Kota districts of Rajasthan. The soils were collected from different industrial areas that could contribute to a higher level of heavy metals contamination. Total eight different locations were selected in the present study, Four different locations were selected in jaipur area are Sitapura Industrial area (location 1), Jhotwara Industrial Area (location 2), RIICO Industrial Area (location 3) and Viswakarma Industrial Area (location 4) and remaining four different locations were selected in Kota area are Indraprastha Industrial area (location 5), Chambal Industrial Area (location 6), RIICO Paryavaran Industrial Area (location 7), Large scale Industrial Area (location 8).

B. Sampling

To avoid contamination of the soil sample, essential cleanness conditions were maintained. The samples were collected randomly in triplicates from different sites of industry area. All samples were collected and put in clean polythene bags and they were sealed in double bags. Use of metal tools was avoided and a plastic spatula was used for sample collection. The soil samples consisting of three subsamples were collected at random by digging the soil at four different depths: from the surface layer (0–5 cm depth), the first feet below the surface (30 cm depth), the second feet below the surface (60 cm depth) and the third feet below the

surface (90 cm depth). Samples were collected with a plastic spade during the winter of 2015, and the collected samples were placed in black polyethylene bag. The samples were labeled appropriately

C. Analysis of the samples -

The soil samples were allowed to dry for 48 h at room temperature. The dry soil sample was disaggregated in mortar pestle. The sample was finely powdered, sieved with a 2 µm sieve and stored in plastic vials. One gram of each sample was weighed and transferred into pre-washed and oven dried beakers. The dried samples were wet digested according to standard protocols and they were labeled properly.

D. pH analysis-

The soil samples were collected from upper surface, first foot, second foot and third foot of sediments in triplicates. The pH was measured as described by Liza Jacob et al. [11]. A soil suspension was made with soil and water in the ratio 1: 2. Ten gram of soil sample was taken in a 50 ml beaker and added 20 ml of distilled water into it. The solution was stirred immediately with glass rod for 30 minutes. It was stirred again just before taking pH reading. The pH was read using pH meter. The electrodes of the pH meter were washed with distilled water after each determination. For standardizing the pH meter, two buffer solutions of known pH values (pH-4 and pH-7) were used.

E. Heavy metal detection-

The detection of heavy metals is accomplished by various methods but here the AAS technique was used, which is relatively simple, versatile, accurate and free from interferences. Heavy metals readily form complexes with organic constituents and therefore, it is necessary to destroy them by digestion with strong acids. Nitric-perchloric acid digestion method was performed for sample preparation [12]. One gram of a sample was placed in 250 ml digestion tube and 10 ml of concentrated HNO3 was added. The mixture was boiled for 30-45 minutes to oxidize all easily oxidizable matter. After cooling, 5 ml of 70 % HClO4 was added and the mixture was boiled gently till the appearance of dense white fumes. The contents were cooled and 20 ml of distilled water was added, and re-boiled to stop the release of any fumes. The solution was cooled again, filtered off through Whatman No. 42 filter paper and transferred to 25 ml volumetric flask. The volume was made up to the mark with distilled water.

All of the digested soil samples were analyzed for their total concentrations of Cd, Cr, Cu, Ni, Pb and Zn by using Atomic Absorption Spectrophotometer (Perkin Elmer A Analyst 300).

F. Transport model

The objective of the transport model is to compute concentrations of heavy metal in the unsaturated soil. The heavy metal movement in the column is only due to the physical transport of the component. The mechanisms of transport considered are advection and dispersion. The retention of each component by the soil matrix is not explicitly considered in

the transport step. Each component is transported independent of the other, i.e., the movement of one component has no influence on the other in the physical step. This is a reasonable assumption, when convection is larger compared to molecular diffusion. A finite difference method was used to discretize the equations. These equations usually have problems of numerical dispersion. In order to circumvent this problem, an Eulerian-Lagrangian approach was adopted [13]. The solution procedure for the transport component was split into two steps. During the first step, only pure convection is considered. Then, the convected concentrations obtained are solved for second-order dispersion using Eularian approach. The system of algebraic equations resulting from discretization at each time step, are solved by formulating a tridiagonal system and invoking the Thomas algorithm.

G. Equation for the transport model

The equation describing the movement of contaminants is

$$\frac{\partial C_k}{\partial t} = \frac{\partial}{\partial z}\left[D\frac{\partial C_k}{\partial z}\right] - \frac{\partial}{\partial z}(v(z)C_k) + R_k \text{ , where } k = 1,2 \dots N_c$$

where C_k is the concentration of the kth component at any spatial location z at any time t, D is the dispersion coefficient, and R_k is the chemical source/sink term representing the changes in aqueous component concentrations.

H. Equations for the flow model-

The flow model is formulated using Richard's equation for unsaturated movement of water in one dimension. The equations governing water movement are

$$q = -K\left(\frac{\partial \psi}{\partial z} - 1\right)$$

$$\frac{\partial \theta}{\partial t} = \frac{\partial q}{\partial z} - S$$

where θ is water content by volume (cm3/cm3), q is the water flux (cm/h), S is the sink term (cm-1), K is the hydraulic conductivity (cm/h), $\psi\ (< 0)$ is the soil matrix potential (cm), z is the vertical coordinate direction taken positive downward, and t is time (h). The two equations can be combined to yield the Richards equation in terms of θ as

$$\frac{\partial \theta}{\partial t} = -\frac{\partial}{\partial z}\left[K(\theta)\left(\frac{\partial \psi}{\partial z} - 1\right)\right] - S(\psi)$$

where the sink term depends on Ψ. The K(θ) and $\psi(\theta)$ are non-linear functions, and have been described by Brooks and Corey [14]. The pore water velocity at any depth is given by

$$v(z) = \frac{q(\theta)}{\theta}$$

The interactions between heavy metals and various ions in both aqueous and solid phases are represented in the form of a set of non-linear algebraic equations. The system of equilibrium equations relates the dependent variables (species) with independent variables (components). A species is defined as a chemical entity to be considered in the transport problem. The species are not limited to aqueous phase, but also include those that are in the solid phase.

Associated with each species is a mass law equation and an equilibrium constant.

III. SOLUTION STRATEGY

The solution space for the transport model described above consists of three domains: spatial, chemical and temporal [15]. The advection-dispersion terms describing aqueous phase transport are spanning over spatial and temporal domains only, and the geochemical equations describing the transformation of heavy metal into different species are spanning over the chemical domain only. In other words, the advection dispersion equations and geochemical equations are decoupled and solved separately. The advantage of this method of solution is that the highly non-linear behavior of geochemical equilibrium is confined to the model describing the geochemistry. Thus, the overall solution system consists of two steps: a physical step in which the advective-dispersive terms of the transport equation are solved, keeping the reaction (sink/source) terms constant, and a chemical step in which the chemical equilibrium equations are solved for the aqueous and solid phase components. For each nodal

point in the spatial domain, a sequential coupling strategy of the physical and chemical steps has been adopted. The physical and chemical coupling is external. The disadvantage of this method is that chemical equilibrium is allowed to occur only at the end of a time step. This does not cause significant errors if small time steps are chosen.

IV. RESULTS AND DISCUSSION

The present study area covers the Jaipur and Kota districts of Rajasthan. Forty eight soil samples were collected from different industrial areas and analyzed. The concentration of six heavy metals (Cd, Cr, Cu, Ni, Pb and Zn) were identified and quantified by using Atomic adsorption spectrophotometer in 4 different locations. Reconnaissance survey was carried out on the surface layer (0–5 cm depth), the first foot below the surface (30 cm depth), the second foot below the surface (60 cm depth) and the third foot below the surface (90 cm depth) to determine the total metal concentration. Sampling was done according to standard procedures. Various results obtained are tabulated and depicted below.

A. pH analysis-

In the present study, soil samples were collected from four zones of Jaipur and four zones of Kota industrial areas. In all the location, when we moved from surface to deep soil area, the acidic nature of soil decreased. In the present study, the soil samples from the industrial area showed an acidic pH. The acidic behavior of soil is responsible for heavy metal leaching, which in turn increases the amount of heavy metals in soil. An acidic soil can free many toxic metals from its combined state which in turn can make the soil toxic.

In Jaipur industrial areas (location 1, 2, 3 and 4), the pH of location 1 ranged from 6.2 (acidic) to 7.2 (alkaline). The upper surface of location 2 was found to be maximally acidic (pH-5.8) and this pH restored near to neutral at third feet (pH-6.8). In location 3, same behavior was observed. On the other hand, in location 4, pH range was 6.1 to 7.3. Maximum alkaline condition was found in the third foot of strata (pH-7.3) at location 4.

Industrial areas of Kota (location 5, 6, 7 and 8) are also showing similar results. In location 5, the uppermost surface is showing maximum acidic condition with a pH value of 5.8. At third feet of strata, the pH become near to neutral with a pH value of 6.8. In location 6, pH values ranges from 5.9 (uppermost layer) to 7.1 (third feet of strata). Location 7 is also showing maximum acidic condition in topmost layer (pH- 6.4) and pH becomes slightly alkaline at third feet of strata (pH-7.2). In the location 8, pH value ranges from 6.3 (uppermost layer) to 7.1 (third foot of sediments).

Table 1: pH values at different locations of Jaipur and kota district

Location	Upper surface (0 Cm)	First feet (30 Cm)	Second feet (60 Cm)	Third feet (90 Cm)
1	6.2	6.4	6.9	7.2
2	5.8	6.2	6.3	6.8
3	5.9	6.2	6.6	6.9
4	6.1	6.6	6.8	7.3
5	5.8	6.3	6.4	6.8
6	5.9	6.7	6.8	7.1
7	6.4	6.7	6.7	7.2
8	6.3	6.6	6.8	7.1

B. Distribution of studied heavy metals in different locations of Jaipur district-

Fig 1, 2, 3 and 4 represents the heavy metal burden in soil samples of Jaipur district. Four different industrial areas were selected in the present study. The survey were carried out in Sitapura industrial area, Jhotwara industrial area, RIICO industrial area and Viswakarma industrial area, which were named location 1, 2, 3 and 4 accordingly.

Fig 1-4 indicates that most of the metals were found in varying concentrations. The mean concentrations of Cd, Cr, Cu, Ni, Pb and Zn in almost all soil samples were significantly higher than background contents of these heavy metals in the soils, suggesting the industrial area are highly polluted. The maximum average concentration is showed by Zn metal (254.16 ppm) in location 4. This was followed by Pb (248.60 ppm) and Cu (227.37 ppm) mean concentrations at location 3 and 4, respectively. The maximum obtained average concentration of Cr was 200.61 ppm (location 1), which was further followed by Ni (91.87 ppm) and Cd (22.5 ppm) at location 4. The maximum obtained average concentrations of heavy metals decreased as follows- Zn > Pb > Cu > Cr > Ni > Cd.

C. Location 1- Sitapura Industrial Area (Fig 1)

Fig 1 represents the descriptive statistics of the heavy metal concentrations of Sitapura industrial area. There was a

remarkable change in the content of heavy metals among the sampled soils. The concentrations of Cd, Cr, Cu, Ni, Pb and Zn varied between 2.56 and 15.42, 56.17 and 374.83, 54.58 and 198.34, 21.65 and 134.87, 58.84 and 284.6, 12.76 and 208.54 ppm, respectively. All of the mean values of the heavy metal concentrations were significantly higher than their normal permitted values. The maximum average concentrations of Cr, Cu and Pb were found in the uppermost surface (200.61 ppm, 144.50 ppm and 184.59 ppm, respectively), while Ni was present maximally in the second foot of sediment (86.85 ppm). The average concentrations of Cd and Zn were highest in the first foot of sediment (8.78 ppm and 123.11 ppm), respectively.

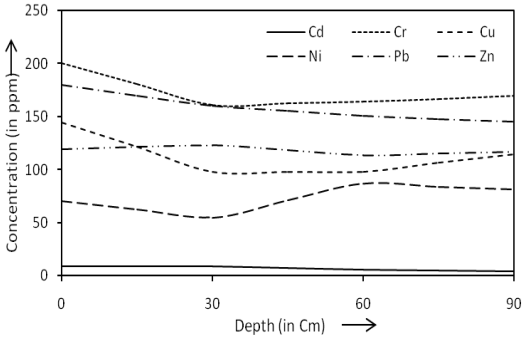

Fig 1: Heavy metals concentrations in soil samples of Sitapura Industrial area: Jaipur district.

D. Location 2 - Jhotwara Industrial Area (Fig 2)

The ranges of the concentrations of the studied metals in Jhotwara industrial area are shown in Fig 2. The Fig 2 shows that the heavy metal concentrations in the upper surface sediments decreased in the following order: Pb > Zn > Cr > Cu > Ni > Cd. In the first foot of sediment sampled, the heavy metal concentrations decreased in the following order: Pb > Cr > Zn > Cu > Ni > Cd. In the second and third foot of sediment sampled, the heavy metal concentrations decreased in the following order: "Pb > Cr > Cu > Zn > Ni > Cd" and "Pb > Cu > Cr > Zn > Ni > Cd", respectively. The average concentrations of heavy metals were predominated mostly in the upper most surface having average values of 15.79 ppm for Cd, 158.59 ppm for Cr, 139.38 ppm for Cu, 54.07 ppm for Ni, 212.41 ppm for Pb and 188.24 ppm for Zn.

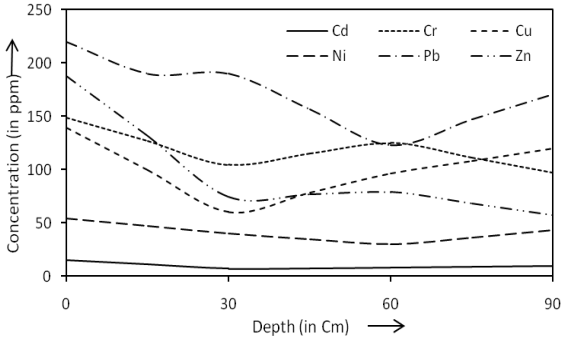

Fig 2: Heavy metals concentrations in soil samples of Jhotwara Industrial Area: Jaipur district.

E. Location 3 - RIICO Industrial Area (Fig 3)

The spatial distribution of heavy metals (Cd, Cr, Cu, Ni, Pb and Zn) in the RIICO industrial area is shown in Fig 3. In the upper surface stratum, the average concentrations of Cr (142.98 ppm), Cu (200.26 ppm) and Pb (248.60 ppm) were obtained at their highest levels. In the first foot of sediment, the average concentration of Zn was highest (210.80 ppm). Other studied metals (Cd and Ni) were highest at second foot level with average values of 14.22 ppm and 89.60 ppm, respectively. The minimum concentrations of Cd (3.95 ppm) and Ni (7.67 ppm) were found in the first foot of sediments, while third foot strata were showing minimum concentration Cr (10.36 ppm) and Cu (17.83 ppm). The lowest concentrations of Pb (19.65 ppm) and Zn (26.98 ppm) were present in the second foot strata and uppermost surface, respectively.

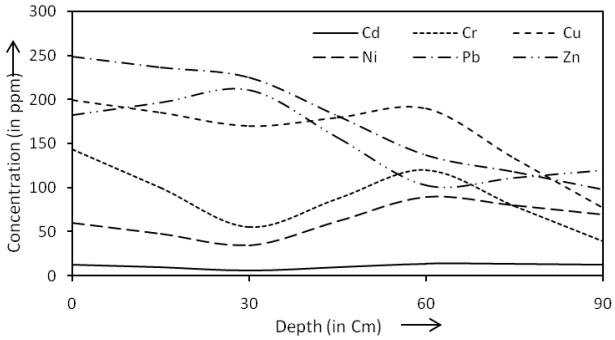

Fig 3: Heavy metals concentrations in soil samples in RIICO Industrial Area: Jaipur district.

F. Location 4 - Viswakarma Industrial Area (Fig 4)

Fig 4 show total concentrations of heavy metals in the Viswakarma industrial area. The studied heavy metals Cd, Cr, Cu, Ni, Pb and Zn concentration levels ranged between 5.87 to 37.15 ppm, 19.67 to 248.16 ppm, 34.56 to 357.78 ppm, 12.87 to 149.98 ppm, 17.84 to 439.67 ppm and 18.89 to 407.87 ppm, respectively with maximum mean values of 22.5 ppm for cadmium, 121.6 ppm for chromium, 227.37 ppm for copper, 91.87 ppm for nickel, 240.30 ppm for lead and 254.16 ppm for Zn. In this study, the following trend of heavy metal contamination was established. Excessive level of Pb was observed in the upper most soil layer (Mean value-240.30 ppm) as compared to all the other elements. In the first, second and third foot of strata, the predominating heavy metal was mainly Cu with an average value of 206.11 ppm and 227.37 and 190.26 ppm, respectively.

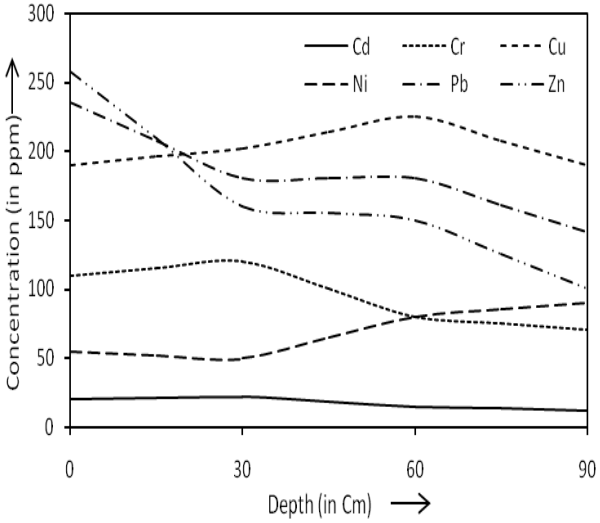

Fig 4: Heavy metals concentrations in soil samples of Viswakarma Industrial Area: Jaipur district.

G. Distribution of studied heavy metals in different locations of Kota district-

The change in the heavy metal concentrations were recorded in 4 different locations of Kota district. Soil samples were collected from the industrial region of Indraprastha, Chambal, RIICO Paryavaran and Large scale area; and these industrial areas were designated as location 5, 6, 7 and 8, respectively. The results concerning industrial areas of Kota are given in Figs (5, 6, 7 and 8).

H. Location 5 - Indraprastha Industrial Area (Fig 5)

Plumbism was evident in all the strata with maximum concentration of Pb (940 ppm) as compared to other studied heavy metals. The concentration of Pb ranges from 36.85 ppm to 940 ppm. The second most prevalent heavy metal was Zn with the average mean values of 312.21 ppm (upper surface), 301.56 ppm (first feet) and 257.56 ppm (second feet). However, in third feet of strata, Zn was predominating heavy metal with the average mean value of 275.52 ppm. Highest mean value for Cd (22.83 ppm) was observed in third foot of strata. Cr and Ni were showing elevated concentrations in second foot layer with the mean values of 174.07 ppm and 86.85 ppm, respectively. Average concentration of Cu was present maximum at first feet of strata (222.65 ppm).

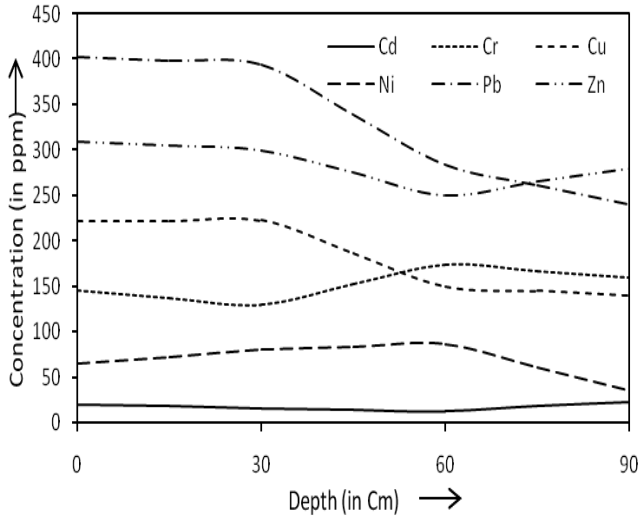

Fig 5: Heavy metals concentrations in soil samples of Indraprastha Industrial area: Kota district.

I. Location 6 - Chambal Industrial Area (Fig 6)

Heavy metal distribution in Chambal industrial area showed elevated levels of all heavy metals in the uppermost surface. The maximum average concentrations of Cd, Cr, Cu, Ni, Pb and Zn in topmost surface were found to be 25.29 ppm, 184.74 ppm, 210.85 ppm, 51.02 ppm, 371.80 ppm and 292.64 ppm, respectively.

Minimum average concentration of Cd, Ni and Pb were present in the third feet of strata (15.06 ppm, 21.36 ppm and 269.87 ppm, respectively), while Cu mean concentration value was least in the first feet of strata (125.85 ppm). Cr and Zn in second foot of sediment were revealing lowest mean concentration values of 104.15 ppm and 169.86 ppm, consequently.

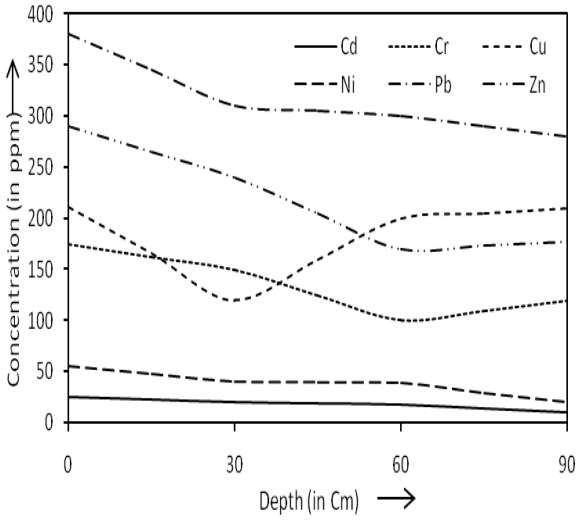

Fig 6: Heavy metals concentrations in soil samples of Chambal Industrial Area: Kota district.

J. Location 7 - RIICO Paryavaran Industrial Area (Fig 7)

Results for Cd, Cr, Cu, Ni, Pb and Zn concentrations in the soil samples of RIICO Paryavaran Industrial Area are presented in Table 7. In the present study, level of cadmium was found in the range of 2.87 ppm to 37.89 ppm. Maximum and minimum mean concentrations of Cd were observed in the uppermost surface soil (21.64 ppm) and first feet of soil (7.27 ppm) samples, respectively. Maximum average Cr and Pb content were found in upper surface (200.11 ppm and 335.27 ppm, respectively), which is much higher than the minimum obtained mean concentration values (62.53 ppm and 221.57 ppm, respectively) from the third feet of strata. The mean concentration values of Cu and Zn were minimum in second feet of strata (174.51 ppm and 159.16 ppm, accordingly) and maximum in uppermost surface (238.23 ppm and 284.64 ppm, respectively). Ni average mean value was highest in third feet of strata (86.72 ppm) and lowest in first feet of sediments (58.22 ppm).

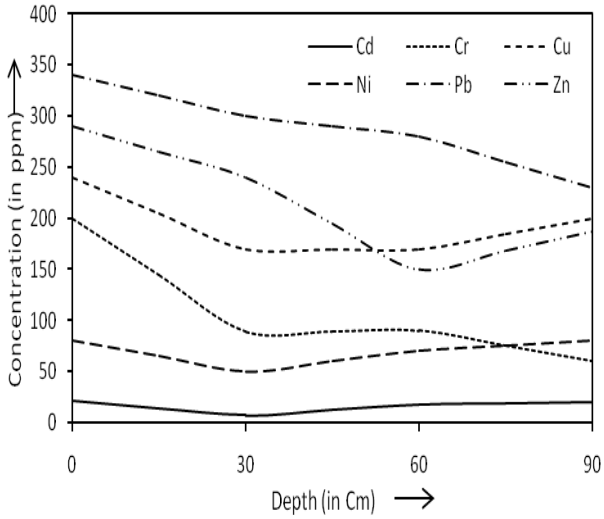

Fig 7: Heavy metals concentrations in soil samples in RIICO Paryavaran Industrial Area: Kota district.

K. Location 8 - Large scale Industrial Area (Fig 8)

Fig 8 shows the content of heavy metals in the soil of the selected area. Maximum heavy metal loads of the soils in the study area are 42.78 ppm for Cd, 358.09 ppm for Cr, 423.98 ppm for Cu, 181.08 ppm for Ni, 528 ppm for Pb and 443.88 ppm for Zn, whereas minimum heavy metal load for Cd, Cr, Cu, Ni, Pb and Zn are 7.89 ppm, 15.9 ppm, 24.68 ppm, 17.95 ppm, 42.98 ppm and 34.98 ppm, respectively. Maximum average concentration of Cd, Cr, Cu Ni, Pb and Zn are present in the uppermost surface with mean values of 28.44 ppm, 177.39 ppm, 253.98 ppm, 85.38 ppm, 359.32 ppm and 272.65 ppm, respectively.

Minimum mean concentration values of Cd, Cr, Cu Ni, Pb and Zn are found to be 14.88 ppm (third feet), 74.32 ppm (first feet), 149.54 ppm (second feet), 42.37 ppm (first feet), 219.65 ppm (third feet) and 159.59 ppm (third feet), respectively.

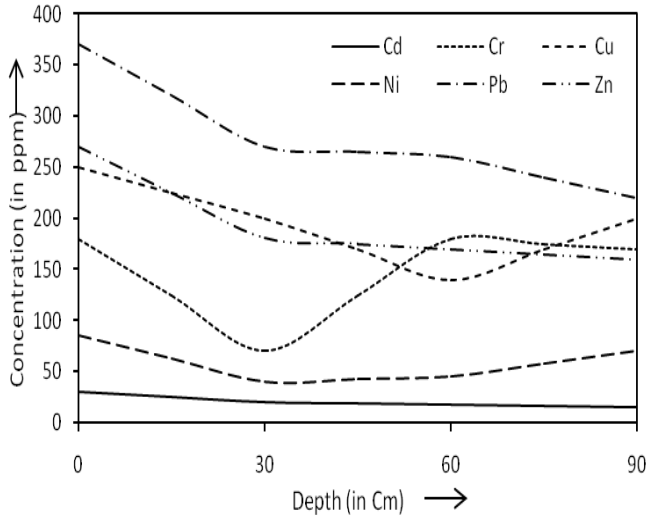

Fig 8: Heavy metals concentrations in soil samples of Large scale Industrial Area: Kota district.

L. Correlation between heavy metals-

Correlation analyses have been widely applied in environmental studies. They provide a useful way to disclose the relationships between multiple variables and thus have been helpful for understanding the influencing factors as well as the sources of chemical components. Heavy metals in soil usually have complex relationships among them. The high correlations between heavy metals in soil may reveal that the accumulated concentrations of these heavy metals come from similar pollution sources. The results of the Pearson's correlation matrix of heavy metals in the surface soils of Jaipur and kota Industrial Area are shown in Table 2 (A) and 2 (B) respectively.

The correlation coefficient between Pb and Zn are 0.71 and 0.74, which indicates a strong linear correlation and a common origin of these metals. Cu and Zn, Cu and Pb formed another correlated pair with a correlation coefficient of 0.52 and 0.51, suggesting they probably originated from the same common sources. From Table 2(A), Cd exhibited strong positive correlations with both Cu (0.62) and Zn (0.47). Cu and Zn occur naturally at abundant levels and are thus barely affected by human activities, which explain their apparent correlation in the surface soils. Cd is also widely scattered in the Earth's crust, and its correlations indicate that its occurrence in the surface soils was mainly due to natural sources. Zn and Cr formed another correlated pair with a correlation coefficient of 0.47 from Table 2(B). The lack of significant linear correlation between, Cr and Ni with other heavy metals from Table 2(A) and Cd with other heavy metals from Table 2(B), suggests that its sources were quite different from those of the others.

Table 2 (A): Pearson's Correlation matrix of heavy metals in the surface soils of Jaipur.

	Cd	Cr	Cu	Ni	Pb	Zn
Cd	1					
Cr	-0.19	1				
Cu	0.62	-0.11	1			
Ni	-0.05	0.10	0.22	1		
Pb	0.29	0.17	0.45	-0.41	1	
Zn	0.47	-0.03	0.52	-0.15	0.71	1

Table 2 (B): Pearson's Correlation matrix of heavy metals in the surface soils of Kota.

	Cd	Cr	Cu	Ni	Pb	Zn
Cd	1					
Cr	0.01	1				
Cu	-0.14	-0.001	1			
Ni	-0.25	0.11	0.35	1		
Pb	-0.18	0.27	0.51	0.22	1	
Zn	0.25	0.47	0.26	0.29	0.74	1

V. CONCLUSION

Heavy metal contamination is a severe environmental problem The results indicated that concentrations of Cu, Zn, Pb, Cd, Hg, and As in almost all the soil samples exceeded the background values in industrial area of Jaipur and Kota cities. Average concentrations of all the studied heavy metals were significantly higher than their normal permissible limit. The study shows that the metals are accumulated in all the strata of soil layer, which clearly indicates soil pollution. These findings have important implications for the

development of pollution prevention and reduction strategies to reduce heavy metal pollution for regions undergoing fast industrialization and urbanization.

REFERENCES

[1] He Z., Shentu J., Yang X., Baligar V.C., Zhang T., Stoffella P.J. (2015). Heavy Metal Contamination of Soils: Sources, Indicators, and Assessment. Journal of Environmental Indicators. 9: 17-18.
[2] Chimezie Anyakora, Teddy Ehianeta and Oghenetega Umukoro. (2013). Heavy metal levels in soil samples from highly industrialized Lagos environment. African Journal of Environmental Science and Technology. 7(9): 917-924.
[3] Dupler D. (2001). Heavy metal poisoning. Gale Encyclopedia of Alternative Medicine. Farmington Hills, MI: Gale Group.
[4] Momodu M., Anyakora C. (2010). Heavy metal contamination of groundwater: the Surulere case study. Res. J. Environ. Earth Sci. 2(1): 29-43
[5] Anyakora C., Nwaeze K., Awodele O., Nwadike C., Arbabi M., Coker H. (2011) Concentrations of Heavy Metals in some Pharmaceutical Effluents in Lagos, Nigeria. J. Environ. Chem. Ecotoxicol. 3(2): 25- 31.
[6] (IARC) International Agency for Research on Cancer. 1993. Beryllium, cadmium, mercury and exposures in the glass manufacturing industry, vol. 58. IARC, Lyon, France. 119-238.
[7] EPA (1998). "Toxicological Review of Trivalent Chromium. CAS No. 16065-83-1. In support of Summary Information on the Integrated Risk Information System (IRIS). U.S. Environmental Protection Agency, Washington, D.C.
[8] Chervona Y., Arita A., Costa M. (2012). Carcinogenic metals and the epigenome: understanding the effect of nickel, arsenic, and chromium. Metallomics. 4(7): 619-27.
[9] Veena Sharma, Arti Sharma, Leena Kansal. (2010). The effect of oral administration of Allium sativum extracts on lead nitrate induced toxicity in male mice. Food and chemical toxicology. 48(3): 928-936.
[10] *Fosmire GJ. (1990). Zinc toxicity. Am. J. Clin. Nutr. 51 (2): 225–227.*
[11] Liza Jacob, Romilly Margaret Mendez, Bindu Antony. (2015). Analysis of the soil properties of an industrial area in Kerala. International journal of scientific & technology research. 4(12): 139-140.
[12] Sharma, R.K., Agarwal, M. and Marshall, F. (2007). Heavy Metals Contamination of Soil and Vegetables in suburban Areas of Varanasi, India. Ecotoxicology and Environmental Safety. 66: 258-266.
[13] N.R. Thomson, J.R. Sykes and W.C. Lennox. (1984). A Lagrangian Porous Media Mass Transport Model. Wat. Resour. Res. 20(3): 391-399.
[14] R.H. Brooks and A.T. Corey. (1964). Hydraulic Properties of Porous Media, Hydrology Paper No. 3, Colorado State University, Fort Collins.
[15] A.L. Walter, E.O. Frind, D.W. Blowes, C.J. Ptacek and J.W. Molson. (1994). Modeling of Multicomponent Reactive Transport in Groundwater, 1. Model Development and Evaluation. Wat. Resour. Res. 30(11): 3137-3148.